

THE FLORIDA STATE UNIVERSITY
COLLEGE OF ARTS AND SCIENCES

CONSTRUCTION AND APPLICATION OF A SPATIAL HURRICANE
CLIMATOLOGY

By

KELSEY SCHEITLIN

A Dissertation submitted to the
Department of Geography
in partial fulfillment of the
requirements for the degree of
Doctor of Philosophy

Degree Awarded:
Summer Semester, 2010

The members of the committee approve the dissertation of Kelsey Scheitlin defended on June 4, 2010.

James Elsner
Professor Directing Dissertation

Robert Hart
University Representative

Victor Mesev
Committee Member

Tingting Zhao
Committee Member

Thomas Jagger
Committee Member

Approved:

Victor Mesev, Chair, Department of Geography

David Rasmussen, Dean, College of Social Sciences and Public Policy

The Graduate School has verified and approved the above-named committee members.

To my parents, B and Jude, for supporting me through nine years of college, and my fiancé Jason, who patiently allowed me to put our lives on hold while I produced this document.

ACKNOWLEDGMENTS

First, I would like to acknowledge Dr. Elsner for his level of commitment to these papers and to my success. Dr. E, your mentorship, life lessons, and all of the wonderful opportunities you provided me will forever be appreciated. I promise you- I did not forget to put your name on the paper! I also thank my committee members- Dr. Zhao, Dr. Mesev, and Dr. Hart- for their time and effort in this project. The published chapters of this dissertation were produced with the help of my coauthors- Dr. Elsner, Dr. Jagger, Dr. Mesev, Jill Malmstadt, Rob Hodges and Shawn Lewers. A special thanks to my entire support system in the Department of Geography, especially those in the bat cave. An extra special thanks to Miss Jillbug Malmstadt, who pulled me through the toughest of times in the past three years.

TABLE OF CONTENTS

List of Tables	vii
List of Figures	ix
Abstract	xiv
1 BACKGROUND	1
1.1 The Hurricane Phenomenon	2
1.2 Hurricane Tracks	3
1.3 Hurricane Climatologies	5
1.4 What is a Spatial Hurricane Climatology?	8
1.5 Objectives	9
1.5.1 Objective 1	9
1.5.2 Objective 2	10
1.5.3 Objective 3	12
1.6 Document Organization	15
2 USING DISTANCE MAPS FOR POLYLINE AVERAGING	16
2.1 Introduction	16
2.2 Methodology	17
2.3 Application in Hurricane Climatology Research	20
2.3.1 Averaging Hurricane Tracks	20
2.3.2 Constructing Historical Hurricane Tracks	24
2.4 Summary	28
3 TOWARD INCREASED UTILIZATION OF HISTORICAL HURRICANE CHRONOLOGIES	30
3.1 Introduction	30
3.2 Early Tropical Cyclones	31
3.2.1 The Chenoweth Archive	32
3.3 Adding a Spatial Dimension	33
3.3.1 Digitizing the Chenoweth Locations	33
3.3.2 Determining a Probable Pathway	35
3.4 The 1766 Hurricane Season	38
3.5 Unusual Archived Cyclones	38
3.6 Sensitivity of the Methodology	42

3.6.1	Omitting an Event Location	42
3.6.2	Applying the Methodology to Recent Hurricanes	43
3.6.3	Filtering the Analogs by Time of Year	43
3.7	Summary	47
4	RISK ASSESSMENT OF HURRICANE WINDS FOR EGLIN AIR FORCE BASE	50
4.1	Introduction	50
4.2	Hurricane Data	52
4.3	An Average Hurricane Track	53
4.4	Hurricane Characteristics Along the Track	55
4.4.1	100-Year Wind Speeds	57
4.4.2	Forward Speed	60
4.4.3	Radius to Maximum Winds	60
4.4.4	Holland <i>B</i> Pressure Profile Parameter	62
4.5	Estimates of Wind Speeds and Wind Damage Losses From HAZUS HM	64
4.5.1	Deterministic Mode	64
4.5.2	Historical Scenario	64
4.5.3	Probabilistic Mode	66
4.5.4	Economic Loss	66
4.6	Summary	68
5	A TRACK-RELATIVE CLIMATOLOGY OF EGLIN AIR FORCE BASE HURRICANES IN A VARIABLE CLIMATE	70
5.1	Introduction	70
5.2	An Average Hurricane Track	71
5.3	Hurricane Characteristics Along the Track	74
5.4	Warm versus Cool SST Years	77
5.5	Summary	78
6	CONCLUSION	82
6.1	Summary of Outcomes	83
6.1.1	Tools	83
6.1.2	Data	83
6.1.3	Analysis	84
6.2	Future Research	84
6.2.1	Comparing Constructed Hurricane Tracks	84
6.2.2	Spatial Patterns of Major Hurricanes	86
6.2.3	Return Levels of Economic Loss	89
6.3	Concluding Remarks	89
A	DIGITIZED CHENOWETH ARCHIVE LOCALITIES	91
	Biographical Sketch	117

LIST OF TABLES

1.1	Years with largest number of articles published with “hurricane” in the title (ISI Web of Knowledge). The years following Hurricane Katrina (2005) and Hurricane Andrew (1992) mark peaks in hurricane research.	2
1.2	The Saffir-Simpson Hurricane Wind Scale. A hurricane reaches a new category with higher sustained wind speeds. Categories 3, 4, and 5 are major hurricanes.	3
3.1	A portion of the Chenoweth Archive (CA) pertaining to the 1766 hurricane season. The date of the first and last events are listed for each cyclone. Location refers to the localities listed in the archive. Method refers to the methods used in this study to digitize the event location (see text). Most cyclones have more than one location.	48
3.2	Parameters used to construct tracks for the 1766 North Atlantic hurricane season. The number of analogs is the number of tropical cyclones from the HURDAT used to determine the track. The minimum distance is the average distance to the Chenoweth locations for the closest analog. The threshold is the minimum distance in the weighted-average distance grids that enclose a continuous pathway.	49
4.1	Hurricanes passing within 150 km of the fiducial point over the period 1851–2008. The maximum sustained wind of the hurricane when it passed within 150 km exceeded 50 m s^{-1} (at least a Category 3 on the Saffir/Simpson hurricane scale). The distance (km) is the hurricane’s closest approach to the fiducial point. Hurricanes were not named before 1950.	53
4.2	Vitals for an extreme hurricane affecting EAFB. The latitude (λ) and longitude (ϕ) are those of the equal-interval points along the average track. The wind speed (m s^{-1}) refers to the 100-year return level for that point. The translation speed (Trans) (m s^{-1}), radius of maximum winds (R_{MW}) (km), pressure (mb), and Holland B profile parameter are obtained from past hurricanes and formulas based on known relationships. The inland column is a binary variable describing whether the point is over water (0) or land (1). These vitals are used to produce a wind field in the HAZUS HM.	63

A.1 Digitized Version of the Chenoweth Archive. The year, month (M1 and M2) and days (D1 and D2) of the first and last event from the hurricane are given. The Storm Number (SN) and maximum intensity (hurricane (HU) or tropical storm (TS)) are as listed in the Chenoweth Archive. The track is the description listed in the archive. The point (Pt) refers to the event number of the given event (1–4) and the location is the description Chenoweth assigned to that point. Last are the method used to digitize the point (M), and the resulting latitude and longitude locations. 92

LIST OF FIGURES

1.1	Hurricanes (tropical cyclones with sustained wind speeds $\geq 33 \text{ m s}^{-1}$) in the North Atlantic basin (1851–2008) (HURDAT).	4
1.2	The influence of the North Atlantic Oscillation (NAO) on hurricane tracks. According to the Bermuda High Hypothesis, a) a positive NAOI steers hurricanes out to sea or towards the east coast of the United States, while b) a negative NAOI steers hurricanes towards the Gulf Coast of the United States (Liu and Fearn, 2000).	6
2.1	Steps for polyline averaging using distance maps. a) Three polylines to be averaged. b) A distance map is created for each polyline. Contour values are the shortest distance from that point to the polyline in units of x . c) The distance maps are averaged, creating an average-distance map. An average polyline is digitized down the center of the contours of the map. d) The average polyline (black) is a geovisualization of the original set of polylines (grey).	19
2.2	10 major hurricane tracks passing nearest Galveston, Texas, 1851–2009. All hurricanes reached major hurricane status (wind speeds $\geq 50 \text{ m s}^{-1}$) within a 100-km radius about Galveston. The shading of the tracks represents the distance of their closest passing to Galveston; the darker tracks having passed nearest the city.	22
2.3	IDW average distance map of the major Galveston hurricane tracks shown in Figure 2.2. Contours are lines of average distance and shown in degrees of latitude. Hurricanes passing nearest Galveston (the darkest tracks in Figure 2.2) are weighted most heavily.	23
2.4	The average major Galveston hurricane track. The track is based off of the IDW-average of the ten closest major hurricanes from 1851–2009.	24
2.5	Ten hurricanes from 1851–2007 passing nearest the points representing Jamaica and Louisiana. The location of the points is based on the methods described in Chapter 3. The darkest tracks passed closer, on average, to the two points.	26

2.6	Average distance map of hurricanes passing nearest Jamaica and Louisiana. Contours are degrees of latitude.	27
2.7	The average track and pathway of hurricanes passing near Jamaica and Louisiana. This is a probable pathway and track for Storm 25 in the Chenoweth (2006) Archive.	28
3.1	Major contributors leading to the Chenoweth Archive. Words in italics denote a source, while bold names represent published tropical cyclone chronologies.	32
3.2	Storm 275 in the Chenoweth Archive. a) The two locations mentioned in the archive for Storm 275 and a straight line through them (first-order track track). b) The ten closest tracks (track analogs) to the locations of Storm 275 shaded by average distance to the locations (km) with the darker shading indicating a closer track. c) Distance from any location across the basin to the closest track analog in degrees of latitude. d) Tropical cyclone pathway constructed by a weighted average of the distance grids of all track analogs. The shaded area encompasses a weighted average distance of less than or equal to 2.25° of latitude. A curve through the shaded area represents a possible (second-order) track for Storm 275.	36
3.3	Tracks for the 1766 North Atlantic hurricane season. The tracks are based on the cyclones listed in the Chenoweth Archive (Storms 93–99) and the method described in section 3.3 using the thresholds listed in Table 3.7. . . .	39
3.4	Distances (km) of the 15 closest modern analogs to the Chenoweth locations for the seven cyclones of the 1766 hurricane season. Distances increase with analog rank, but relatively rapidly for some cyclones (Storm 4).	40
3.5	Storm 96 in the Chenoweth Archive. a) Connecting the event locations provides a first-order approximation to the track. b) Using the event locations together with ten modern analogs provides a second-order approximation. c) A third-order approximation to the track is obtained by blending the first- and second-order approximations in a 1 to 1 ratio. d) Another third-order approximation using a blend in a ratio of 3 to 1 in favor of the direct track. . .	41
3.6	Pathways constructed for Storm 97 by using some localities (marked by a square), and omitting others (marked by an asterick). a) Using all three localities: Lesser Antilles, Puerto Rico, and off South Carolina. b) Omitting the location off South Carolina. c) Omitting the Puerto Rico location. d) Using only the Puerto Rico location.	44

3.7	Pathways and tracks constructed for Hurricane a) Charley (2004) using event locations: West of Jamaica, Western Cuba, and off the South Carolina coast and b) Dennis (2005) using event locations: North of Jamaica, Western Cuba, and Pensacola, Florida.	45
3.8	The track of Hurricane Gilbert and pathways created using analogs restricted to the months of a) August and September, and b) October and November. . .	46
4.1	Study area. Eglin Air Force Base (striped) is located in the Florida Panhandle, comprising of portions of Santa Rosa, Okaloosa, and Walton counties. . .	51
4.2	Tracks of the 10 major hurricanes passing within 150 km of the fiducial point over the period 1851–2008. The fiducial point represents a worst-case landfall scenario for the Eglin Air Force Base. The gray scale on the tracks corresponds to the distance from the fiducial point, with the darker tracks indicating closer approaches.	54
4.3	Average distance maps. The maps are based on using the a) 10 and b) 24 major hurricanes passing closest to the fiducial point over the period 1851–2008. Contours indicate the weighted average distance of the set of hurricanes. The outer contour encompasses the area that has an average distance less than 3° of latitude and the inner contour encompasses the area that has an average distance less than 0.75°, with a 0.25° contour interval. The average track is a line through the shortest distances on the average distance map and perpendicular to the contours.	56
4.4	Points along the average EAFB hurricane track. Points are equally spaced at a 100-km intervals from the fiducial landfall point. Hurricane characteristics are determined at these locations to create a track-relative climatology. . . .	57
4.5	Intensities and tracks of the extreme event and Hurricane Opal. a) Wind speed (m s^{-1}) profiles of the extreme event (black) and Hurricane Opal (gray) along their respective tracks. Landfall values are marked with an asterisk. Values are given at 100-km intervals, with distances in kilometers before (negative) and after landfall plotted on the horizontal axis. The 100-year return levels are for a 35-km radius around the given point. Return levels are calculated using an application of Elsner et al. (2008). The vertical lines are the 90% confidence interval. Wind speeds for Opal are the value of the closest one-hour observation. b) Equal interval points along the track of the extreme event (black) and Hurricane Opal (gray).	59

4.6	Track selection and forward speeds. a) Tracks of the 34 hurricanes passing within a 100-km great circle distance of the track point 300 km from the landfall location. The forward speed of each hurricane as it passed within 100 km of the location is used to compute the average. b) Average forward speeds (m s^{-1}) as a function of distance before and after landfall. Vertical bars indicate the \pm on standard errors above the mean speed. The number of hurricanes used in the averaging are shown above the horizontal axis.	61
4.7	Maximum wind gusts (m s^{-1}) for a) the extreme event and b) Hurricane Opal. The respective hurricane tracks are shown as a black line. One maximum wind gust is provided for each census tract. The extreme event produces wind gusts of 34–58 m s^{-1} . Hurricane Opal produces wind gusts of 31–45 m s^{-1}	65
4.8	Wind speed gusts for the Santa Rosa Island census tract. The curve shows 100-year return levels of wind gusts from the HAZUS HM probabilistic output. The points and error bars are from the HAZUS HM deterministic output using extreme hurricane vitals for EAFB.	67
5.1	Tracks of hurricanes affecting Eglin Air Force Base (EAFB). All 26 tracks came within 100 km of Santa Rosa Island, FL (30.4°N and 86.8°W) based on data from 1851–2008. The gray shading is proportional to the distance the track came to the landfall location. Darkest tracks are those that passed nearest the island.	72
5.2	Average hurricane track for EAFB. The average track is the solid line drawn through the minimum distance contours of the average-distance map. The average-distance map is based on 26 hurricanes affecting EAFB over the period 1851–2008.	73
5.3	The average EAFB hurricane track depicted as a series of equal-interval points spaced 100 km apart and centered on the landfall location of EAFB. The tracks of all hurricanes passing within 100-km radius of the point 500 km from landfall are also depicted. Hurricane characteristics (intensity, forward speed, etc) are averaged based on the maximum value obtained from the hourly data as the hurricane passes through the circle. The process is repeated for each point.	74
5.4	Hurricane characteristics along the average track. Average a) wind speeds and b) translation speeds at 100-km intervals along the track. Distances in kilometers before (negative) and after landfall are plotted on the horizontal axis. Standard errors (s.e.) about the mean are drawn as vertical lines and the number of hurricanes used in the averaging are shown above the horizontal axis.	76

5.5	Average hurricane intensities along the average track for hurricanes during a) cool and b) warm SST years. Distances in kilometers before (negative) and after landfall are plotted on the horizontal axis. Standard errors (s.e.) about the mean intensities are drawn as vertical lines and the number of hurricanes used in the averaging are shown above the horizontal axis.	79
5.6	Average hurricane forward speed along the average track for hurricanes during a) cool and b) warm SST years. Distances in kilometers before (negative) and after landfall are plotted on the horizontal axis. Standard errors (s.e.) about the mean translation speed are drawn as vertical lines and the number of hurricanes used in the averaging are shown above the horizontal axis.	80
6.1	Two reconstructions of Storm No. 314. The shaded area is our climatological pathway, and the line is a digitized version of the hand-drawn track of Michael Chenoweth. Comparisons like this may help refine the technique for reconstructing historical hurricanes.	85
6.2	Creating an average Galveston hurricane track. a) The 10 hurricanes (wind speeds $\geq 33 \text{ m s}^{-1}$) passing nearest Galveston between 1851 and 2008. b) The average distance map of the 10 tracks. These tracks have slightly less in common than the 10 major hurricane (wind speeds $\geq 50 \text{ m s}^{-1}$) tracks used in Figure 2.2 as indicated by their average distance map in Figure 2.3.	87
6.3	Creating an average Galveston tropical storm track. a) The 10 tropical storms and hurricanes (wind speeds $\geq 18 \text{ m s}^{-1}$) passing nearest Galveston between 1851 and 2008. b) The average distance map of the 10 tracks. These tracks have slightly less in common than the 10 hurricane tracks used in Figure 6.2 as indicated by their average distance map.	88

ABSTRACT

The tracking of hurricanes, largely controlled by the organization of the presiding pressure systems, determines whether or not any given hurricane will strike a coastline. Some of the climatic influences, such as the North Atlantic Oscillation, show annual- or decadal-variability. This means that particular locations will have typical hurricane tracks that may vary with the climate. Therefore, it makes physical sense to summarize large sets of hurricane tracks by creating an average track.

A hurricane climatology describes the typical hurricane to affect a location. This dissertation proposes expanding the hurricane climatology by adding a spatial dimension in the form of an average track. This is referred to as a spatial hurricane climatology. Since a hurricane track is a polyline, the construction of a spatial hurricane climatology requires averaging spatial polyline data. The technique introduced in this dissertation uses distance maps to average a set of polylines. Three applications of spatial hurricane climatologies are also detailed in this work. First they are used to construct historical hurricane chronologies. This has the possibility of providing an additional 150 years of hurricane data, providing a glimpse into hurricanes prior to the American industrial revolution. The second application is a risk analysis of local-scale hurricane winds. The technique uses statistics of past hurricanes and places them in a deterministic model. This can be performed for any coastal area, and provides wind gusts and economic loss estimations for a once-in-100-year event. Because the statistics are easy to manipulate, this allows for simple analysis of the affects of climate change. This is done as the final application of the technique. These are only a few examples of the uses of spatial hurricane climatologies, and the ideas presented in this research provide a basis for future studies on spatial hurricane patterns, as well as the analysis of spatial polyline data in general.

CHAPTER 1

BACKGROUND

Climate change is currently among the most prevalent topics of scientific inquiry. Is the atmosphere warming? What will happen to global sea level if the glaciers melt? What about droughts, severe weather and hurricanes? Hurricanes already cause considerable damage along our coastlines. A possible increase in the frequency or intensity of hurricanes in a warmer climate has brought an already prominent field to the forefront of climatology research.

A quick search for journal articles on the Institute for Science Information (ISI) website shows that in recent years, about one peer-reviewed article (on average) is published each day with the word “hurricane” in the title (Table 1). Topics of these papers include affects of climate on tropical cyclone intensity (Emanuel, 2005; Elsner et al., 2008b), frequency (Pielke et al., 2005; Oouchi et al., 2006), and duration (Webster et al., 2005). Spikes of interest in hurricane research occurred after major hurricane events, such as Hurricane Andrew (1992) and Hurricane Katrina and the active 2005 hurricane season. The rate of publications has decreased each year since Katrina, but maintains relatively high. Perhaps the current elevated interest is related to the growing concerns associated with climate change. Interestingly enough, the number of ISI publications with “hurricane” listed as a topic, however, continues to steadily increase, likely indicating more recent interest in widespread hurricanes impacts.

All of this research by leading climate scientists and yet there are still some basic hurricane questions left unanswered. Yes, strides have been made in understanding the thermodynamics of hurricanes (Emanuel, 1986, 1999), and what controls their maximum potential intensity (Holland, 1997) and their likelihood of reaching it (Emanuel, 2000). Statistical models can estimate hurricane probabilities with confidence (Elsner and Bossak, 2001; Elsner and Jagger, 2004, 2006; Jagger et al., 2001; Jagger and Elsner, 2006) and deterministic models can estimate their losses (Vickery et al., 2006a,b). The ability of dynamical models to reproduce a hurricane or entire season of hurricanes is rather impressive (Hoke and Anthes, 1977; Emanuel, 1995; Walsh et al., 2004).

But Kerry Emanuel, a leading hurricane scientist, is quick to mention during his presentations that we do not know why there are, on average, 80 hurricanes per year around the globe (also discussed in (Emanuel, 2004)). We know that the frequency and intensity of North Atlantic hurricanes fluctuates with sea surface temperature (Emanuel, 1987;

Table 1.1: Years with largest number of articles published with “hurricane” in the title (ISI Web of Knowledge). The years following Hurricane Katrina (2005) and Hurricane Andrew (1992) mark peaks in hurricane research.

Year	Number of Articles
2006	440
2007	397
2008	372
2005	331
2009	323
1993	133

Elsner et al., 1999; Wentz et al., 2001), El Niño Southern Oscillation (Bove et al., 1998; Elsner et al., 1999, 2001), and other climate controls. But there are still unanswered questions regarding some fundamental concerns such as mean hurricane frequencies. Thus, the research presses on. Climate change may not be a major topic of this dissertation, but understanding today’s hurricanes is the first step towards understanding tomorrow’s. And the better the understanding of today’s hurricanes, the more accurate the future projections, allowing for informed mitigation and preparation.

1.1 The Hurricane Phenomenon

It all begins with a disturbance. Perhaps a cluster of thunderstorms begin to organize off of the western coast of Africa. After persisting for 24 hours they earn the title of tropical disturbance. Sometimes the cluster continues to strengthen and organize, and develops a closed circulation. The disturbance is now called a tropical depression. Warm sea surface temperature (SST) (preferably $\geq 80^\circ$ F) and little wind shear aloft favors continued strengthening. New titles are earned with incremental increases in sustained wind speeds. Formally, sustained winds are the average speed over a 1-minute period at roughly 30 feet above the ground.

Sustained wind speeds of 17 m s^{-1} indicate a tropical storm. At this point the storm is named. Names such as Isabel, Charley, and Katrina make the storm sound much more welcome than coastal populations feel they are. The storm has also taken on a distinctive appearance. The clouds take on a curved pattern, organizing into spiral bands of thunderstorms as the coriolis force spins the storm in a counter-clockwise motion in the northern hemisphere.

If the tropical storm intensifies to 33 m s^{-1} it becomes a hurricane. More than half of North Atlantic tropical cyclones reach this status (Elsner and Kara, 1999). There are five categories of hurricanes, as described by the Saffir-Simpson Hurricane Wind Scale (Ta-

Table 1.2: The Saffir-Simpson Hurricane Wind Scale. A hurricane reaches a new category with higher sustained wind speeds. Categories 3, 4, and 5 are major hurricanes.

Category	Wind Spd (m s^{-1})	Damage
1	33–42	Minimal
2	43–49	Moderate
3	50–58	Extensive
4	59–68	Extreme
5	≥ 69	Catastrophic

ble 1.1). Category 3, 4 and 5 hurricanes are often referred to as major or intense hurricanes. The hurricane continues to organize as it strengthens. An eye forms in the center of the hurricanes, devoid of wind and rain and clearly visible on most satellite images. It is in the wall of this eye where the strongest winds of the entire hurricane are located. Attempts to understand the formation of the eye began as early as 1940s, but it is still not completely understood (Riehl, 1948; Malkus, 1958; Willoughby, 1998).

The hurricane is an awe-inspiring force, especially when one considers its purpose- to redistribute the excess heat of the tropics towards the sun-neglected poles. But the effects of the hurricane are more daunting than inspiring. They are the costliest and deadliest of all atmospheric storms, having killed more people worldwide in the last 50 years than any other natural force (Elsner and Kara, 1999). They occur in most of the world’s ocean basins, but this work focuses on those of the North Atlantic. These hurricanes account for 11% of global hurricane activity (Elsner and Kara, 1999) and cause an average of \$10 billion in damage in the United States annually (Pielke Jr. et al., 2008). They destroy lives, buildings, and even the economy.

There are many geographic considerations in the hurricane problem. Hurricanes are prone to strike some coastlines more often than others. The population density and economy of the landfall location greatly influence damage and loss amounts. While physicists model the thermodynamics of a hurricane, perhaps it is the role of the geographer to model the spatial behavior of a hurricane, which is represented by a single line traveling across space- the hurricane track.

1.2 Hurricane Tracks

Each year, coastlines are threatened by tropical cyclones forming over the warm ocean. When the threat is fulfilled and a hurricane makes landfall, the damage can be catastrophic and the effects far-reaching. The National Hurricane Center (NHC) tracks the hurricanes from their genesis through their decay. The NHC currently hosts the Hurricane Database (HURDAT; best track) which contains location, intensity, and size information for observed

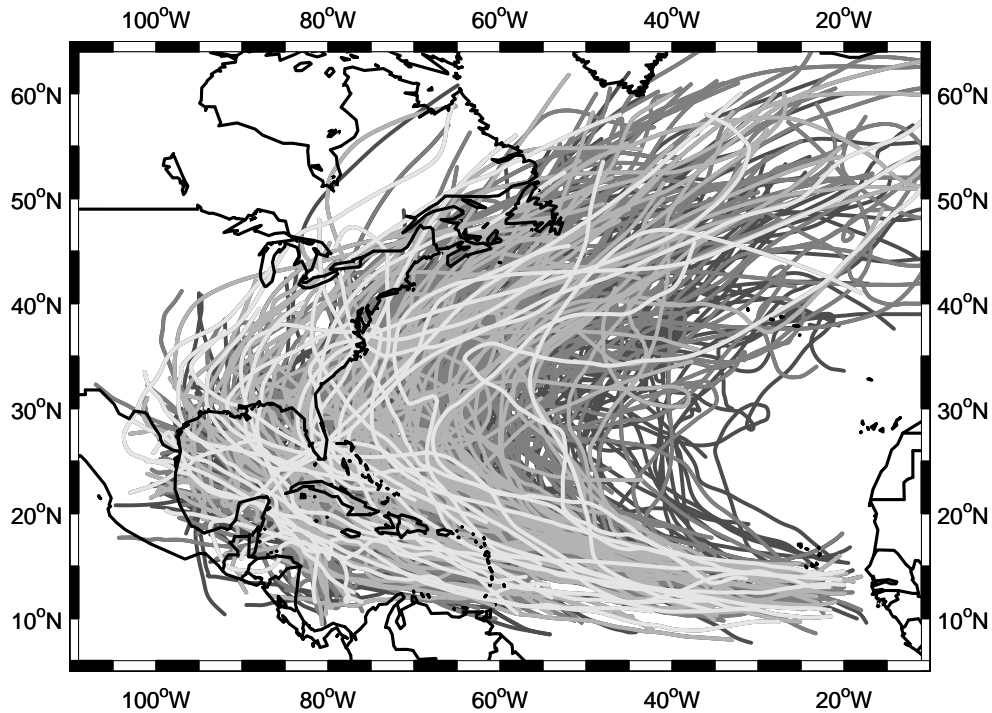


Figure 1.1: Hurricanes (tropical cyclones with sustained wind speeds $\geq 33 \text{ m s}^{-1}$) in the North Atlantic basin (1851–2008) (HURDAT).

North Atlantic, Gulf of Mexico and Caribbean Sea tropical cyclones since 1851. The best track data set currently contains approximately 1400 tropical cyclones (1851–2009), 819 of which reached hurricane strength. Every six hours during the tropical cyclone’s lifespan, data are gathered through reconnaissance flights, remote sensing images, and surface observations. Connecting the dots between the six-hourly observation locations provides an estimated track for a given hurricane (1.1).

The spatial behavior of hurricanes is of utmost importance. A given hurricane’s track controls the fate of our most populous coastal cities. The track is largely controlled by presiding climate conditions, which steer the hurricane in a somewhat predictable manner. The North Atlantic Oscillation (NAO) has perhaps the largest control on North Atlantic hurricane tracks. Mathematically, the NAO Index (NAOI) is the difference in sea-level pressure between Iceland and the Azores (Elsner and Bossak, 2004). A positive (negative) NAOI indicates relatively higher pressure over the Azores (Iceland) (Elsner et al., 2000a). Physically, this pressure difference controls the positioning of the mid-latitude jet stream

and the sub-tropical high (Elsner et al., 2000b). When NAOI values are positive (negative), the sub-tropical high tends to be stronger (weaker) and located further east (west) (Elsner et al., 2001). Hurricanes are steered around the sub-tropical high in a clockwise fashion (Figure 1.2). The Bermuda High Hypothesis states that a positive NAOI pushes hurricanes out to sea or towards the east coast of the United States. This is often referred to as recurving. Meanwhile, a negative NAOI encourages North Atlantic hurricanes to travel west into the Gulf of Mexico (Liu and Fearn, 2000; Elsner and Kara, 1999). This, in turn, affects local hurricane frequency along the U.S. coastline.

The NAO example shows that seasonal climate scenarios dictate basin-wide tracking patterns. This is seen as frequency fluctuations at the local level, the result being an increase or decrease in hurricane activity at a given location. The NAO's largest effects are on the steering of hurricanes but it is one of the most important considerations for seasonal predictions. Because an existing hurricane is not dangerous until it approaches habited land. Thus, while a majority of hurricane research focuses on the factors influencing the intensity and frequency of hurricanes, their spatial behavior should not be neglected. An understanding of the dynamics and tracking of hurricanes together allows for the most complete understanding and better predictions.

A hurricane's track is more important than just determining where it makes landfall. Two hurricanes may make landfall at the same location but have different effects. The path the hurricane takes to get there affects its intensity. Hurricane Opal (1995), for instance, rapidly intensified while crossing the Gulf of Mexico due to a warm core ring associated with the loop current (Hong et al., 2000). A different track could have limited intensification by avoiding the abnormally warm sea surface temperatures. Another example is the effect that the angle of landfall has on local storm surge. Depending on the coastline, a hurricane making landfall perpendicular to the shore results in different storm surge heights than one traveling along the coast. In these cases, the specific tracking of a hurricane is very important.

That being said, a set of hurricanes affecting a particular location will often exhibit similar spatial behavior. In other words, a location is affected by a typical track. This idea is the basis of this dissertation and is discussed in detail in the next section. The remainder of this chapter introduces hurricane climatologies and defines what is coined a spatial hurricane climatology. The construction and application of spatial hurricane climatologies is the topic of this dissertation. This is shown through three research objectives, to be described later in this chapter.

1.3 Hurricane Climatologies

As the name suggests, hurricane climate is the study of the hurricane-climate relationship. This includes climate's influence on seasonal, annual, and decadal hurricane activity. There is also an interest in the hurricane's affect on climate (Hart et al., 2007).

The climatology of an area can be thought of as its "average weather." Thus, the hurricane climatology for a particular location describes its "average hurricane." This can

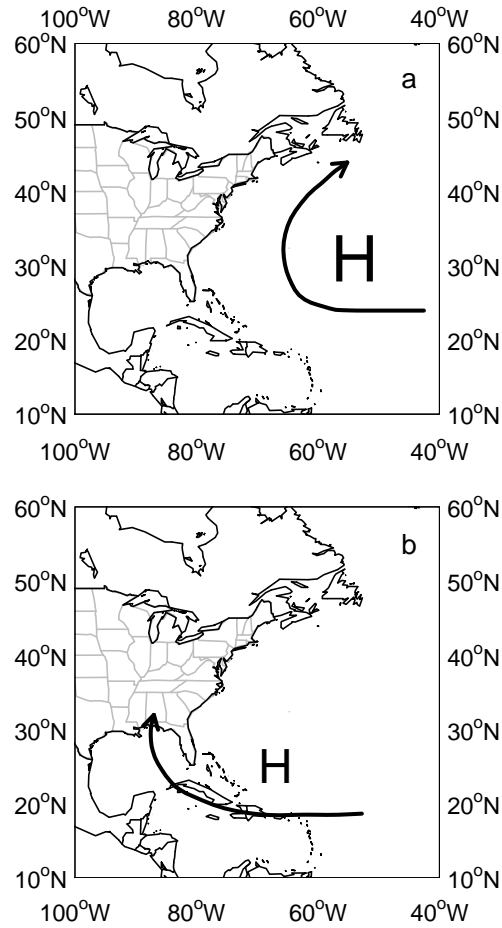


Figure 1.2: The influence of the North Atlantic Oscillation (NAO) on hurricane tracks. According to the Bermuda High Hypothesis, a) a positive NAOI steers hurricanes out to sea or towards the east coast of the United States, while b) a negative NAOI steers hurricanes towards the Gulf Coast of the United States (Liu and Fearn, 2000).

include the typical hurricane intensity, size, forward speed, and frequency of occurrence. So a hurricane climatology is the statistics of past hurricane activity over some time period for a location. Hurricane climatologies are usually created using past hurricane information and statistical models.

A hurricane climatology can be created for a point location (city) region, or even an entire basin. Elsner and Bossak (2001) breaks the coastline into regional segments to look at the larger scale hurricane climate along the U.S. coast, while Malmstadt et al. (in press) focuses on city-wide frequencies. The study area is an important consideration because there are physical reasons why hurricane activity can vary greatly even within a state. The Florida coastline experiences substantially different return rates in the panhandle and Miami area (Malmstadt et al., in press). This means the two areas have different hurricane climatologies, and the results depend on the scale of the study area.

Scale is an important consideration in a hurricane climatology. According to Blaut (1961), space is inseparably fused with time, so nothing in the physical world can be only spatial or temporal, rather a process that marries the two. This is true for hurricanes, and understanding their variability requires attention to both spatial and temporal patterns, and how they are inter-related. This is also related to the division of a study area. For frequency counts the area in which the events are counted is important. Hurricanes follow a poisson distribution, meaning they are rare events without many occurrences in a small area (Elsner, 2003). The lack of a large sample provides difficulty in achieving statistical significance. To understand hurricane frequency specific to a smaller area, it is sometimes worthwhile to look beyond that area to gain more information. This helps two issues in frequency calculations: 1) the data problems due to the rarity of the event itself and lack of an extensive record, and 2) the misrepresentation that occurs when random borders are drawn to designate the spatial categorization of binary hurricane counts. Using information outside of the area of question solves the border problem because one place does not “own” the hurricane, and provides a larger data set for analysis. This idea was introduced in Elsner and Jagger (2008) and applied to Florida cities in Malmstadt et al. (in press). In Chapter 4, this technique is used to apply intensity information to a spatial hurricane climatology.

Hurricane climatologies provide information about local hurricane rates and intensities, and how they vary with climate fluctuations. They are usually statistical in nature, with some having an empirical (Elsner and Bossak, 2001) or dynamical twist (Jagger et al., 2001). A common goal for hurricane climatologies is to improve local hurricane knowledge for operational use (Elsner and Jagger, 2006). A hurricane climatology is essential for hurricane loss models used by insurance, financial, and government sectors to estimate damage losses (Watson and Johnson, 2008). Chapter 4 shows how one is placed in a deterministic model to gain information about economic loss from a specific event.

A hurricane climatology usually explains the frequency of hurricanes and their characteristic at landfall. This type of point information is important, but does not tell the entire story. This work focuses on adding extensive spatial information to the hurricane climatology.

1.4 What is a Spatial Hurricane Climatology?

The spatial behavior of hurricanes is an important part of a hurricane climatology- for both the general and the particular. The “general” refers to broad or seasonal spatial patterns. We may see this as a track type- such as recurving versus straight-moving due to the influence of the NAO. This causes a change in hurricane frequency (more or less storms) in different areas. The “particular” is storm-specific. The tracking of a specific hurricane affects its intensity and/or storm surge heights. Thus, the general and particular influence the local climatology in different ways. Generally, the larger-scale spatial patterns play more of a role on the frequency of events, while the smaller-scale track changes influence the intensity. Another reason for this is that the smaller-scale track shifts may not change frequency. For example, the general pattern may send a hurricane towards the western Gulf of Mexico. Meanwhile, smaller-scale track influences may guide the hurricane towards Galveston, or perhaps 20 miles south of Galveston. The frequency of the Galveston hurricane is the same regardless because the city will feel the effects, but the intensity felt at the city depends on how the track will shift and where it will make landfall. Though the intensity of the storm is the same, where it makes landfall determines what intensity a location will experience. This is yet another illustration of the hurricane climatology’s dependence on scale.

The track of a hurricane is obviously important, but when it comes time to develop a hurricane climatology most attention goes to point characteristics without much concern for spatial hurricane patterns. Even when a hurricane climatology is created for a larger area, such as a coastline, hurricane information is obtained where they intersect the coastline with no interest in their spatial behavior before or after they affect the area of interest. Indeed, spatial patterns are inherent in the point hurricane climatology characteristics, especially in frequency counts. But expanding the spatial scale from a point to an entire track can provide more local-scale hurricane information. This allows the hurricane to be visualized as a dynamic object, changing over time and space. That is where a spatial hurricane climatology comes into use.

The spatial hurricane climatology expands the hurricane climatology to describe the average spatial characteristics of a hurricane. Since a hurricane’s spatial representation is its track, the term “spatial hurricane climatology” can literally be interpreted as the average hurricane track. A spatial hurricane climatology can be created for a specific location, month, sea surface temperature, etc. It represents a set of tracks with one average track. Similar to the typical hurricane climatology, a spatial climatology can include a number of hurricane characteristics by attaching information to the track. I refer to this as a track-relative climatology because it describes the climatology of a set of hurricanes along a similar path, with emphasis on the common track. More details on track-relative climatologies are in Chapters 4 and 5.

1.5 Objectives

This dissertation focuses on the spatial hurricane climatology- specifically its construction and application. The intent of the dissertation is to develop a tool kit for creating a climatology of hurricane tracks in the form of an average track, and to use this technique to gain insight into select hurricane climatology problems. This is achieved through three objectives.

1.5.1 Objective 1

The first objective of this dissertation is to develop a method for averaging spatial polyline data. The methodology described in Chapter 2 utilizes distance maps to create an average polyline from a set of spatial polylines. This technique is useful for the goal task (averaging hurricane tracks), but can also be used with other spatial polyline data sets. The methodology can be modified to calculate, in addition to the average polyline, a weighted-average polyline, cumulative distance, distance differences, and various other mathematical functions. For the case of averaging hurricane tracks, an inverse-distance weighted approach is presented.

Constructing a spatial hurricane climatology. A spatial hurricane climatology consists of a “climatological” or “average” hurricane track for a location. A hurricane track is a polyline, each track consisting of a set of line segments. Constructing a spatial hurricane climatology requires averaging a set of polylines. The first objective of this dissertation is to develop a technique for averaging spatial polylines. This is detailed in Chapter 2, and involves the use of distance maps.

A distance map is a map that displays the distance from a particular object to any point on the map. In this case, the distance map shows distances from a hurricane track. The track has a value of 0 (because it is 0 units away from itself), with the distances increasing as you move farther away. The distances can be shown as contours, which resemble a series of distance buffers around the track.

The distance maps are an efficient tool for averaging hurricane tracks. Other techniques that may be used for a similar purpose usually view the hurricanes as a set of observation points. For example, a kernel density of a set of observations from multiple hurricanes can show where there is the greatest density of hurricane observations, signifying more hurricanes nearby. However, since hurricanes move at different different speeds, slower moving hurricanes have more observations in a smaller space. This causes a density of points for a single hurricane, falsely resembling agreement between multiple hurricanes. Another issue with kernel density is that the units of density do not have any real-world relevance. The distance map method does not have either of these issues, allowing the entire track to be averaged and results in units of average distance. This work uses degrees longitude, but it may be changed to other distance units such as km. The distance map technique has proven to be straight forward with relatively few free parameters.

The first step to averaging a set of polylines is creating a distance map for each polyline. In the case of hurricanes, a distance map is created for each track. The distance maps

are subsequently stacked and averaged. The average distance map is shown in contours of average distance. A line digitized through the center of the contours is the average polyline. When applying the method to hurricanes the average polyline is an average track, which provides a spatial dimension to the hurricane climatology. This dissertation outlines two specific applications of a spatial hurricane climatology- to reconstruct historical hurricanes and to analyze hurricane risk. The first is solely based on the spatial aspect of the climatology, while the second creates a multi-dimensional hurricane by adding hurricane characteristics to the average track.

1.5.2 Objective 2

The second objective of the dissertation is to use the polyline-averaging technique to construct tracks of hurricanes listed in historical hurricane chronologies. Such chronologies are tables of documented hurricane accounts, most occurring before 1851. Each cyclone is associated with a set of one to four locations. The locations are qualitative descriptions of places that made record of the hurricane. The first step in constructing tracks for the hurricanes is to digitize the qualitative locations by assigning appropriate latitude/longitude coordinates. Next, past hurricane tracks that have passed by the archived locations are found, and averaged according to the distance map technique from Chapter 2. The inverse-distance weighted average track of the past hurricane tracks is used to represent a likely track for the historical storm.

Constructing historical hurricane tracks. The record of past tropical cyclones provides an important means to evaluate the hurricane hazard. Most contemporary hurricane research uses hurricane data since 1851, but this is not always seen as sufficient. Some researchers have taken an interest in “reconstructing” hurricanes prior to this date. Two main sources are being used to uncover past hurricane events- geologic proxies and historical documents. Historical documents are especially intriguing because they often provide multiple accounts of one hurricane, creating a paper trail of events over a spatial domain. A collection of hurricanes uncovered through document sources, such as newspapers, ship logs, and farmer’s diaries, is referred to as a hurricane chronology.

Historical chronologies are a source of information about tropical cyclones prior to the modern era. The focus of Chapter 2 is on the Chenoweth Archive, which is a table in Chenoweth (2006). The archive lists 383 tropical cyclones occurring during the 18th and 19th centuries (specifically, 1700–1855). Each cyclone is described by one–four qualitative locations reported to have felt its effects. Objective two of the dissertation is to construct tracks for the historical events based on these locations, demonstrating a novel way the archive can be used to articulate historical tropical cyclone activity across space.

Constructing tracks for historical hurricanes presents a few interesting geographical issues. The process itself is a historical and qualitative GIS application, because the historical hurricane data are qualitative in nature. Thus, the data require special considerations with regard to analysis and uncertainty. The first step to the process is to assign each location in the archive a set of latitude/longitude coordinates approximating the descriptive location. This is an attempt of converting qualitative data into something purely quantita-

tive. Error can occur in four places during the qualitative-quantitative conversion. First, the newspaper report (or other source) may have recorded something wrong. A wrong date, location, or exaggeration of the wind speeds creates an error in the data set. Chenoweth (2006) describes how the archive was carefully instructed to avoid inclusion of these errors when possible. Next, there may be error associated with Chenoweth's interpretation of the newspapers and ship logs. Many of the sources were in other languages or difficult to read. Some may have been vague or confusing. Chenoweth only included the tropical cyclones for which he had reasonable confidence in the source documents. Third, the digitized coordinates are only an attempt to approximate the locations Chenoweth described, but may not be a perfect interpretation. Finally, the broad descriptions of some locations (for example "Gulf of Mexico") make accuracy especially difficult. But this is not the first time that the qualitative historical documents have been quantified for inclusion in modern research. Past research has quantified information that has seemingly no numerical value, such as explanations and gestures (Chi, 1997). Chenoweth (2007) does something similar to the goal of this project, by converting the wind descriptions from chronologies into quantitative values. This research requires the same but for the spatial descriptions.

The archive may provide qualitative descriptions, but it is describing inherently quantitative data- locations (coordinates) and wind speeds. Thus, while the previous paragraph describes this research as a qualitative-quantitative problem, it may be more of a historical GIS application. It is not necessarily the qualitative characteristic of the data that provides difficulties, rather the interpretation of historical information. Historical GIS requires a more error-sensitive approach to data modeling, taking into account the inherent precision and/or accuracy issues of out-dated data sets (Gregory and Ell, 2006). The user must be aware of the error associated with individual data points, while appreciating the value of the set as a whole. Thus, while the digitization of the descriptive locations may not be exact, the track construction process is done in such a way to make use of the valuable data without a need for detailed precision.

Once coordinates are assigned to the qualitative locations, known hurricanes that passed nearby the set of locations are selected. The selected hurricane tracks are modern analogs to the historical hurricane. The modern analogs are averaged using the distance map technique, meaning distance maps are created for each track and they are stacked and averaged. Although instead of using a direct average, an IDW average is used, weighting the tracks that passed nearest the locations the heaviest. A line drawn down the center of the contours of the IDW distance map is the average track. This track is a possible track for the historical tropical cyclone. It is also useful to visualize a pathway for the hurricane by shading in a chosen contour. This provides a wider-ranging track for the historical hurricane and ensures that the locations given by the source documents and Chenoweth are likely included, regardless of misinterpretation during the digitization procedure.

Chapter 3 shows how the procedure is used to generate tracks for the Atlantic tropical cyclones of 1766. Sensitivity of the methodology to changes in event location and event timing are also tested. The chapter shows that historical hurricane chronologies, when combined with a history of cyclone tracks, can provide useful information about the older events that is not directly related to where the original information was gathered. An entire set of

constructed historic tracks should help climatologists better understand long-term variations in tropical cyclone activity. Constructing the tracks may also lead to increased evidence about the hurricane itself, by providing information about additional undocumented landfalls in areas lacking documented history. In the United States this includes states such as Florida, Mississippi, Texas and Louisiana that only have written documents available for “hurricane hunting” since the mid-1800s. Hints from hurricanes uncovered through other documents may help uncover landfalls in these areas under-represented in historical archives. Also, by combining the reconstructed tracks with geologic proxy evidence, historical hurricane chronologies can be enhanced and improved. Some research already involves combining historical hurricanes uncovered through proxies with those of the best track era (Chenoweth and Divine, 2008; Elsner et al., 2008a; Woodruff et al., 2008). This research helps marry the data sets by making the historical data more comparable to the modern record, and encourages increased use of the historical record. As with the best track data set that is continually updated, the historical hurricane tracks can and should be altered upon new-found information.

The result of Chapter 3 is a method for constructing tracks for the historical hurricanes. It is possible to add intensity or other information to the track if reasonable data exist. Chapters 4 and 5 show how hurricane characteristics may be added to an average track.

1.5.3 Objective 3

The third objective of the dissertation is to analyze hurricane risk using a spatial climatology. This is illustrated in Chapters 4 and 5. The focus of Chapter 4 is major hurricanes (Category 3, 4, and 5) and their economic impact on Eglin Air Force Base (EAFB). This requires an average major EAFB hurricane track, which is created using past EAFB hurricane tracks and the distance map technique from Chapter 2. Characteristics of a 100-year event are added to the track, based on information from past hurricanes. These characteristics are run through a deterministic model to obtain loss estimations. Chapter 5 also creates an average EAFB track, but this time for hurricanes of all strengths. Characteristics along the track are compared for warm and cool SST anomaly years to analyze the affects of climate variability on the typical EAFB hurricane.

A 100-year EAFB hurricane. Hurricane winds present a significant hazard for coastal infrastructure. An operational application of the spatial hurricane climatologies is demonstrated through their utilization in risk analysis of hurricane winds. In Chapter 4, the local risk of extreme wind speeds is estimated using a spatial hurricane climatology with a deterministic wind field model. The method is applied to Eglin Air Force Base (EAFB) located in the Florida Panhandle.

First, the distance map technique is used to create an average major hurricane track for a landfall location that represents the worst-case scenario for EAFB. Next, information about local hurricane characteristics is added to the track. Since interest lies in the most extreme hurricanes, the characteristics are those of the strongest hurricanes. The intensity is based on extreme-value statistical model estimates of 100-year wind speeds at locations along the average track based on past nearby hurricanes. This is based off of the technique

demonstrated by Malmstadt et al. (in press). Other characteristics added to the track include radius of maximum winds, central pressure, and the Holland B pressure profile parameter. The track and characteristics together are a track-relative climatology for EAFB.

The climatology is put into a deterministic model in order to estimate economic loss from such an event. Deterministic models take information (such as a set of hurricane characteristics), run it through a series of equations based on physical relationships, and produce the same result each time (as opposed to a stochastic model which contains some room for random variation by providing ranges in the form of probability distributions). HAZUS is the deterministic hurricane model used in Chapter 4. The HAZUS Hurricane Model (HM) deterministic mode consists of five model components: the hurricane hazard model, terrain model, wind load model, physical damage model, and loss model (Vickery et al., 2006a).

The hurricane hazard model simulates the track and wind field of the hurricane. The model, described in detail in Vickery et al. (2000a,b) has been through extensive validations. For example, observed hurricane landfall intensities were compared to those of a 100,000 year simulation. Recently, the hurricane hazard model has been extended to estimate rainfall rates in addition to basic hurricane characteristics such as wind speed, pressure, and translation speed. The model simulates the hurricane track through its entire lifespan, whether or not it makes landfall (Vickery et al., 2006a).

The terrain over which a hurricane travels is a critical component for understanding the hurricanes wind loads and damage. Increased friction associated with a rougher land surface causes a decrease in the hurricanes sustained wind speeds. Peak wind gusts, however, are not as greatly affected by surface roughness (Zhu, 2008). The HAZUS HM uses the terrain model to appropriately incorporate the wind speed-surface roughness relationship. The terrain model contains surface roughness data based on land use land cover (LULC) maps. LULC maps were acquired from two locations: the National Land Cover Data, compiled by the Multi-Resolution Land Characteristics Consortium, and the Florida Water Management District. The maps classify location by LULC type, such as urban, agriculture, wetlands, etc. Estimations of surface roughness were made for each LULC class, allowing for the creation of a HAZUS surface roughness map. The map contains local surface roughness estimations for use in the wind load modeling (Vickery et al., 2006a).

The wind load model has two components- wind pressure modeling, and windborne debris modeling. The wind pressure model uses empirical data from wind tunnel tests to estimate directionally dependent wind-induced pressures (Vickery et al., 2006a). Wind pressures are important due to their strain on buildings, resulting in building damage and causing windborne debris. Windborne debris modeling is a critical component of a physical damage model. HAZUS has two windborne debris models: one for residential debris, and another for roof gravel, which acts as a missile during high winds. The wind load model provides information to estimate wind-induced damage and loss (Vickery et al., 2006a).

Using detailed building stock information, the physical damage model estimates the damage associated with the given wind load. The physical damage model predicts the failure of building components due to progressive failures, internal pressures, duration effects, and changes in wind direction and speed. The model focuses on damage to the exterior of

the buildings, including the windows, roof cover, roof deck, joint failures, and wall failures. Five damage states are used to describe the amount of damage to each of the buildings: no damage or very minor damage, minor damage, moderate damage, severe damage, and destruction (Vickery et al., 2006b). The economic loss model uses the information from the physical damage model to estimate hurricane wind-induced losses. The economic loss model takes into account actual building losses, loss of contents and inventory, and loss of building use (Vickery et al., 2006b).

A major difference between HAZUS and other hurricane wind models is that the ultimate goal of HAZUS is to estimate economic loss. The economic loss estimates are based on census building stock information, which is broken down by census tract. Thus, the HAZUS wind estimates are provided in the same format. HAZUS HM output includes a wind field, tables of damage-related information, and summary paragraphs explaining notable findings. Since the deterministic model provides economic loss, this allows economic loss to be part of the spatial climatology and provides a simple way to analyze changes in loss associated with climate change. Chapter 4 shows the estimated loss associated with a 100-year EAFB hurricane, but the methodology may be altered to model hurricanes of any strength for a chosen coastal location.

The impact of climate variability on the typical EAFB hurricane. Chapter 4 applies local-level hurricane statistics to a deterministic model to obtain wind gusts and economic loss information. This type of approach- using local statistics in a deterministic model- is often overlooked, but has recently been used in a similar project for local storm surge analysis (Lin et al., in press). Instead, many climatologists focus on using global climate models (GCMs), later scaling down to obtain local-scale information. The main issue with this practice is that a model of global scale has difficulty discerning smaller phenomena such as hurricanes.

Another advantage of the statistical to deterministic method is that the model input can easily be altered for further analysis. The aforementioned GCM-downscaling technique involves intricate global information that is not easily changed. The deterministic models often contain complex stochastic data modeling, such as the HAZUS probabilistic mode which is based on a 100,000 year simulation of hurricanes. The easiest way to include climate variability is probably in the statistics rather than attempting to alter global circulation or deterministic models.

In the case of hurricanes, the track can be easily altered for warmer or cooler climates in order to look for climatic affects on hurricanes. The probabilistic estimation provided by HAZUS can provide a similar analysis but is inherent with more vigorous calculations that are not capable of being altered with climate. Chapter 4 shows that the method presented in this dissertation provides results similar to HAZUS but with simpler calculations that may easily be altered to analyze the results of a shifting climate. This is demonstrated in Chapter 5, which compares the characteristics along an average EAFB track during warm and cool SST anomalies.

Similar to Chapter 4, Chapter 5 begins with an average EAFB hurricane track. Instead of having an interest in major hurricanes the interest here is in the typical hurricane and

how it varies with climate anomalies. Using the same methodology as Chapter 4, the typical EAFB hurricane track is created based off of past EAFB hurricane tracks and the IDW-distance map technique. All hurricanes coming within 100 km of the base since 1851 are used to create the track. Next, the average intensity and translation speed of the hurricanes are applied to the average track. When graphed as a profile along the track, the characteristics show the average intensification pattern of the typical EAFB hurricane and the forward motion of the hurricane as it approaches the shore.

Once the characteristics of the average EAFB hurricane are determined, they may be compared to the characteristics of past hurricanes occurring in warm and cool SST anomaly years. The process of obtaining characteristics for the average tracks is repeated, this time using only hurricanes during the warmest and coolest tercile (33%) of Caribbean SST years since 1951. The average translation speed and intensity of the warmest and coolest years are compared, providing information about how SST affects the typical EAFB hurricane. As in Chapter 4, the methodology may be easily repeated for a different coastal location.

1.6 Document Organization

The remainder of this document discusses these three objectives in detail. Chapter 2 explains the construction of spatial hurricane climatologies, and Chapters 3–5 describe three applications of the methodology in hurricane climatology research. Each of these chapters (2–6) are publications submitted to a separate journal or book, so there is some overlap in definitions and methodology descriptions. The titles of the chapters reflect the names of the publications. The coauthor(s) for the publications are also listed at the start of each chapter. Finally, Chapter 6 discusses the outcomes of the dissertation and other possible applications for spatial climatologies in hurricane research.

Funding for individual parts of this dissertation are noted on the first page of each chapter. The speculation and opinions expressed in such chapters are those of the author(s) and do not necessarily reflect those of the funding agencies. All statistical analyses were performed using the open source software environment R (<http://www.r-project.org>).

CHAPTER 2

USING DISTANCE MAPS FOR POLYLINE AVERAGING

A version of this chapter of the dissertation will be submitted to the *International Journal of Geographical Information Science*. The coauthors on the paper are Dr. Victor Mesev and Dr. James Elsner. This chapter introduces a technique for averaging polylines, which is useful for gaining understanding of the spatial behavior of hurricanes. This paper describes two specific areas in hurricane climatology where the technique may be helpful. These ideas are described in detail in Chapters 3, 4, and 5.

2.1 Introduction

Hurricane data are gathered every six hours during the storm's lifespan. The data include intensity, size and location information. When plotted, these observation points show the location of the storm at six-hour increments. "Connecting the dots" of the observation points creates a hurricane track. The track itself is a polyline, or a set of connected line segments.

Manipulating or analyzing polyline sets is difficult due to the lack of technology created for the analysis of tracks (Wentz et al., 2003a). Polyline data provide a challenge in geographic data analysis and representation (O'Sullivan and Unwin (2003) discuss this in some detail), especially in large quantities. Geovisualization procedures may be used to explore the behavior of a large set of polylines (Siirtola, 2000). Polyline averaging is an example of a geovisualization procedure that may be useful for polyline sets by summarizing the data in a simple format. A real-world application could be averaging animal migratory patterns to obtain information about the spatial behavior of a particular species.

This chapter is not the first to address polyline averaging, but it is unique in that it addresses polylines in a spatial plane. Polyline averaging has previously been used for the geovisualization of parallel coordinates (PCs). PCs are sets of polylines providing two-dimensional visualization of multivariate data (Inselberg and Dimsdale, 1990). PCs have been used for exploratory visual analysis of hurricane climate data (Steed et al., 2009) and health statistics (Edsall, 2003). While PCs are useful for visualizing large data sets in a space-efficient and interactive manner, they too may consist of an overwhelming number

of lines. This causes difficulty differentiating between polylines. In this case it may be useful to view the trend of the set of polylines, rather than the entire PC set. Siirtola (2000) describes a way to geovisualize a set of PCs using an average polyline. Averaging provides information about the overall behavior of the data set in a simple way. A benefit of averaging is that it is less computationally demanding than other geovisualization methods, such as hierarchical clustering, and provides a dynamic, interactive approach to data visualization (Siirtola, 2000).

PC averaging is relatively simple because a set of PCs consists of straight line segments with an identical range of values. Geographic data, on the other hand, are often line segments of varying lengths and ranges scattered throughout space. Unlike PCs there is no common starting point or connections between the polylines. Similar to PCs, averaging spatial polylines may be useful to analyze the overall pattern or behavior of the data.

The goal of this chapter is to provide an algorithm for averaging polylines over space. The method employs what is referred to as a distance map. Distance maps were used as early as 1944 to assess the average distance between farms across the United States, thereby reflecting farm distributions over space (Mather, 1944). Euclidean distance maps have been used in geographic research as part of modeling and geovisualization techniques. Specific examples include examining the shortest paths between points, cluster analysis, and skeletonization (Danielsson, 1980; Russ, 1989). More recently distance maps have been used in GIS for risk analysis of natural disasters (Chen et al., 2006). Most often, the term distance map refers to a map of gridded values. The value of each pixel is the distance from that location to the closest pixel with a value of zero (Hirata, 1995). The method presented here uses a similar idea, where the polylines have a value of zero and the value of each pixel is its distance to the polyline following the shortest route.

Section 2.2 presents the technique of averaging polylines using distance maps. First, a random set of polylines is generated. A distance map is created for each polyline, showing the shortest distance from that line to each point in the map. Next, the distance maps are stacked and averaged to create an average-distance map. The map is displayed as contours of average distances in units of x . A polyline digitized down the center of a chosen threshold contour is considered the average polyline. Section 2.3 highlights the utility of the polyline-averaging technique in hurricane climatology research. This involves an enhanced methodology that employs inverse-distance weighted averaging, and shows the relevance of the method in modern GIS applications, such as historical and qualitative GIS. A summary and conclusion are in Section 2.4.

2.2 Methodology

This section describes an algorithm for averaging a set of polylines. The procedure is detailed in Figure 2.1. The example shown here describes the procedure for three polylines with a range of $[0,1]$. Each polyline has a value for x at every $0.01y$, where $x = y + a$, and a is normally distributed with a mean of 0 and standard deviation of 0.1. It is useful to envision the set of polylines as the tracks of three skiers going down the same slope. The

goal of this section is to find the average track that the skiers take down the mountain.

The first step to polyline averaging is converting each polyline into a distance map. The maps are raster or grid data files with a distance value associated with each position. The value at any point on the map is the distance from that point to the polyline at its closest passing. The line has a value of zero and the values increase as you move farther away. Each polyline has its own distance map with its distances displayed as a series of contours. The contours can be thought of as buffers of various distances around the polyline. The distance maps for each skier's track are shown in Figure 2.1b.

The next step to constructing an average polyline is to average the set of distance maps. The values on the maps can be averaged using simple map algebra. The distance maps are stacked by aligning them according to their similar locations. Then, for each particular location on the distance map, the distance values of the three maps are averaged. The average distance values are mapped on a contoured average distance map. Each point on the map is the average value of all of the distance maps at that point. In other words, the contour values indicate the average distance from that point to each polyline in the set. Areas of smaller distance values represent the most agreement between the polylines, and a value of zero means all of the polylines intersect at that point.

For the ski-track example, my interest is in the average path the skiers took down the slope. The three individual distance maps are used to create an average-distance map of the skiers' tracks. The average-distance map of the tracks is shown in Figure 2.1c. A value of some number v on the distance map indicates that the three tracks are, on average, v units of x away from that point.

Next, the average-distance map is used to construct an average polyline. First, the range of the line must be chosen. In other words, for what approximate range of y values does the average line make sense? Similar to the parallel coordinate example, this example uses a restricted range ($[0,1]$), making the selection of an appropriate range simple. This is not always the case with physical phenomena and the range selection is sometimes a subjective parameter. The physical mechanism determining the range of the skiers' tracks is the top and bottom of the ski slope.

After a range is chosen it is used to determine the threshold contour. The threshold is the smallest closed contour that covers the entire range. As shown in Figure 2.1c, the contour threshold for the sample polyline set is 0.05, as it is the smallest continuous contour over the selected range.

Finally, the average polyline is digitized down the center of the threshold contour. The average polyline can be thought of as the valley of the contour lines, or the least-cost route if the distance map is viewed as a cost-density field (Wentz et al., 2003b). Figure 2.1d shows the average track together with the three individual ski tracks. Here the line is manually drawn but the process may be automated depending on the software being used.

An additional consideration for the average polyline construction is the detail of the polyline's behavior, determined by the length of the digitized line segments. The lines segments for the ski slope example are digitized to reflect the nature of the data, which are long linear segments. Some spatial polylines such as hurricane tracks, on the other hand, consist of relatively smaller line segments, so the average polyline reflects this level of

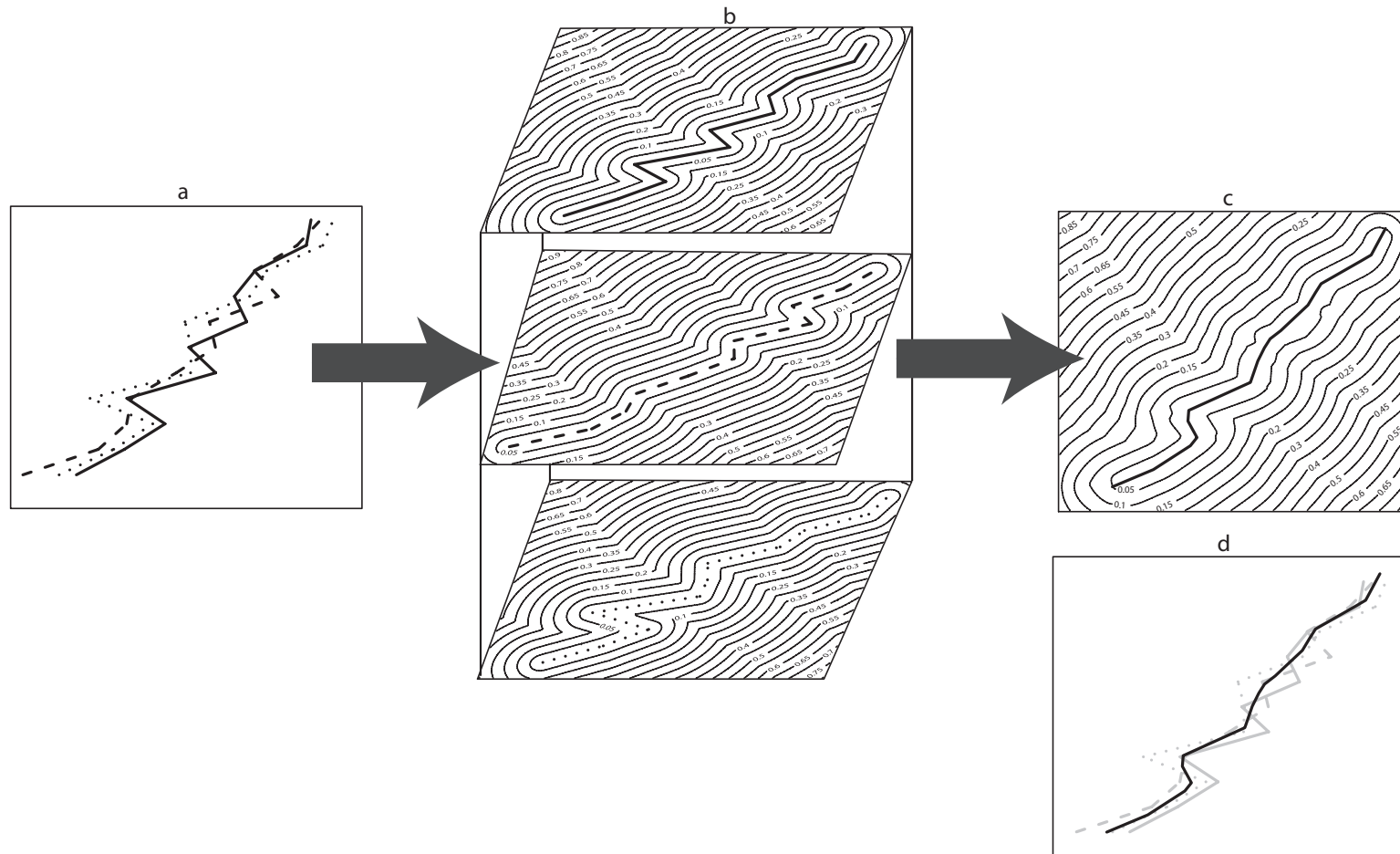


Figure 2.1: Steps for polyline averaging using distance maps. a) Three polylines to be averaged. b) A distance map is created for each polyline. Contour values are the shortest distance from that point to the polyline in units of x . c) The distance maps are averaged, creating an average-distance map. An average polyline is digitized down the center of the contours of the map. d) The average polyline (black) is a geovisualization of the original set of polylines (grey).

detail. Section 2.3 outlines applications of the distance map polyline-averaging technique in hurricane climatology research.

2.3 Application in Hurricane Climatology Research

Hurricane tracks are an example of spatial polyline data. Hurricane data are recorded as observation points at a given time interval, but the storm itself travels along a continuous track across space. Due to the complexity in spatial line data analysis, hurricane tracks are often summarized as counts within a chosen area. For example, Zandbergen (2009) uses GIS to analyze the spatial patterns of hurricane tracks to evaluate the local exposure to various hurricane intensities. The analysis lies heavily upon the cumulative number of tracks, treating the hurricanes as count data. Spatial hurricane information is often obtained through clustering techniques or other methods that group similar storm tracks.

The distance map averaging technique presented in this chapter provides the opportunity for a more geographically-sensitive approach to a spatial hurricane climatology. This section outlines two uses for the distance map methodology in hurricane climate research. First, distance maps are used to determine an average hurricane track affecting a specific location. Then distance maps, in combination with information about past hurricanes, help fill in the gaps of historical hurricane data.

2.3.1 Averaging Hurricane Tracks

A hurricane climatology, as discussed in Chapter 1, is used to describe the typical hurricane affecting an area. This may include the intensity, size, and return rate of the hurricanes, but usually lacks extensive spatial information. The path of the typical hurricane is a useful addition to a hurricane climatology. One way to construct a typical track for an area is by averaging past tracks that made landfall nearby. For example, what is the typical hurricane track affecting Galveston, Texas? This can be determined using the distance map averaging technique.

The first step towards constructing an average Galveston hurricane track is collecting prior Galveston hurricane information. Hurricane data are obtained from a version of the Hurricane Database (HURDAT) maintained by the National Hurricane Center with hourly-interpolations of location and intensity for tropical cyclones in the North Atlantic basin from 1851–2009 (as described by Jagger and Elsner (2006)). The hurricane track is a polyline connecting the hourly location estimations. Major hurricanes (Category 3 or higher on the Saffir Simpson Hurricane Wind Scale) are the most dangerous threat to the coastal location, so I will focus on these intense storms (wind speeds $\geq 50 \text{ m s}^{-1}$).

The ten major hurricanes tracking nearest to Galveston, Texas are selected from the data set (Figure 2.2). The selected hurricanes are referred to as analogs. These track analogs are used to find the typical major hurricane track to affect Galveston. The analogs are ranked by their closest passing to Galveston, evident by their shading in Figure 2.2. The darkest tracks are those that passed nearest the city. All of the analogs maintained major hurricane

intensity within 100 km of Galveston.

A distance map is created for each track analog as shown in the previous section. The maps are in the Mercator projection so distances are slightly exaggerated to the north where the earth's curvature is not reflected in the distances between lines of longitude. This should not affect the averaging outcome in the range of latitude used for the hurricane track constructions. Next, the distance maps are averaged. In order to show the climatological behavior of hurricane tracks relative to Galveston, the tracks that have passed nearest the location (the darkest tracks in Figure 2.2) may be considered more important than those farther away. This can be accounted for in the map algebra. Instead of taking the average of the distance maps, an inverse-distance weighted (IDW) average is used.

The IDW average is modified by a distance-decay parameter to adjust for diminishing importance with increasing distance. The formula for the average distance map ($D(\mathbf{s})$) using IDW is

$$D(\mathbf{s}) = \frac{\sum_{k=1}^{10} w_k D_k(\mathbf{s})}{\sum_{k=1}^{10} w_k}, \quad (2.1)$$

where $w_k(\mathbf{s}) = \frac{1}{d(e, t_k)}$ and $d(e, t_k)$ is the great-circle distance from the track to Galveston. This weights the nearest tracks more heavily than those further away, allowing them to have more influence on the average track. Since an IDW average is used, the entire database of tracks may be used in the averaging rather than selecting only the closest few. Those that are farther away will have little affect on the track due to the distance decay parameter. However, it benefits to use the smaller sample since it is computationally simpler with nearly identical results. Chapter 4 shows the affect of using an increased number of track analogs.

The IDW-average distance map of the major Galveston hurricane tracks are shown in Figure 2.3, with distances shown in contours. The contours form a bullseye pattern around Galveston since all of the tracks have that area in common. The distance values then increase moving in any direction from the city. The contour gradient is greater latitudinally than longitudinally because the tracks are more similar in the north and south direction.

The average distance map can be thought of as the distance map of an average track. The difference between the average-track distance map and the original set of distance maps is that the average track does not have a value of zero. Instead the average track is a line down the smallest values of average distance. The line is drawn through a chosen range of values. In this case the data have no defined range, so choosing the range of the average polyline is not as simple as the ski track example. The line can be drawn through the range of the entire data set, but this causes a problem where one track extends much farther in either direction. Also, there is likely little interest in the hurricane track far north where the hurricanes have significantly decayed and perhaps transitioned into extratropical cyclones. For such a case, an appropriate range and threshold contour are determined based on the intent of the procedure. For example, perhaps interest is in typical Galveston hurricane movement across the Gulf of Mexico. Then the range is the Gulf of Mexico and the contour threshold is chosen for this range.

In this instance, the 4° contour is the smallest contour that covers the range of interest.

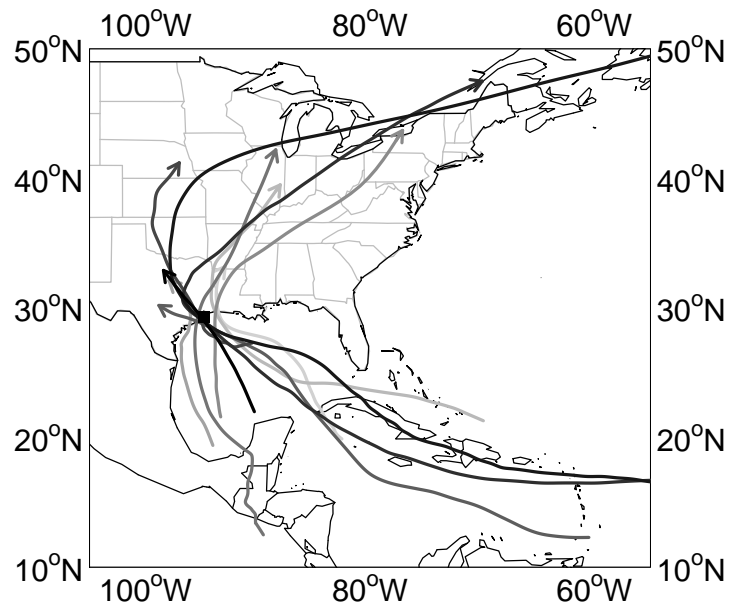


Figure 2.2: 10 major hurricane tracks passing nearest Galveston, Texas, 1851–2009. All hurricanes reached major hurricane status (wind speeds $\geq 50 \text{ m s}^{-1}$) within a 100-km radius about Galveston. The shading of the tracks represents the distance of their closest passing to Galveston; the darker tracks having passed nearest the city.

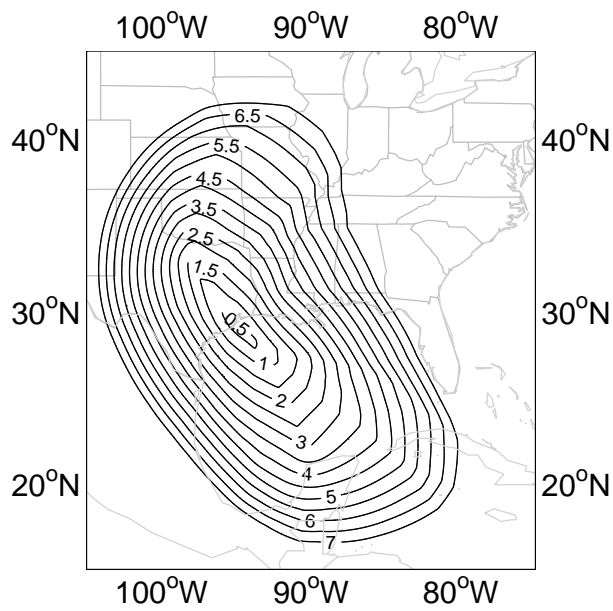


Figure 2.3: IDW average distance map of the major Galveston hurricane tracks shown in Figure 2.2. Contours are lines of average distance and shown in degrees of latitude. Hurricanes passing nearest Galveston (the darkest tracks in Figure 2.2) are weighted most heavily.

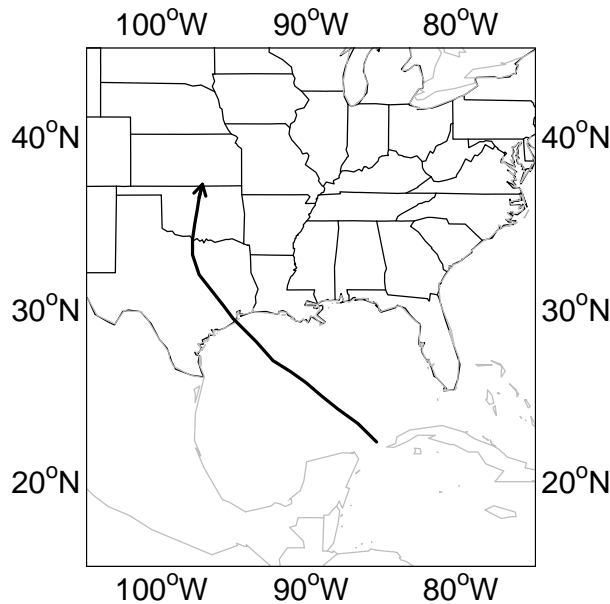


Figure 2.4: The average major Galveston hurricane track. The track is based off of the IDW-average of the ten closest major hurricanes from 1851–2009.

The average track is digitized down the center of this contour (Figure 2.4). The track shows that the average hurricane arrives at Galveston after traveling between Cuba and the Yucatan Peninsula and through the Gulf of Mexico.

The average track adds a spatial dimension to a Galveston hurricane climatology. It can be enhanced by adding the typical hurricane characteristic along the track, which can also be gathered from past hurricanes. Adding such characteristics to the track creates a multi-dimensional Galveston hurricane (Scheitlin and Elsner, 2010). This hurricane can be modeled in a deterministic loss model to estimate the wind profile and economic loss associated with the hypothetical hurricane (Chapter 4). This adds economic loss estimates to the Galveston hurricane climatology. The process of applying statistical information to deterministic models is seen in other recent local-scale hurricane climate projects Lin et al. (in press), and provides a resolution not possible in global climate models.

2.3.2 Constructing Historical Hurricane Tracks

The previous section describes how to characterize the typical hurricane affecting an area by finding an average track. The average track is based on past hurricanes that passed nearby since 1851. Data of this temporal extent are sufficient for this purpose, but difficulties arise with attempting to model long term hurricane trends, such as in climate change

research, using ~ 150 years of data. Hurricane climatologists have taken interest in expanding the data set by reconstructing historical (pre-1851) hurricanes using geological proxies and historical documents. Historical documents begin to uncover possible tracks of past storms. Multiple records of one hurricane may be found in various sources, providing a paper trail of reports across the hurricane's track. For example, Chenoweth (2006) contains a list of historical hurricanes, each one associated with one–four qualitatively-described locations. The archive is discussed in detail in Chapter 3.

One of the goals of this dissertation is to construct a continuous track for a historical hurricane by filling the gaps between documented reports. This is similar to a space-time geography problem where different algorithms are used to create continuous tracks for moving objects where there is missing data (Wentz et al., 2003a). Hurricanes, however, are a special case because it is known that they move in climatological patterns. I propose filling in these gaps of historical documents with help of the distance map averaging technique and information from known hurricane tracks.

Hurricanes provide a unique example because we know that they take regular paths across space relative to the current climate conditions (Elsner, 2003). Therefore, hurricanes striking similar places may have similarities in their paths. For many of the archived historical hurricanes only two locations are known along the track. Past hurricane tracks that have affected similar locations can provide more information about the behavior of the historical storm in question.

This section details how the distance map technique can be used to construct a historical hurricane from the Chenoweth (2006) historical hurricane archive. Storm 25 is used as an example. Historical documents such as ship logs and newspapers place the hurricane at Jamaica and Louisiana in September 1722 (Chenoweth, 2006). The first step to reconstructing the historical event is representing these locations with appropriate latitude and longitude coordinates. The methods for doing so are provided in Scheitlin et al. (2010) and described in Chapter 3. The method depends on the type of location given. Jamaica, being an island, uses Method 4 and the centroid of the island is used to represent the location. Louisiana uses Method 3 for states, and the centroid of the Louisiana coastline is used. The coordinates used to represent these locations and all other locations in the Chenoweth (2006) archive are listed at myweb.fsu.edu/jelsner/extspace/ChenowethArchive.csv. Using these coordinates in conjunction with information from known storm tracks, a likely track for the historical hurricane is created.

The next step is to gather analogs for the historical event. The ten hurricanes passing nearest Jamaica and Louisiana from 1851–2009 are selected. The hurricanes are ranked by their distance from the coordinates used to represent Jamaica and Louisiana. The distance is calculated by averaging the distance of the hurricane's nearest passing of the two locations. Figure 2.5 shows the two locations and the ten nearest-passing hurricanes. The darkness of the track shading indicates the tracks rank in distance, the darkest tracks passing nearest the points. Each hurricane averaged less than 100 km from the points.

Next, distance maps are created for each of the ten hurricanes. The distance maps are stacked and IDW-averaged according to the corresponding hurricane's distance from the two locations. Thus, the black track in Figure 2.5 has the most weight on the average

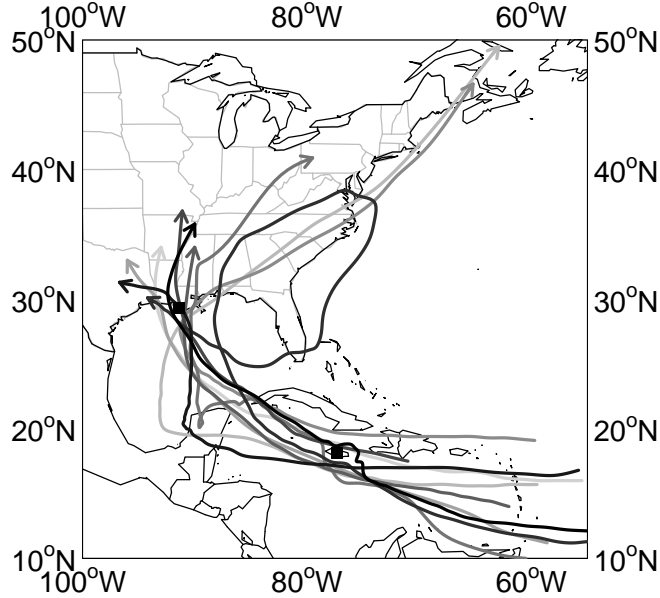


Figure 2.5: Ten hurricanes from 1851–2007 passing nearest the points representing Jamaica and Louisiana. The location of the points is based on the methods described in Chapter 3. The darkest tracks passed closer, on average, to the two points.

distance map. Contours of the average distance map are shown in Figure 2.6. The average distance map can be thought of as the distance map of the reconstructed historical hurricane.

Figure 2.7 highlights a portion of the IDW-distance map encompassing distances within the three degrees longitude contour. This depicts a realistic pathway for the historical storm based off of known hurricane tracks. This is a meaningful way to look at the historical hurricane for two specific reasons. First, as in most historical GIS applications, there are errors inherent in the data. Viewing the hurricane as a pathway accounts for these errors in some way, by showing that the hurricane likely took some route through the pathway. Also, searching for more geologic or documented evidence of the hurricane in the pathway area may uncover the hurricane's affects or undocumented landfalls that could be added to the chronology and help create a more accurate track.

The track for the historical hurricane may be digitized down the center of the average distance map. The hurricane likely did not follow this exact track, but the procedure helps us visualize hurricanes uncovered in historical documents, provide additional possible landfall points, and conforms historical hurricane data to the modern tropical cyclone data sets. An entire set of tracks provides insight into hurricanes prior to the American Industrial Revolution, and can help hurricane climatologists uncover long-term hurricane

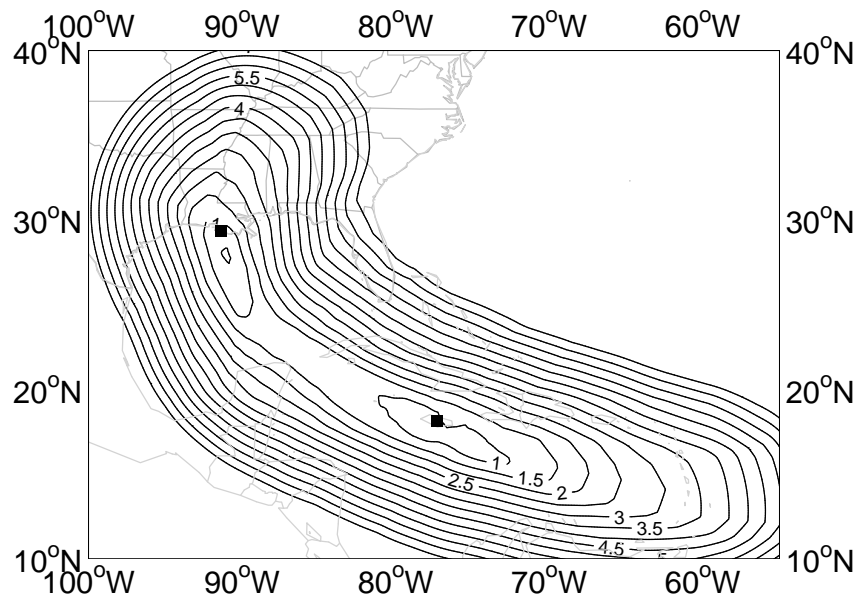


Figure 2.6: Average distance map of hurricanes passing nearest Jamaica and Louisiana. Contours are degrees of latitude.

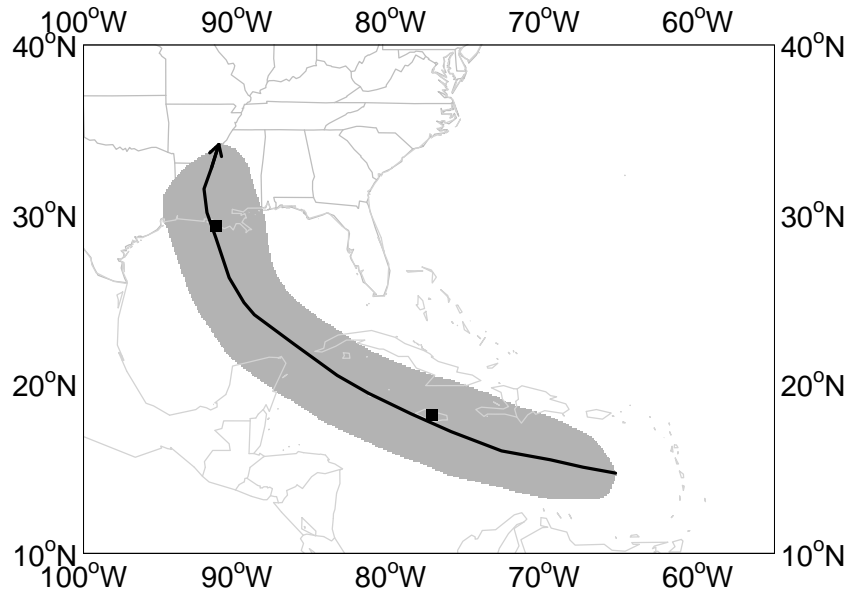


Figure 2.7: The average track and pathway of hurricanes passing near Jamaica and Louisiana. This is a probable pathway and track for Storm 25 in the Chenoweth (2006) Archive.

patterns. The methodology for constructing historical hurricanes is presented in detail and further analyzed in Chapter 3.

2.4 Summary

Hurricane tracks are an example of spatial polylines. Because of the large number and nature of the data they may be difficult to visualize, analyze and manipulate. Averaging is one way to summarize a set of polylines. This chapter introduces a way to average polylines using distance maps. This method is preferred because it is relatively easy to understand, maintains real-world units, and has few free parameters.

Depending on the data, the technique is useful as a geovisualization of a complex data set or something as specific as creating an average hurricane track for a coastal location. The average hurricane track for a location based on past hurricanes is a spatial hurricane climatology- adding a spatial dimension to the hurricane climatology. Two applications of this technique for hurricane research were introduced in this chapter and are described in more detail in the upcoming chapters.

Section 2.3 shows how the distance maps can be manipulated using different types

of math algebra. In the hurricane example, an IDW average is used to weight the tracks relative to their importance. Other mathematical functions may be applied depending on the purpose for the geovisualization. For example, the difference between distance maps can be used to show annual differences in animal migratory tracks.

One way the polyline averaging technique may be improved is by providing error estimation for the average polyline. Uncertainty information could be obtained by using an additional procedure such as polyline similarity testing (Kuijpers et al., 2006). This technique can be used in two ways. First, the similarity between the set of polylines will provide information regarding the relevance of an average polyline. If the polylines have little similarity then the average polyline may not have physical relevance. After an average polyline is created, polyline similarity testing can provide information about the difference between the average polyline and the original set of polylines. This provides the user some information about the uncertainty associated with the average. Calculating the standard distances from the average polyline to the polyline set is another way to obtain similar information. Such testing should also help determine a reasonable range of values for which the average polyline should be digitized. Additionally, it would be useful to estimate the error associated with utilizing the Mercator projection and determine if an alternate projection would more accurately depict the map distances.

The remainder of this dissertation discusses the use of distance-map averaging in hurricane research. The concluding chapter describes more examples of where the technique may be employed in hurricane climate research.

CHAPTER 3

TOWARD INCREASED UTILIZATION OF HISTORICAL HURRICANE CHRONOLOGIES

This chapter of the dissertation is a version of a paper of the same title, published in the *Journal of Geophysical Research* in February 2010 (Scheitlin et al., 2010). The coauthors on the paper are Dr. James Elsner, Jill Malmstadt, Robert Hodges, and Dr. Thomas Jagger. The relevance of this work to the dissertation as a whole is that it uses the methodology presented in Chapter 2 to reconstruct historical hurricane tracks. The work was supported by the U.S. National Science Foundation (ATM-0738172) and the Risk Prediction Initiative (RPI08-2-002) of the Bermuda Institute for Ocean Sciences.

3.1 Introduction

Recent destructive hurricane seasons have led to an increased awareness of the field of hurricane climatology. While the comprehension of hurricane climatology grows with each related research publication, there are arguments as to the accuracy of long-term variability assessment due to temporal brevity of hurricane records (Chenoweth and Divine, 2008). Since these long-term trends provide a basis for understanding the climate change-tropical cyclone relationship, it is important that strides be made toward improving the quality and temporal extent of the North Atlantic tropical cyclone data set. In fact, the record of past hurricanes is among the most important means to evaluate the hurricane hazard, so extending the data base of hurricanes by several hundred years is valuable.

The data set used most often by hurricane researchers is the Hurricane Database (HURDAT), maintained by the National Hurricane Center. HURDAT contains data for all observed tropical cyclones from the Atlantic Ocean, Gulf of Mexico, and Caribbean Sea since 1851. The HURDAT record (also known as the best-track record) is continually updated and re-analyzed in order to make it consistent and accurate. However, the relatively short time period of tropical cyclone data sets limits the ability of climatologists to determine long-term (50–100-yr) variability. In response to this challenge researchers have begun using methods to uncover hurricanes from the 18th and 19th centuries.

The purpose of this chapter is twofold: 1) To provide a digitized version of the Chenoweth (2006) historical tropical cyclone list (Chenoweth Archive) and, 2) To illustrate a procedure for estimating the likely pathway of cyclones in the archive. The work is an extension of Elsner et al. (2008a) where geological records of pre-historical hurricanes at a single location over time are compared with the record of modern cyclones. Here it is shown how historical archives of spatial locations affected by tropical cyclones can be summarized across space with the help of a record of modern cyclones. This is done by applying the polyline averaging technique presented in Chapter 2.

Section 3.2 provides a brief description of the Chenoweth Archive and places it in the context of other methods for uncovering past tropical cyclone activity. Section 3.3 lists the methods for digitizing the archive and gives details on how to determine a cyclone path from digitized locations and tropical cyclone analogs from the modern record. Section 3.4 examines the active 1766 hurricane season, and Section 3.5 explains how the methods can incorporate “unusual” historical cyclones as is the case for the fourth cyclone of 1766. Section 3.6 answers questions about the sensitivity of the methodology. Section 3.7 summarizes the research efforts.

3.2 Early Tropical Cyclones

Evidence of early hurricanes can be obtained from proxy data and historical documents. Proxies in the form of coral cores, tree rings, and overwash sediments in coastal lakes can be used to detect hurricanes back through the middle Holocene (Liu and Fearn, 1993, 2000). These proxies are useful in providing information pertaining to centennial- and millennial-scale tropical cyclone variations (Murnane and Liu, 2004). While these proxies may reveal long-term variability in tropical cyclone occurrences, smaller-scale fluctuations over the time period are difficult to discern due to lack of temporal precision.

While proxy approaches provide a glimpse of hurricane activity locally through time, historical documents can sometimes provide clues about the path of hurricanes across space. This chapter focuses on data about early hurricanes uncovered from historical documents. The available time-span and overall quality of these data vary for different regions of the world, with China having the longest history of written documents, spanning the last 3500 years (Louie and Liu, 2003). While written history in North America and the Caribbean begins much later, the additional evidence of tropical cyclone occurrence from written records provides a larger data set for understanding long-term hurricane trends than is provided by HURDAT.

Historical archives are largely qualitative in nature, consisting of descriptions of cyclone location and intensity. Quantifying these data is important to encourage their use in contemporary hurricane research. Chenoweth (2007) provides quantitative interpretations of tropical cyclone intensity for storms affecting the Lesser Antilles and Jamaica. For example, a document which reads “wind very high” is interpreted as an approximate wind speed of 17 ms^{-1} (35 kt). This chapter focuses on the quantification of the locational descriptions, examining one way a historical archive of North Atlantic tropical cyclones

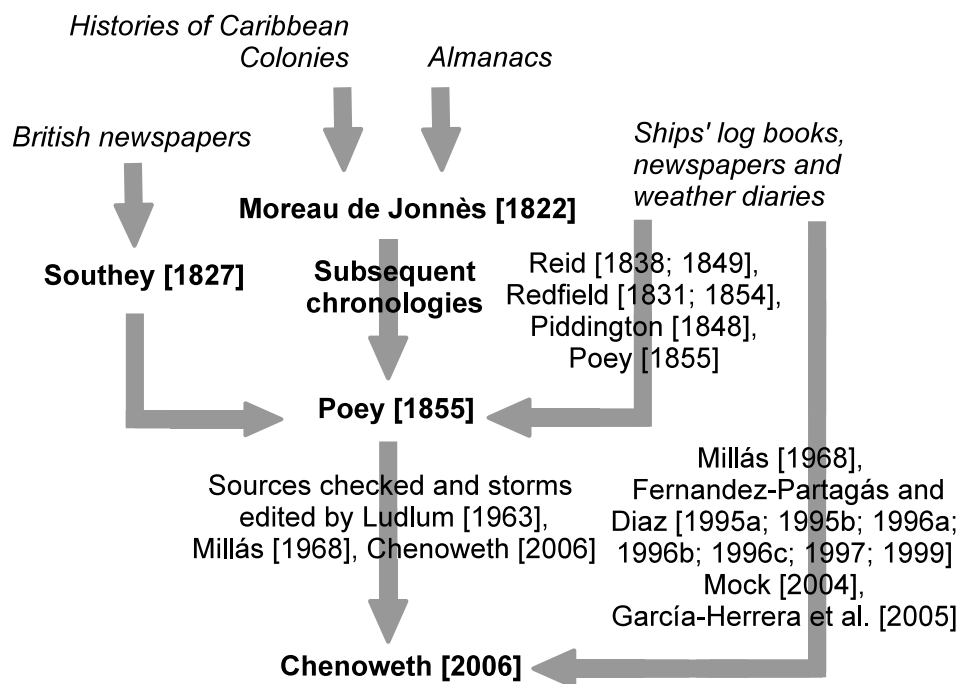


Figure 3.1: Major contributors leading to the Chenoweth Archive. Words in italics denote a source, while bold names represent published tropical cyclone chronologies.

(Chenoweth, 2006) can be used to give more information about tropical cyclone tracks.

3.2.1 The Chenoweth Archive

Examination of historical documents to uncover Atlantic-basin tropical cyclones began centuries ago, with researchers putting in countless hours of work looking through hundreds of thousands of ship logs, almanacs and newspapers (García-Herrera et al., 2004). A schematic of the research that went into the Chenoweth Archive is shown in Figure 3.1. The first attempt towards a chronological list of hurricanes is attributed to Moreau de Jonnès in 1822 (Chenoweth, 2006). The Poey chronology of 1855 is considered the most comprehensive of its time.

In 2006, Michael Chenoweth produced a list of tropical cyclones (inclusive of hurricanes and tropical storms) from 1700–1855 by taking into account all previous historical archives and research. Table 4 of Chenoweth (2006) is a list of the most widely-accepted tropical cyclone accounts, and is what we consider here as the Chenoweth Archive. Chenoweth’s chronology begins in 1700 because logbook records and newspapers are abundant by this time, and most of the tropical cyclones on the Poey list occur after 1700 Chenoweth (2006).

The archive contains 383 published and independently-confirmed tropical cyclones that traversed the Atlantic basin between 1700 and 1855. The Chenoweth Archive is available at www.aoml.noaa.gov/hrd/hurdat/Chenoweth/index.html (Chenoweth, 2006).

A few caveats are in order. This archive is a comprehensive chronology of all previously uncovered tropical cyclones after Chenoweth's careful edits and source checking. It does not contain more recently uncovered cyclones by Chenoweth himself. Moreover, although here Table 4 of Chenoweth (2006) is referred to as the Chenoweth Archive, it does not represent all that is known about these historical events. More information is available with Michael Chenoweth on individual events, especially for some of the later cyclones on the list, but this additional information is not in a digital format at this time.

Table 3.7 lists a portion of the Chenoweth Archive corresponding to the 1766 season. Each cyclone is listed chronologically with a start and end date (referring to the first and last observation of the cyclone), and an associated location of the region affected. Not present in Table 3.7, the Chenoweth Archive also lists whether the cyclone was included in previous chronologies, the number of log books and newspapers checked for validity, and an estimate of whether the affect was likely due to a hurricane or tropical storm for each location.

3.3 Adding a Spatial Dimension

The Chenoweth Archive provides a glimpse into North Atlantic tropical cyclone activity prior to the American Industrial Revolution. This is important in the context of climate change as related to anthropogenic greenhouse gas increases. This chapter introduces an attempt to digitize the Chenoweth Archive for the purpose of making it more useful for researchers. We then use this digitized archive together with the HURDAT record to generate a pathway for each tropical cyclone in the archive, giving a spatial dimension to cyclones that began as newspaper accounts.

The procedure is performed in two steps. First, the Chenoweth Archive locations are digitized. The digitization is done using nine different methods depending on the locational information provided in the archive. Second, modern tropical cyclone tracks are used as location analogs and a likely pathway is found based on the distance of the analog to the archive's locations.

3.3.1 Digitizing the Chenoweth Locations

Each tropical cyclone in the archive is defined by as few as one to as many as four observation locations (events), resulting in a total of 742 events. The average is 2.1 events per cyclone. Since events consist of reports from recurring locales (e.g. Jamaica), less than half of the event locations are unique. The descriptions of the locations range from specific (e.g. latitude and longitude coordinates), to broad (e.g. "New England"). In order to provide a spatial version of the Chenoweth Archive, each of the events are assigned approximate latitude/longitude coordinates (digitized). The following methods were used to digitize the

coordinates depending on the specificity of the description given in the archive:

Method 1. Latitude/longitude coordinates are given: If coordinates are given, these exact coordinates are used to represent the event location. For example, according to the Chenoweth Archive, the second event of Storm 96 affected the location 17°11' N, 69°49' W. Most of these locations are coordinates recorded in ship log books and are therefore located over the ocean. Thirteen percent of all event locations in the archive require this type of digitization.

Method 2. City name is given: If the name of a city is given, either in the United States or international, the latitude and longitude of that city are found using a valid source, such as the United States Geological Survey. For example, according to the Chenoweth Archive, the third event of Storm 98 affected Pensacola, Florida. Eight percent of all event locations in the archive require this type of digitization.

Method 3. State or country names are given: Most states or countries given are coastal areas, likely representing where the tropical cyclone made landfall. Therefore, if a coastal state or country is named, the center of the coastline is used to represent the location. For example, according to the Chenoweth Archive, the second event of Storm 94 affected Texas. Fourteen percent of all event locations in the archive require this type of digitization. If an inland state or country name is given, the event is considered a “special case” (see Method 9).

Method 4. Island name is given: If the event location is an island, the coordinates of the geographic center of the island are used. For example, according to the Chenoweth Archive, the second event of Storm 97 affected Puerto Rico. Twenty-six percent of all event locations in the archive require this type of digitization.

Method 5. Water body is given: If a water body such as a sea, gulf, or bay is listed, the coordinates of the approximate geographic center of the water body are used. For example, according to the Chenoweth Archive, the first event of Storm 94 affected the Gulf of Mexico. Two percent of all event locations in the archive require this type of digitization. Since an ocean is large, it is considered a special case (e.g. the first event of Storm 95 is listed as affecting the Atlantic.)

Method 6. Directional description is given: For some events the location description includes a direction from a land mass, such as “west of,” “off the coast of,” or “near” a given area. For example, according to the Chenoweth Archive, the second event of Storm 93 affected south of Jamaica. We assume that for most of these event types, the effects were felt and reported at the location listed, but the eye of the tropical cyclone did not traverse the area. Instead the cyclone struck a nearby location, which is being described by direction from the area reporting the storm. The average North Atlantic tropical cyclone radius is 3° of latitude as defined by the circular area encompassing relative vorticity values less than $1 \times 10^{-5} \text{ s}^{-1}$ (Liu and Chan, 1999). Therefore, a location listed as “south of Jamaica” is assumed to be within 333 km (approximately

3° of latitude) of the most south-central point of Jamaica. For the purposes here, a directional description is defined as 1° of latitude (approximately 111 km) away from the base point, as farther distances could imply the cyclone is closer to a different land mass that could instead be defined as a distance away from that land mass. Twelve percent of all event locations in the archive require this type of digitization.

Method 7. Coastline is given: If a coastline is listed, the coordinates of the geographic center of the coastline are used. For example, according to the Chenoweth Archive, the fourth event of Storm 55 affected the U.S. Gulf Coast. Two percent of all event locations in the archive require this type of digitization.

Method 8. Portion of an area is given: Many events are described as a specific portion of a political or geographic area. Methods used in this case are similar to those above; the coordinates of the geographic center of the portion of the area are used. For example, according to the Chenoweth Archive, the second event of Storm 129 affected western Haiti, and is therefore represented by the coordinates of the center of the western quadrant of Haiti. Similarly, if the area listed is part of a coastline, the coastline is portioned off and the coordinates of the center of the appropriate quadrant are used. For example, according to the Chenoweth Archive, the second event of Storm 315 affected the Southeast U.S. Coast. Eight percent of all event locations in the archive require this type of digitization.

Method 9. Special Cases: If the location does not fit one of the cases above, it is considered a special case. Some examples include broad areas (e.g. Storm 4 affecting New England) or island chains (e.g. Storm 11 affecting the Lesser Antilles). The coordinates for these locations are chosen following as closely as possible to the methods described in the above cases. Fifteen percent of all event locations in the archive require this type of digitization.

3.3.2 Determining a Probable Pathway

The above methods are applied to all 742 events listed in the Chenoweth Archive. A complete list of all events by date and spatial coordinates is available from myweb.fsu.edu/jelsner/extspace/ChenowethArchive.csv, and in the appendix (Table A.1). Figure 3.2a shows the digitized locations for Storm 275 in the archive, described as affecting Haiti and the northeast coast of Florida. While the locations are not the exact coordinates of the center of the cyclone, one can assume that these locations felt its direct affects, and in most cases the cyclone's eye passed nearby. The coordinates serve as event locations to assist in determining a pathway of the archived cyclones. A straight line connecting the event locations provides what is called a first-order approximation to a possible track.

Additional information about tropical cyclones in the archive can be gained with the help of a track climatology. Previous research has shown tropical cyclones move across the Atlantic in a somewhat predictable manner (Elsner and Kara, 1999; Brettschneider, 2008). However, track patterns fluctuate on annual and decadal time scales (Elsner et al., 2000a).

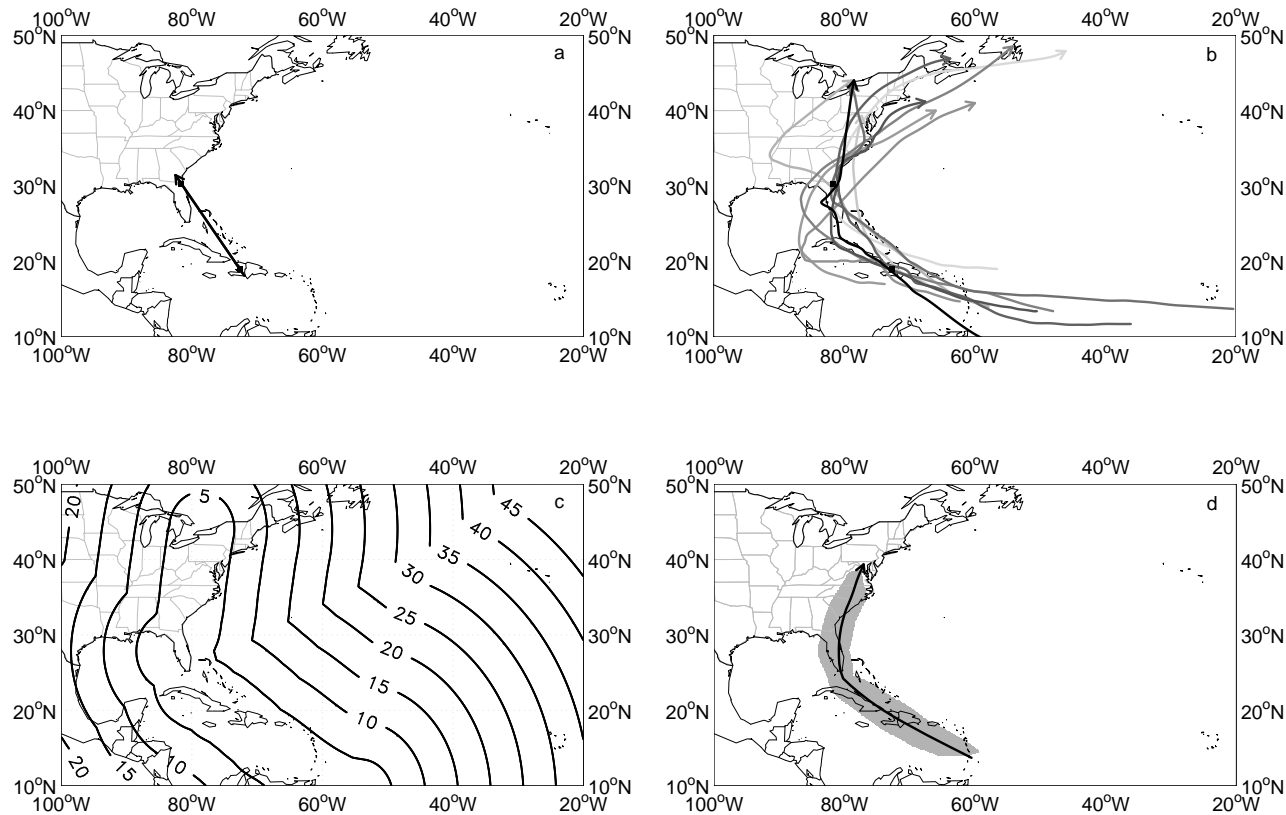


Figure 3.2: Storm 275 in the Chenoweth Archive. a) The two locations mentioned in the archive for Storm 275 and a straight line through them (first-order track track). b) The ten closest tracks (track analogs) to the locations of Storm 275 shaded by average distance to the locations (km) with the darker shading indicating a closer track. c) Distance from any location across the basin to the closest track analog in degrees of latitude. d) Tropical cyclone pathway constructed by a weighted average of the distance grids of all track analogs. The shaded area encompasses a weighted average distance of less than or equal to 2.25° of latitude. A curve through the shaded area represents a possible (second-order) track for Storm 275.

Indeed a seasonal forecast of U.S. hurricane probability requires not only knowing how many cyclones will form, but where they will track (Elsner and Jagger, 2006). Here it is assumed that the same steering flows have influenced hurricanes throughout the centuries and that hurricane tracks have had a similar response to those influences, making it possible to create pathways for historic hurricanes based on known tracks in the modern record. It is further assumed that the data set used here contains a large enough sample of cyclone tracks to represent most possible climate scenarios.

The hourly-interpolated track data (Jagger and Elsner, 2006) are used to find modern tropical cyclones that have passed near the Chenoweth event locations. The higher temporal resolution ensures that cyclones traveling quickly past the event location are not missed. The code used to select modern tracks (and other routines used in this study) is developed within the R package for statistical computing.

Figure 3.2b shows the ten closest tracks (analogs) to the event locations of Storm 275, which was the 3rd known tropical cyclone of 1825, occurring during late September. The ten tracks are ranked according to their average great-circle distance from the event locations (analog rank). While the historical cyclone almost surely did not follow any one of these specific tracks, it likely traversed a similar pathway, which can be represented by a “probable” pathway.

There are various ways to determine a pathway, the one presented here being an inverse distance weighting (IDW) approach. This method is preferred because it weights the modern cyclone tracks based on their inverse distance to the event locations. The IDW approach also has the advantage that it is easy to understand and has relatively few free parameters. Here the ten closest modern tracks are used. As shown in section 3.5, the larger the analog rank, the larger the average distance from the locations so the less weight it has on determining the pathway.

The IDW approach begins by converting each of the modern analogs into a distance grid, the values of each grid point representing the closest distance that point is from the track (Figure 3.2c). The track itself has a value of zero where it intersects the grid. Distance grids (D_k) for all ten modern analogs are then averaged using IDW, so that the average distance grid is weighted towards the modern analog tracks that are closest to the historical storm. The formula for the IDW is given in Equation 2.1, where $d(e, t_k)$ is the average great-circle distance from the event locations (e) to a given track (t_k). Then, from the average distance grid ($D(\mathbf{s})$) a maximum threshold value is chosen that provides an area encompassing the tracks of the closest cyclones on their closest approach to the event locations.

Figure 3.2 shows the tropical cyclone pathway for Storm 275. The pathway is constructed by determining the area enclosing a 2.25° latitude threshold. The threshold indicates that average distances are less than this value within the region. The threshold distance is a tuneable parameter, but here is chosen to provide a small, but spatially continuous corridor that likely includes the event locations. A line is manually-drawn down the center of the pathway provides what is called a second-order approximation to a track.

Storm 275 provides a good example where the second-order track provides a realistic depiction of the hurricane’s movements. While the hurricane was only reported in Haiti

and Northwest Florida, it could have had additional effects over a larger portion of Florida and possibly the Carolinas. Despite this evidence, it would not be surprising if there is no record of Storm 275 affecting the peninsula of Florida, as most of the state was not settled until the early 20th century (Landsea et al., 2004).

3.4 The 1766 Hurricane Season

The procedure outlined in the previous section produces a probable pathway and a realistic track for a hurricane listed as a set of events in a historical archive. While this track is almost certainly not the actual track of the archived cyclone, the probable pathway defines a corridor that bounds an area for realistic tracks based on past climate scenarios.

Figure 3.3 shows the tropical cyclone tracks for the 1766 season based on the method described above. The minimum distances and the threshold for the pathway is listed in Table 3.7. The third cyclone of the season has the smallest minimum distance (22 km), while the fourth cyclone has the largest minimum distance (509 km). The track is manually drawn through the center of the pathway. Longer tracks result from either event locations being dispersed more widely across the region, and/or relatively more similarities between the modern-analog tracks. The start and end points of the track are placed just outside the objectively determined pathway to make them easier to see.

This particular season consisted of one tropical storm and six hurricanes, and would be considered average (in terms of the number of hurricanes) by today's standards. While it is possible there were additional weaker tropical cyclones that remained unobserved, the Chenoweth Archive represents a sample of historical tropical cyclones, especially for areas such as Jamaica and the Caribbean, where historical records are more numerous. In addition to the number of tropical cyclones in 1766, constructed tracks for this season highlight possible uses of the data set.

The seventh recorded tropical cyclone of the 1766 season (Figure 3.3) could have made an additional landfall in central or south Florida. As previously alluded to, Florida tropical cyclone records are scarce prior to the 20th century. Thus it would not be surprising if a storm striking Florida in 1766 went unreported. As the cyclone continued, it is less likely to have hit South Carolina at tropical storm strength or greater, as South Carolina archives are more prevalent and have been examined in detail with no signs of a storm in 1766 (Mock, 2004). Therefore, the probable pathway based on the modern analogs is a good depiction of where the hurricane likely went.

3.5 Unusual Archived Cyclones

While the procedures outlined here can provide pathways for a large portion of historical tropical cyclones in an automated way, a climatologically-based track might not be the most appropriate for cyclones with only a few or no close modern analogs. An example is the fourth tropical cyclone of the 1766 season (Storm 96 in the Chenoweth Archive), described as affecting the Lesser Antilles, 23°45'N 64°03'W, 33°00'N 57°00'W, and finally

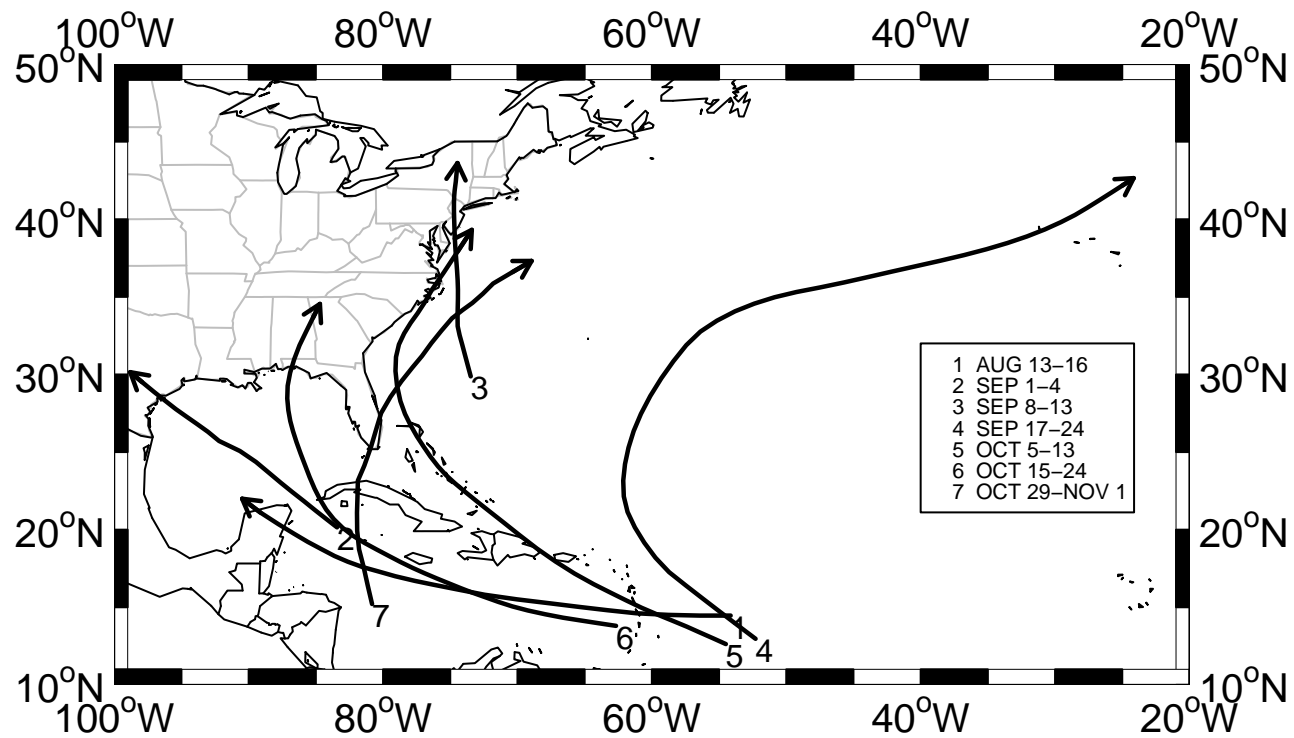


Figure 3.3: Tracks for the 1766 North Atlantic hurricane season. The tracks are based on the cyclones listed in the Chenoweth Archive (Storms 93–99) and the method described in section 3.3 using the thresholds listed in Table 3.7.

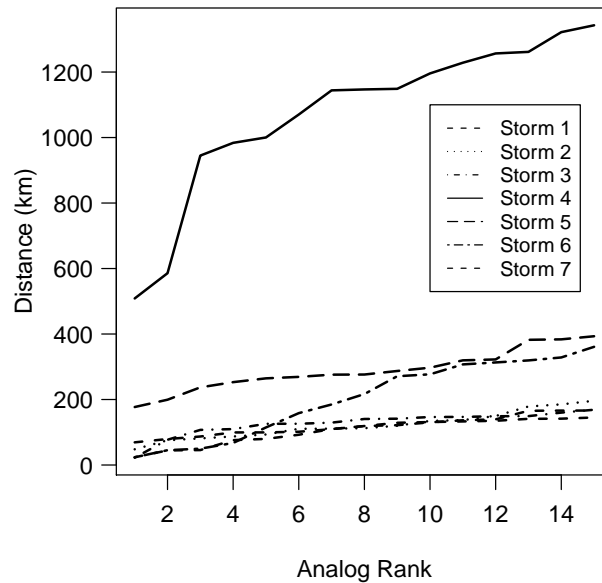


Figure 3.4: Distances (km) of the 15 closest modern analogs to the Chenoweth locations for the seven cyclones of the 1766 hurricane season. Distances increase with analog rank, but relatively rapidly for some cyclones (Storm 4).

the Azores. The event is unusual in that it affected both the Lesser Antilles and the Azores. Also, the event is defined by four locations fairly evenly spaced across the North Atlantic. The unusualness of the cyclone is verified by a search for modern analogs. No recorded modern cyclone hit both the Lesser Antilles and the Azores, and the closest approach of any modern track averages 509 km to the event locations. Figure 3.4 depicts the distance of the 15 closest analogs for the cyclones in the 1766 season, showing that not only does Storm 96 have no close analogs, but the average distance to the location increases relatively rapidly as a function of analog rank.

The first-order track approximation of the Chenoweth events of Storm 96 (Figure 3.5) depicts a reasonable hurricane path, with the missing piece being the curvature of the cyclone. Using the automated procedure and ten analog tracks results in a pathway and track depicted in Figure 3.5b. Note the pathway does not include the Chenoweth event location over the Lesser Antilles (although it does include a portion of these islands). Thus, while some tropical cyclones will be well represented by their second-order track approximation, others need to take into account the actual event locations when creating the pathway. In fact it might make sense to blend the pathways created by connecting the Chenoweth event locations with the pathway generated by the modern analog climatology. This blend represents what is called a third-order track approximation.

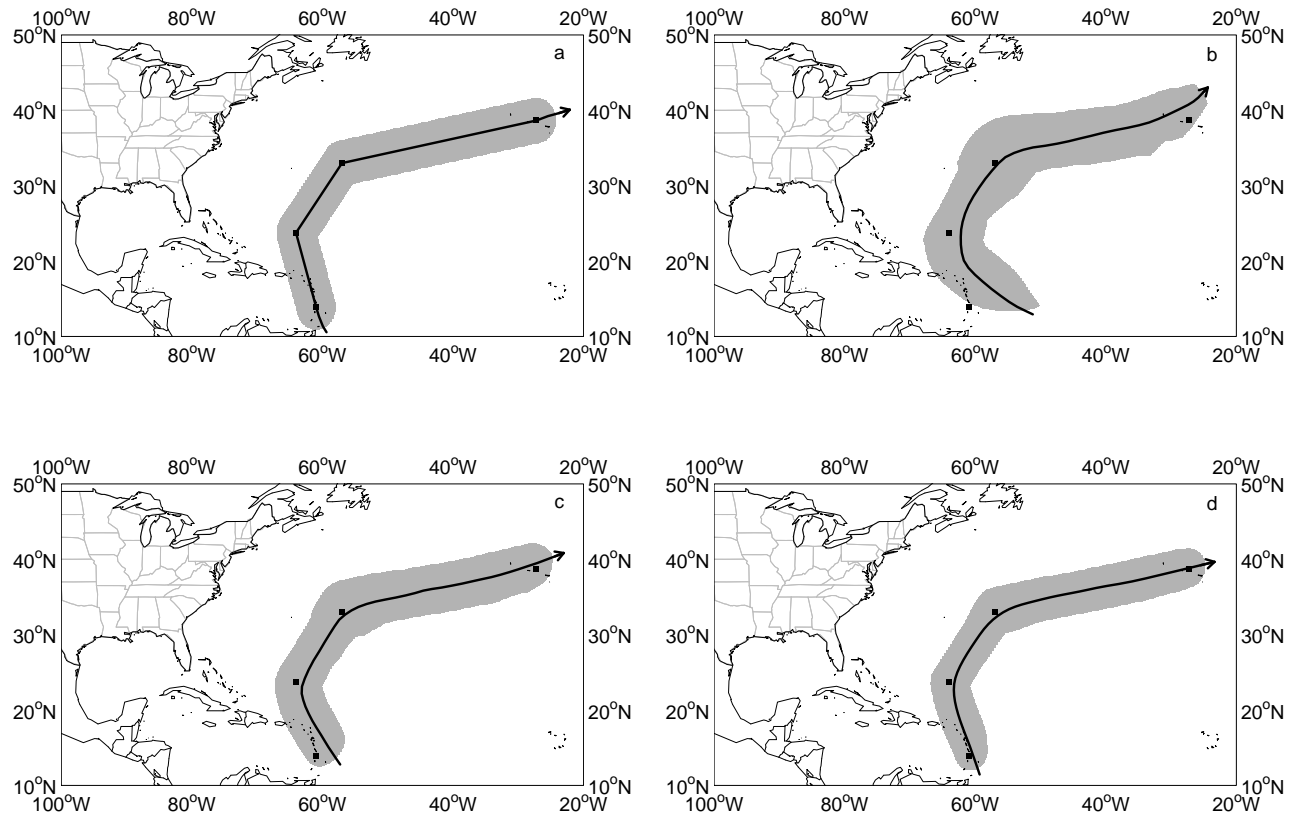


Figure 3.5: Storm 96 in the Chenoweth Archive. a) Connecting the event locations provides a first-order approximation to the track. b) Using the event locations together with ten modern analogs provides a second-order approximation. c) A third-order approximation to the track is obtained by blending the first- and second-order approximations in a 1 to 1 ratio. d) Another third-order approximation using a blend in a ratio of 3 to 1 in favor of the direct track.

Figure 3.5c shows a new pathway, calculated using the second-order track as 50% of the input and the first-order track as the remaining 50% percent. This approximation provides a better fit to the Chenoweth archive locations as the pathway now includes all four of the Chenoweth locations. Another option, shown in Figure 3.5d, uses the first-order track as 75% of the input and the second-order track as 25%. This pathway seemingly depicts the most appropriate rendition of the historic event, with the track down the center of the pathway passing all of the event locations within a reasonable distance. The weight ratio of the first-order and second-order tracks used in the third-order approximation will vary depending on the specific event. Thus in cases where the modern climatology provides less information relative to the historical event locations the procedure can be modified to include a direct track between the event locations and a “tuning” parameter that weights the analog tracks relative to the direct track.

3.6 Sensitivity of the Methodology

Here the performance of the above methodology (second-order approximation) is examined under three experiments. First, pathways are constructed for the same event by leaving out a location in the archive. Second, the methodology is applied to a few known hurricanes where the information about the hurricane is degraded to the level available in the archive and a comparison of the pathway is made with respect to the known track. Third, a pathway is constructed using only hurricanes that correspond in time (within a month or so) of the event time and compared with a pathway constructed using hurricanes over a different part of the season.

3.6.1 Omitting an Event Location

Here the sensitivity of the methodology is examined by omitting event locations. The archived cyclones are associated with one to four event locations, each location being a part of the methodology to construct the probable pathway. The number of locations for each cyclone affects the construction of pathways. For example, here four different pathways for Storm 96, the fifth storm of the 1766 hurricane season, are considered.

Figure 3.6a shows the pathway created using all three localities provided in the Chenoweth Archive (Lesser Antilles, Puerto Rico, and off the South Carolina coast). The pathway in Figure 3.6b is created using only the first two locations, omitting the point off South Carolina. This pathway is shorter and does not contain the final event location. The third attempt, shown in Figure 3.6c, utilizes the first and third locations, omitting Puerto Rico. The pathway created here, however, still contains Puerto Rico and resembles the pathway in Figure 3.6a which uses all three points. Finally, Figure 3.6d depicts a pathway constructed using only the Puerto Rico locality. This pathway does not contain either of the omitted locations, although it does contain part of the Lesser Antilles and leaves open the possibility that the historical cyclone approached South Carolina. The best case scenario comes from a pathway with the largest number of localities for the particular cyclone. However, when

data are especially limited, the most productive localities in terms of creating a realistic track are those farther separated across space.

3.6.2 Applying the Methodology to Recent Hurricanes

Here the sensitivity of the methodology is examined by how well known tracks fit the estimated pathway. First, a known recent hurricane track is marked only by three locations based on its actual track and common locations in the Chenoweth Archive. These locations are then used to construct a pathway following the above methodology, excluding the track of the particular cyclone of interest from the analog search.

Figure 3.7a shows the pathway created for Hurricane Charley of 2004 using the event locations of West of Jamaica, Western Cuba, and off the South Carolina coast. The actual track of Charley is also shown. The methodology does well as there appears to be a good spatial correspondence between the pathway and the track. On the other hand, Figure 3.7b shows the same for hurricane Dennis of 2005. The event locations used to create the pathway are North of Jamaica, Western Cuba, and Pensacola, Florida. The spatial correspondence in this case is less precise as the pathway runs through the Greater Antilles and across the northern Gulf coast, while the track of Dennis is south of Puerto Rico and Hispanola.

3.6.3 Filtering the Analogs by Time of Year

It is well known that tropical cyclones track in varying directions depending on the time of year (Elsner and Kara, 1999). A hurricane originating over the Gulf of Mexico or the western Caribbean during the early or later part of the season will tend to have a considerably greater northward component to its track compared to one originating over the central Atlantic during September. Thus it may be beneficial to restrict the search for analogs to those cyclones that occur near the same time of year as the historical hurricane. This may be especially helpful for those historical cyclones with less data, since the time of year may give more information about the storm's behavior.

Figure 3.8 provides an example using Hurricane Gilbert of 1988. The only location used to create the pathway is the island of Jamaica. Since Gilbert occurred during September, the left panel shows the pathway constructed using only analogs from the months of August and September (middle two months of the season). In contrast, the right panel shows the pathway using analogs from October and November. As expected, the pathway corresponding to the mid-season analogs better resembles the cyclone's actual path, depicting the westward component common in this part of the basin during this part of the season. The pathway corresponding to the late-season analogs shows a pathway directed to the north, and is not representative of this cyclone's actual track. Thus, the most appropriate rendition of the pathway of Hurricane Gilbert is created when the search of analogs is restricted based on the month of occurrence. It should be noted that pathway sensitivity will be considerably less severe when more than one event location is given in the archive, as the additional locations will better fix the direction of motion.

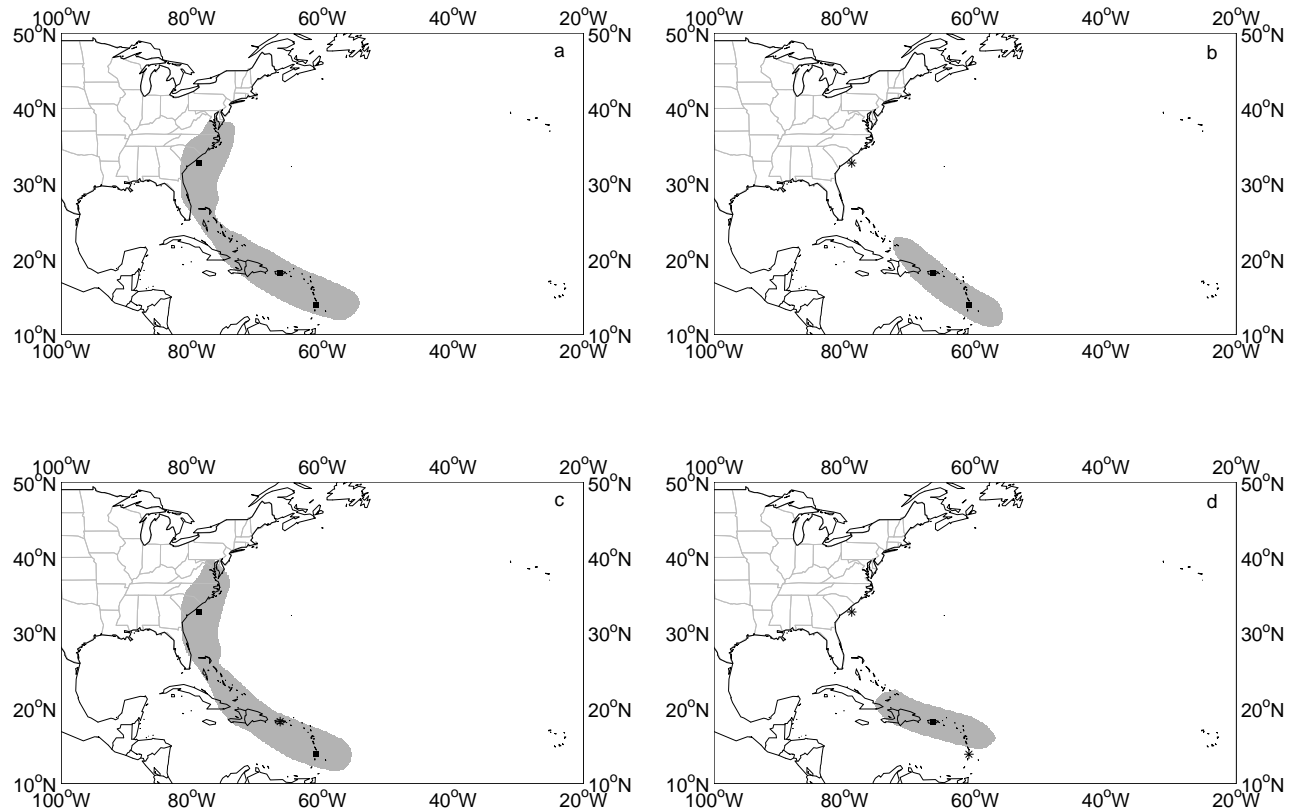


Figure 3.6: Pathways constructed for Storm 97 by using some localities (marked by a square), and omitting others (marked by an asterick). a) Using all three localities: Lesser Antilles, Puerto Rico, and off South Carolina. b) Omitting the location off South Carolina. c) Omitting the Puerto Rico location. d) Using only the Puerto Rico location.

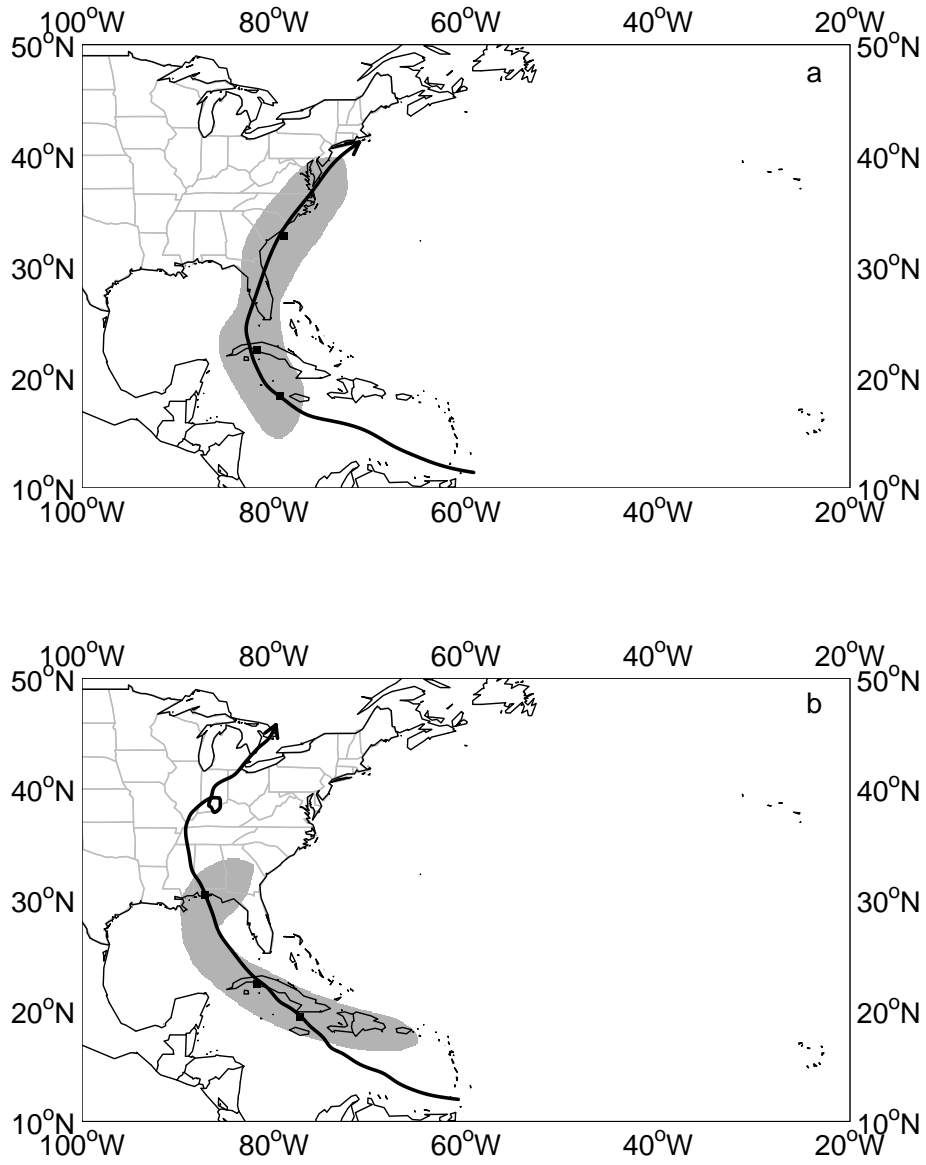


Figure 3.7: Pathways and tracks constructed for Hurricane a) Charley (2004) using event locations: West of Jamaica, Western Cuba, and off the South Carolina coast and b) Dennis (2005) using event locations: North of Jamaica, Western Cuba, and Pensacola, Florida.

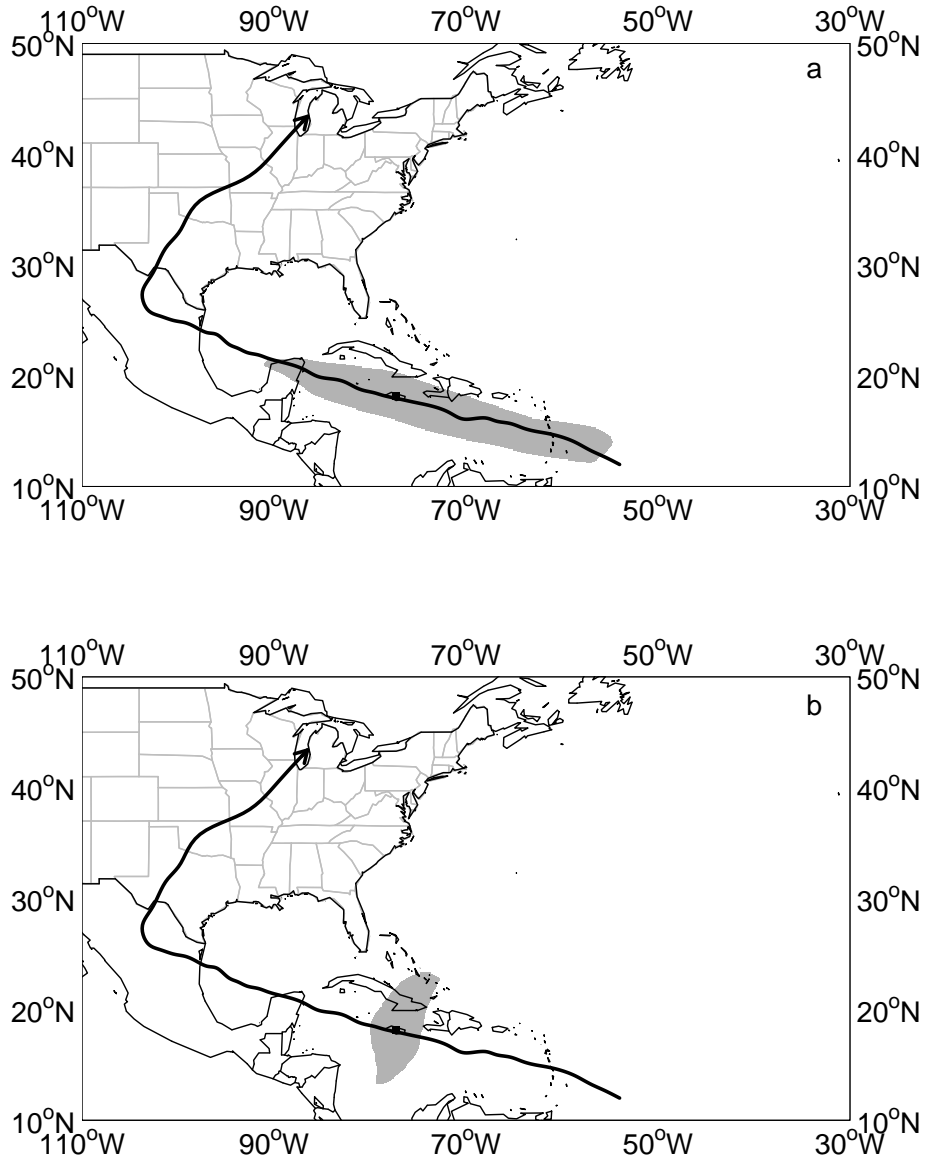


Figure 3.8: The track of Hurricane Gilbert and pathways created using analogs restricted to the months of a) August and September, and b) October and November.

3.7 Summary

A long record of past hurricane occurrences is the best way to assess future risk. While a complete and comprehensive record of all past hurricanes will remain elusive, information about previously undocumented cyclones is being uncovered through historical document searches and geological proxies. The present work is an initial attempt to make greater use of the limited information from historical hurricane archives. The major conclusion is that it is relatively straightforward to create a probable pathway for archived tropical cyclones based on a few event locations and a climatology of modern analog tracks. The pathway encompasses an area of possible tracks capable of improving information about tropical cyclone strikes in areas lacking extensive records or geologic proxy information. In turn, the pathway can be used to help uncover additional information about historical tropical cyclones. For instance, it might be worthwhile to examine historical documents from south Florida during late September or early October of 1825 for evidence of a cyclone corresponding to Storm 275 in the Chenoweth Archive.

Although the methods discussed here rely largely on a climatology of modern hurricane tracks, not all event-specific characteristics are lost. The seventh storm of the 1766 season is evidence that it is possible to discover unusual tropical cyclone tracks relative to the set of modern records. Tropical cyclones such as these could result in additional insight into temporal variations in hurricane-track patterns. Ultimately, this chapter provides a digitized version of the Chenoweth (2006) historical hurricane chronology and a methodology for depicting a probable pathway based on the event locations and modern tracks. Once pathways and tracks are created for all of the tropical cyclones in Chenoweth (2006) they can be used by climatologists to better understand long-term hurricane variability.

The methodology can be improved in a couple of ways. The certainty associated with localities in the Chenoweth Archive varies based on the description given. Thus, weighting the modern analogs towards the more certain locations might give a more accurate depiction of the historical cyclone's pathway. Second, a distribution of cyclone intensities at locations along the constructed historical track could be added to the historical track data base. Finally, the method could be used in concert with other specific information about the cyclone's path to generate an even more realistic track. An alternative approach would be to determine the posterior probability distribution that the historical track came within a specified distance of any location in the basin. This Bayesian approach provides a statistical framework for understanding the behavior of tropical cyclones in historical hurricane chronologies.

Table 3.1: A portion of the Chenoweth Archive (CA) pertaining to the 1766 hurricane season. The date of the first and last events are listed for each cyclone. Location refers to the localities listed in the archive. Method refers to the methods used in this study to digitize the event location (see text). Most cyclones have more than one location.

Event		CA			Latitude	Longitude
Month	Day	Storm No.	Location	Method	(°N)	(°E)
8	13	93	Martinique	4	14.65	-61.01
8	16	93	south of Jamaica	6	16.74	-77.27
9	1	94	Gulf of Mexico	5	24.82	-90.14
9	4	94	Texas	3	28.40	-96.38
9	8	95	Atlantic	9	31.36	-35.09
		95	Off Virginia	6	37.29	-74.58
9	13	95	west of NYC	6	40.70	-75.00
9	17	96	Lesser Antilles	9	13.90	-60.97
		96	2345N 6403W	1	23.75	-64.05
		96	33N 57W	1	33.00	-57.00
9	24	96	Azores	9	38.65	-27.22
10	5	97	Lesser Antilles	9	13.90	-60.97
		97	Puerto Rico	4	18.23	-66.48
10	13	97	off South Carolina	6	32.77	-78.92
10	15	98	South of Haiti	6	16.52	-74.04
10	24	98	Pensacola, FL	2	30.42	-87.22
10	29	99	Havana	2	23.12	-82.35
11	1	99	east of Florida	6	28.50	-79.53

Table 3.2: Parameters used to construct tracks for the 1766 North Atlantic hurricane season. The number of analogs is the number of tropical cyclones from the HURDAT used to determine the track. The minimum distance is the average distance to the Chenoweth locations for the closest analog. The threshold is the minimum distance in the weighted-average distance grids that enclose a continuous pathway.

Season Sequence No.	CA Storm No.	Minimum Distance (km)	Threshold (°lat)
1	93	69	2.00
2	94	48	2.00
3	95	22	2.00
4	96	509	4.00
5	97	178	3.00
6	98	24	2.75
7	99	24	2.75

CHAPTER 4

RISK ASSESSMENT OF HURRICANE WINDS FOR EGLIN AIR FORCE BASE

This chapter of the dissertation is a version of a paper of the same title, submitted to Theoretical and Applied Climatology in March 2010. The coauthors on the paper are Dr. James Elsner, Shawn Lewers, Jill Malmstadt, and Dr. Thomas Jagger. The relevance of this work to the dissertation as a whole is that it employs a spatial climatology of tropical cyclones in order to assess risk of extreme hurricane winds for Eglin Air Force Base. The work was supported with a contract from the Strategic Environmental Research and Development Program (SERDP SI-1700). Additional support came from the U.S. NSF (ATM-0738172).

4.1 Introduction

Hurricanes cause an average of \$10 billion in damage in the United States annually. In 2004 and 2005, the damage totaled \$150 billion. Approximately 85% of U.S. hurricane damage comes from major hurricanes (Category 3 or higher on the Saffir Simpson Hurricane Wind Scale), while they comprise only 24% of landfalling hurricanes (Pielke Jr. et al., 2008). A noted increase in the intensity of the strongest hurricanes in recent times (Elsner et al., 2008b) is of particular concern for estimates of future losses 100 years from now.

The frequency of hurricane strikes and the amount of damage they cause varies by location. The occurrence and magnitude of historical hurricanes can be used to estimate the return period of wind speeds exceeding a specified threshold. The return period (average time between successive events) can be made local by extrapolation (Elsner et al., 2008a). Damage estimates are more complicated and must take into account location-specific vulnerability. Inter-annual variability in hurricane frequency and damage losses at the coast are related to ocean temperature, the El Niño Southern Oscillation, the North Atlantic Oscillation, and solar activity (Elsner et al., 1999; Pielke Jr. and Landsea, 1999; Elsner and Jagger, 2004, 2006; Jagger et al., 2008).

The potential for a particular hurricane to cause damage depends on the strength of its winds, its forward speed, and its geographic size. For a given landfall location the damage potential also depends on local population and economy. This chapter uses a fixed location and considers the distribution of hurricane characteristics along an average track, producing

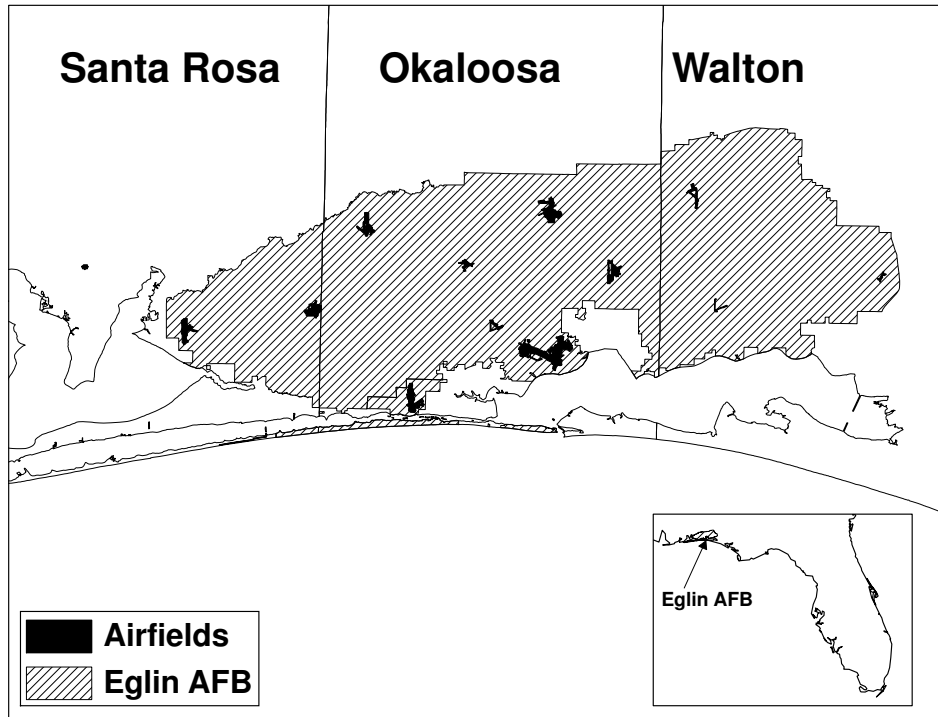


Figure 4.1: Study area. Eglin Air Force Base (striped) is located in the Florida Panhandle, comprising of portions of Santa Rosa, Okaloosa, and Walton counties.

a track-relative climatology. In short, historical hurricane tracks are used to construct a “mean” hurricane track for a given coastal location. Hurricane characteristics are gathered at 100-km increments as the storm approaches the shore. The characteristics are displayed as profiles along the average track. The characteristics are used to model a hurricane wind field and damage estimates using the HAZUS-MH Hurricane Model (HM).

The geographic focus of Chapters 4 and 5 is the Eglin Air Force Base (EAFB) located in panhandle region of Florida (Figure 4.1). These chapters represent a first step toward investigating the effects of near-term (next 100 years) risk to military infrastructure located in low coastal or near-coastal areas due to predicted changes in climate and sea level. Models project global sea level rises over the next 100 years on the order of 0.5 m, which will increase hurricane storm surge penetration. As a result, EAFB and similarly situated coastal military facilities will likely experience significant changes to environmental resources and man-made infrastructure. Shoreline retreat, increased flooding and erosion, and greater wind loads and storm surge will all contribute to increased losses. This chapter focuses on the threat of extreme hurricane winds based on the current climate, with particular emphasis on the 100-year event. The next chapter examines how the average EAFB hurricane changes with climate.

The methodology is divided into three main parts: the construction of an average hur-

ricane track, the determination of hurricane characteristics along this track, and simulation of hurricane wind gusts in the HAZUS HM. Section 4.2 describes the data used to construct the average track and to accumulate the hurricane characteristics. Section 4.3 details the generation of the average track for EAFB by using distance maps. In Section 4.4 the track is represented by equal-interval points, for which hurricane characteristics are found. These characteristics are shown as profiles along the track. In Section 4.5 a subset of hurricane characteristics, referred to as hurricane vitals, are used to simulate the hurricane, with HAZUS HM being the platform. The HAZUS HM provides wind fields and damage estimates for an extreme event following the average track. The 100-year wind gust over Santa Rosa Island estimated from hurricane simulations compares favorably with the wind gust estimated by the approach presented here. Section 4.6 provides a summary and conclusion.

4.2 Hurricane Data

Hurricane loss models are important for insurance, financial, and government sectors to estimate damage losses. These models require several subcomponents, including wind and vulnerability models, and a hurricane climatology for the specific area. The hurricane climatology is often based off the historical record, providing information about the recurrence rate and characteristics of past hurricanes (Watson and Johnson, 2008).

Past hurricane data are acquired from the HURDAT, which contains data for tropical cyclones observed in the Atlantic Ocean, Gulf of Mexico, and Caribbean Sea since 1851. This chapter uses the same data set as previous chapters, which is the Jagger and Elsner (2006) hourly-interpolations of HURDAT. Past hurricanes are used to create the average track and obtain climatological hurricane characteristics. Additionally, data from Demuth et al. (2006) are used for information on hurricane size.

The present work expands the idea of a hurricane climatology to include a track-relative climatology of hurricane characteristics specific to a given location. In other words, I seek to provide climatological hurricane characteristics along a track based on past tropical cyclones that affected the area in question. The hurricane characteristics are subsequently used to model an extreme hurricane wind event affecting EAFB. Therefore, my interest is in a track that would likely produce a worst-case scenario for EAFB and threaten military infrastructure.

For several reasons, the largest threat to EAFB is a hurricane striking the western side of the base, with much of the base on the immediate eastern side of the track. Keim et al. (2007) show that for average- or large-size hurricanes, the maximum winds extend forward and to the right about 50–100 km from the eye. This encompasses an area twice as large as the area of winds to the left of the eye. Wind speeds on the forward right quadrant of the storm are also greater due to the cumulative effect of the hurricane wind speed about the circulation and the forward motion of the tropical cyclone (Elsner and Kara, 1999). The increased winds on the right side increase the storm surge (Simpson and Riehl, 1981). Tornadoes (Pearson and Sadowski, 1965) and lightning (Corbosiero and Molinari, 2003) are also more common in this right-forward quadrant of a landfalling hurricane.

Table 4.1: Hurricanes passing within 150 km of the fiducial point over the period 1851–2008. The maximum sustained wind of the hurricane when it passed within 150 km exceeded 50 m s^{-1} (at least a Category 3 on the Saffir/Simpson hurricane scale). The distance (km) is the hurricane’s closest approach to the fiducial point. Hurricanes were not named before 1950.

Year	Name	Distance (km)
1926	Not Named	57
1995	Opal	67
1975	Eloise	74
2005	Dennis	85
1985	Elena	87
1894	Not Named	92
1851	Not Named	105
2004	Ivan	114
1877	Not Named	130
1979	Frederic	133

The landfall location chosen for the average track for EAFB is situated at 30.4°N and 86.8°W , on Santa Rosa Island, Florida. This point is located approximately 30 km southwest of the geographic centroid of EAFB, in the western portion of the base property. A hurricane making landfall here places much of EAFB in the most destructive portion of the hurricane. This location is a worst-case landfall scenario for the base and is the fiducial landfall point for the track-relative climatology.

Next, an average track is created for the worst-case landfall location by examining past hurricanes making landfall near the fiducial point. Hourly-interpolated data are used to find the strongest hurricanes in history that passed nearby. Each of these cyclones reached major hurricane intensity within 150 km of the fiducial point. In Figure 4.2, the tracks are ranked according to their average great-circle distance from that point, shown by gray-scaling. Table 4.1 lists attributes for the corresponding hurricanes, including year, name (once naming of tropical cyclones was implemented), and distance to the fiducial point. The next section describes a method to create an average track from these 10 tracks.

4.3 An Average Hurricane Track

There are various ways to determine an average track from a set of hurricanes making landfall at a particular location. The method used in this chapter is the inverse-distance weighted (IDW) averaging method introduced in Chapter 2. This method weights the particular hurricane track inversely to the distance between the hurricane’s closest approach to the fiducial point. In other words, the hurricanes tracking nearest the fiducial point have

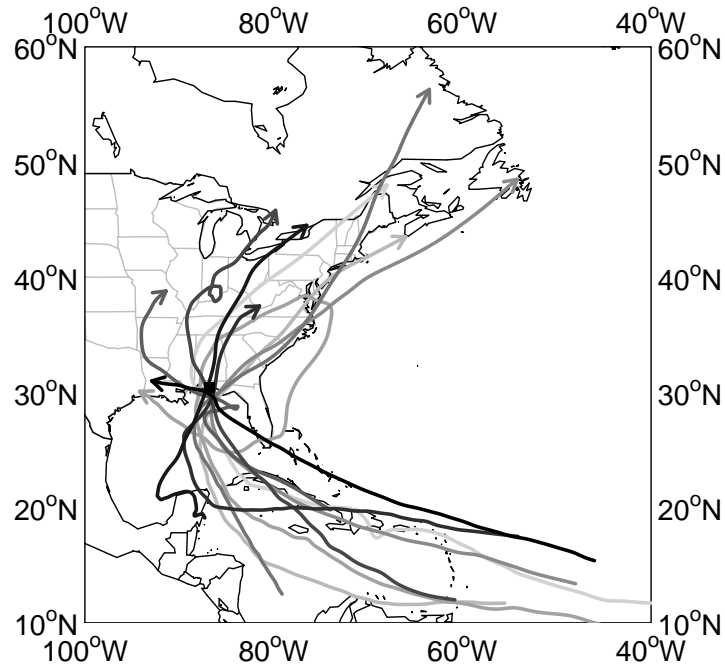


Figure 4.2: Tracks of the 10 major hurricanes passing within 150 km of the fiducial point over the period 1851–2008. The fiducial point represents a worst-case landfall scenario for the Eglin Air Force Base. The gray scale on the tracks corresponds to the distance from the fiducial point, with the darker tracks indicating closer approaches.

the most influence on the average track.

A distance map is made for each of the tracks in Figure 4.2. On each distance map, distances to the corresponding track are computed on a common 0.1° longitude grid. The track itself has a value of zero, with distances increasing away from the track. The distances are given in degrees of longitude. The 10 distance maps ($D_k(\mathbf{s})$, for $k = 1, \dots, 10$) are subsequently averaged using IDW, so that the average distance map is weighted towards the tracks that are closest to the fiducial point. The formula for the average distance map ($D(\mathbf{s})$) using IDW is given in Equation 2.1, where $d(e, t_k)$ is the great-circle distance from the Eglin Air Force Base (e) to a given track (t_k).

The average distance map is shown in Figure 4.3 with contour masks representing the weighted-averaged distance of the closest strong hurricanes to EAFB. The outer-most contour encompasses the area that has average distances less than 3.0° of longitude and the inner-most contour encompasses the area that has average distances less than 0.75° . Contours are shown at 0.25° intervals. This geovisualization of the combined set of tracks provides some information about the spatial distribution of intense hurricanes affecting the area. The contour gradient in the direction of the track is tighter post-landfall than pre-landfall. This indicates that past EAFB hurricanes have more in common prior to landfall than after. One reason for this could be the susceptibility of a decaying hurricane post-landfall to be controlled by the variable synoptic conditions. Meanwhile, stronger hurricanes will follow a more predictable manner based on larger-scale climate forcing. Drawing a line through the shortest distances on the average distance map and perpendicular to the contours provides an average hurricane track (Scheitlin et al., 2010).

The average distance map is relatively insensitive to the number of hurricanes chosen, which is a function of the distance threshold used to select the hurricanes. This can be seen by repeating the analysis using a search radius twice as large (300 km). This increases the sample size from 10 to 24 hurricanes. The track having the greatest distance to the fiducial point increases from 33 km using the set of 10 hurricanes to 274 km with the larger set of 24 hurricanes, but the average distant maps are quite similar. This insensitivity is a consequence of the inverse-distance weighting scheme. The remainder of this chapter is based on the track corresponding to the smaller sample size (Figure 4.3a).

4.4 Hurricane Characteristics Along the Track

Next, hurricane characteristics are added to the average track for EAFB. This is done at equally-spaced points along the track, including the fiducial landfall location (Figure 4.4). A spacing of 100 km is used. Since the human-affecting part of the hurricane is mostly before and directly after landfall, the portion of the track that is used covers its movement across the Gulf and its initial inland penetration. The number of track locations is arbitrary but using a 100-km spacing ensures some uniformity in wind speeds.

Hurricane characteristics are obtained for the purpose of creating an EAFB track-relative climatology, and for simulating an extreme EAFB hurricane event in the HAZUS HM. The model requires a set of values along a prescribed track that characterize the hurricane.

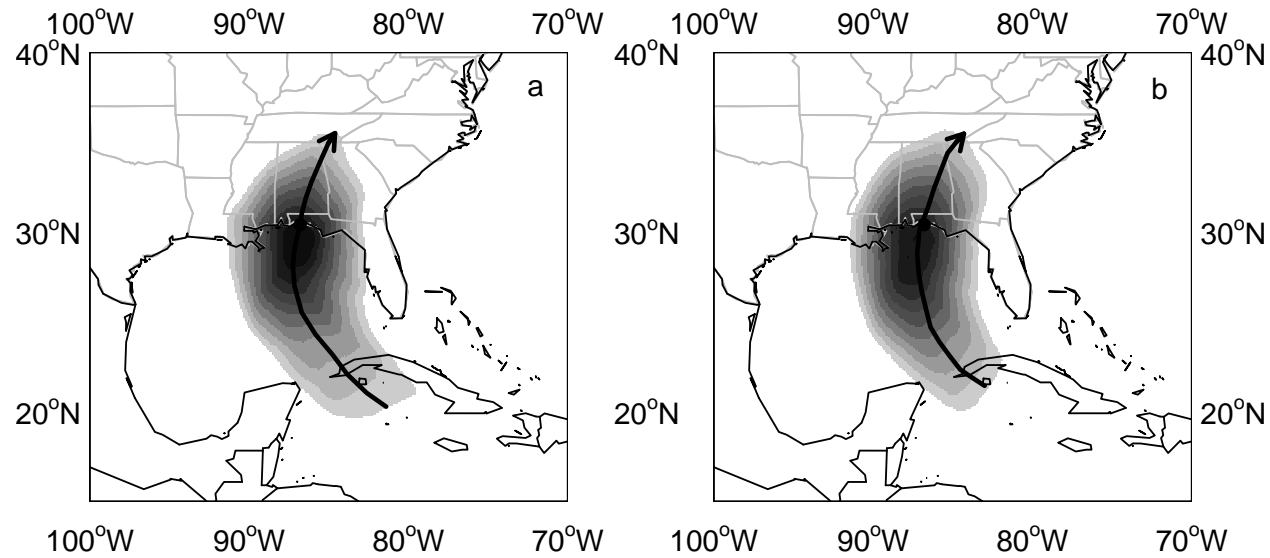


Figure 4.3: Average distance maps. The maps are based on using the a) 10 and b) 24 major hurricanes passing closest to the fiducial point over the period 1851–2008. Contours indicate the weighted average distance of the set of hurricanes. The outer contour encompasses the area that has an average distance less than 3° of latitude and the inner contour encompasses the area that has an average distance less than 0.75° , with a 0.25° contour interval. The average track is a line through the shortest distances on the average distance map and perpendicular to the contours.

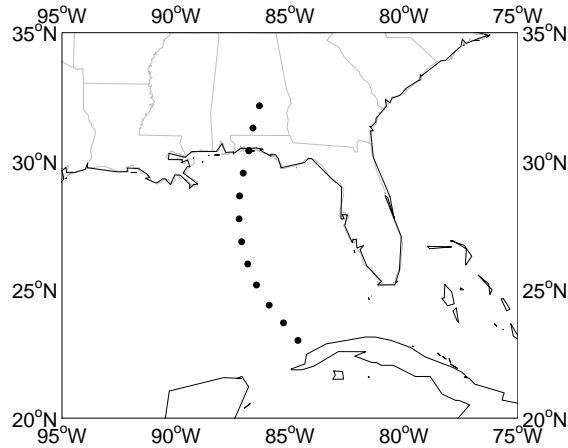


Figure 4.4: Points along the average EAFB hurricane track. Points are equally spaced at a 100-km intervals from the fiducial landfall point. Hurricane characteristics are determined at these locations to create a track-relative climatology.

These values, called “vitals,” include information about location, intensity, forward speed, size, central pressure and wind speed decay. The vitals are obtained from historical data and known empirical relationships as described below.

4.4.1 100-Year Wind Speeds

Total damage depends to a large degree on the hurricane’s maximum wind speed. Maximum wind speed refers to the estimated strongest (10-m, 1-min sustained) winds somewhere in the eyewall of the hurricane. The strongest winds are typically found on the right side of the hurricane track when looking in the direction of the storm’s forward motion. The radial distance from the center of circulation to the location of the strongest winds is called the radius to maximum winds (R_{MW}) and is, on average, 35 km for hurricanes over the Gulf of Mexico (Vickery and Wadhera, 2008).

Since the focus of this chapter is the highest wind speed that can be expected, on average, in any 100-year interval for locations along the track. Under the assumption that the maximum wind speed of any hurricane occurs within 35 km of the center of the storm, hurricanes that have come within this distance of the particular location are selected. The hurricane wind speeds are ranked from fastest to slowest and determine the parameters of an extreme-value distribution. However the historical record of hurricanes is too short to have many such hurricanes, so searching at larger distances provides more hurricanes and to accurately estimate the parameters of the distribution. Linear regressions of the distribution parameters on search radius allows us to estimate the parameters at the 35-km radius. These estimated parameters are subsequently used to determine the highest wind speed that

can be expected within the 35 km radius in any 50-year interval. This 50-year return level wind speed is used as the 100-year return level wind speed based on the assumption that the strongest winds are typically on the right side of the hurricane track and it is just as likely for a hurricane to track to the right of the location as it is to track to the left of the location. The method is developed and described in Elsner et al. (2008a), and applied to Florida in Malmstadt et al. (in press).

The above procedure for estimating the 100-year wind speed at a location is repeated independently for all locations along the track with results shown in Figure 4.5. The points indicate the estimated 100-year return level wind speed. The 90% confidence interval about this estimate is indicated by the vertical line. The set of locations is along the track (shown by black circles in panel b) with the distance prior to, and after, landfall marked along the horizontal axis. The peak 100-year sustained wind speed is 58 m s^{-1} at the location along the track 600 km before landfall. At landfall the 100-year wind speed is 48 m s^{-1} with a 90% confidence interval on this estimate between 44 and 51 m s^{-1} .

The 100-year wind speeds are strongest for locations prior to landfall and get weaker as the locations get closer to the coast. The weakest winds occur over land. Based on the historical record of hurricanes in the northern Gulf of Mexico, EAFB can expect an approaching strong hurricane to begin decaying approximately 550 km from landfall. Thus if the hurricane maintains a forward speed of 6.5 m s^{-1} , the weakening begins about one day before the time of landfall.

The tendency for pre-landfall weakening is common to hurricanes in the Gulf of Mexico, but its cause has received less attention than the more relevant concern of inland hurricane decay (Kaplan and DeMaria, 1995, 2001). Vickery and Wadhera (2008) suggest that tropical cyclones in the Gulf of Mexico exhibit a weakening 6–24 hours prior to landfall that is not exhibited in hurricanes striking other parts of the U.S. coast. This weakening is characterized by an increase in central pressure p and an increase in the R_{MW} , creating a more uniform distribution of the pressure gradient force across the diameter of the hurricane.

Information on Hurricane Opal of 1995 is shown in Figure 4.5 for comparison. Opal took a track farther to the west as it approached the base than the average EAFB track (see Figure 4.5b) although the landfall locations are only 30 km apart. Opal's hourly wind speed values are interpolated to the 100 km-spaced pre- and post-landfall locations. The wind speed profiles are similar, although the extreme hurricane generally has higher wind especially at large distances from the coast. Opal intensified rather rapidly reaching a wind speed of 60 m s^{-1} (Powell and Houston, 1998) over a warm-core ring in the waters of the Gulf approximately 450 km from the coast (Hong et al., 2000). Opal decayed just as rapidly, making landfall with 42 m s^{-1} winds. This speed is just below the 90% confidence interval of the 100-year return level. Opal's intensity values were used in creating the 100-year return levels.

Likely causes for pre-landfall decay of hurricanes in this region include movement away from the warm core ring, entrapment of dry continental air (Levinson et al., 2009), and the interaction of continental aerosols (Khain et al., 2008). Opal's more dramatic decay could have resulted from enhanced advective mixing of dry continental air due to an upper-level

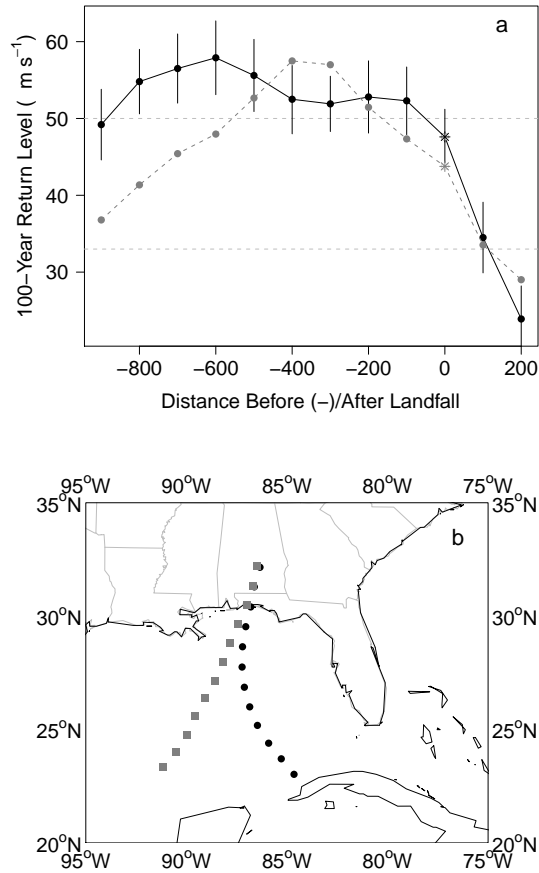


Figure 4.5: Intensities and tracks of the extreme event and Hurricane Opal. a) Wind speed (m s^{-1}) profiles of the extreme event (black) and Hurricane Opal (gray) along their respective tracks. Landfall values are marked with an asterisk. Values are given at 100-km intervals, with distances in kilometers before (negative) and after landfall plotted on the horizontal axis. The 100-year return levels are for a 35-km radius around the given point. Return levels are calculated using an application of Elsner et al. (2008). The vertical lines are the 90% confidence interval. Wind speeds for Opal are the value of the closest one-hour observation. b) Equal interval points along the track of the extreme event (black) and Hurricane Opal (gray).

trough over the coast (Shay et al., 2000).

4.4.2 Forward Speed

The amount of hurricane damage at a given location depends also on the amount of time the wind blows, which is a function of the hurricane's forward speed and size. A hurricane moving slower over an area will cause more damage than a hurricane moving faster, all else being equal. The forward speed of hurricanes passing within a 100-km radius of the locations are used to compute an average. If a hurricane has more than one observation in the search radius, the maximum observed value is used in the calculation. The search domain for the location 300 km from landfall and the average translational speed as a function of distance along the track are shown in Figure 4.6. Results show that, on average, hurricanes approaching EAFB move at speeds of 6–7 m s⁻¹ with a slight acceleration prior to landfall. After landfall there is a significant increase in forward velocity as the hurricanes get pushed northward and eastward under the influence of the mid-latitude jet streams.

4.4.3 Radius to Maximum Winds

The size of a hurricane is characterized by the radius to maximum winds (R_{MW}). Formally, R_{MW} is defined as the distance from the center of the cyclone to the farthest extension of the maximum wind speeds. A typical R_{MW} is 30–50 km (Hsu and Yan, 1998). Vickery and Wadhera (2008) note that in the Gulf of Mexico there is no statistically significant relationship between R_{MW} and latitude or Δp , which is the difference in the cyclone's central and peripheral pressures. Thus, the R_{MW} can not be approximated using any of the information already obtained. Vickery and Wadhera (2008) note three traits of Gulf of Mexico landfalling hurricanes. First, the average R_{MW} is estimated to be 35 km. Second, there is a notable change in R_{MW} associated with the decay of a Gulf hurricane as it approaches the coast. Finally, Gulf of Mexico landfalling hurricanes are smaller, on average, than their Atlantic coast counterparts.

To check these relationships in the study area, R_{MW} data are obtained from the extended best-track database (Demuth et al., 2006). The database contains information for most North Atlantic tropical cyclones since 1988. For 1988 and 1989 the data are from the vortex messages of aircraft reconnaissance missions. For 1990–present, the data are from the National Hurricane Center archives, estimated from operational data sources including ship reports, aircraft reconnaissance data and satellite imagery. Information is provided at six-hour intervals. I focus on major hurricanes estimates within a region of the northern Gulf of Mexico off the coast of EAFB. Within this region the average R_{MW} is 33 km with a standard error of 12 km. As Vickery and Wadhera (2008) suggest, there is no significant correlation between R_{MW} and maximum wind speeds, or R_{MW} and latitude. Thus, the Vickery and Wadhera (2008) estimation of 35 km is used as a constant R_{MW} through the length of the track.

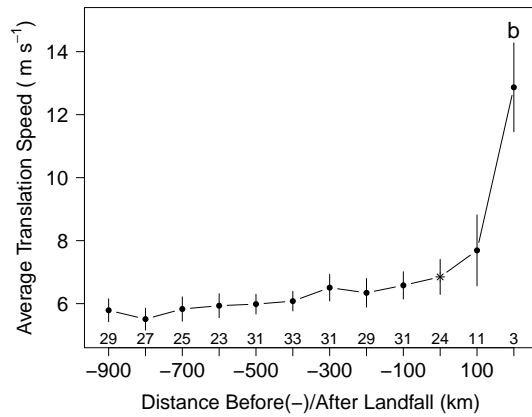
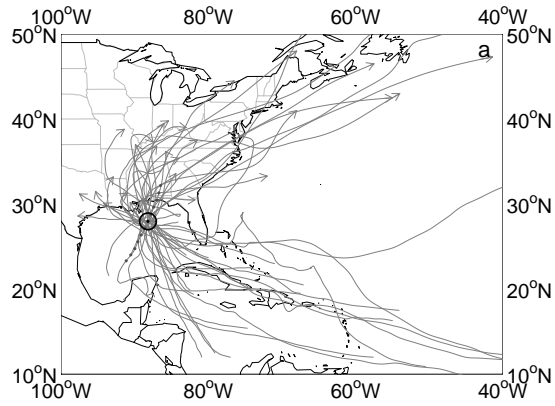


Figure 4.6: Track selection and forward speeds. a) Tracks of the 34 hurricanes passing within a 100-km great circle distance of the track point 300 km from the landfall location. The forward speed of each hurricane as it passed within 100 km of the location is used to compute the average. b) Average forward speeds (m s^{-1}) as a function of distance before and after landfall. Vertical bars indicate the \pm on standard errors above the mean speed. The number of hurricanes used in the averaging are shown above the horizontal axis.

4.4.4 Holland B Pressure Profile Parameter

The decrease of wind speeds away from the R_{MW} is described by the Holland B parameter. Specifically, Holland B dictates the shape of the surface air pressure field of a hurricane. The values are non-dimensional and range between 1 and 2.5. Holding R_{MW} and central pressure constant, a decrease in B indicates a weaker maximum wind speed with more dispersed pressure gradients across the wind field (Holland, 1980). In other words, after the hurricane reaches its peak wind speed, wind speeds gradually decrease away from the eyewall in a nonlinear fashion. Thus a lower value of B , all else being the same, indicates a larger area subjected to the strongest winds, but the maximum wind speed is relatively weaker. Constant pressure and R_{MW} with a higher value of B cause a higher maximum wind speed but a quicker decrease in velocity beyond the R_{MW} .

Vickery and Wadhera (2008) provide the following empirical formula for Holland B for landfalling hurricanes based on observations of R_{MW} and latitude (ϕ):

$$B = 1.811 - 0.00557R_{MW} - 0.01295\phi \quad (4.1)$$

This equation is used at each of the track locations. The values of B range from 1.32 at the first location to 1.20 at the location farthest inland.

The complete set of vitals for each track location is listed in Table 4.2. The list is ordered by location along the track from farthest from coast to farthest inland. The minimum central pressure values are obtained from the wind-pressure relationship of Brown et al. (2006) for Gulf of Mexico hurricanes. The “Inland” tag is set to 1 for locations over land.

Table 4.2: Vitals for an extreme hurricane affecting EAFB. The latitude (λ) and longitude (ϕ) are those of the equal-interval points along the average track. The wind speed (m s^{-1}) refers to the 100-year return level for that point. The translation speed (Trans) (m s^{-1}), radius of maximum winds (R_{MW}) (km), pressure (mb), and Holland B profile parameter are obtained from past hurricanes and formulas based on known relationships. The inland column is a binary variable describing whether the point is over water (0) or land (1). These vitals are used to produce a wind field in the HAZUS HM.

ϕ	λ	Wind Speed (m s^{-1})	Translation Speed (m s^{-1})	R_{MW} (km)	Central pressure (mb)	Holland B	Inland
23.0	-84.6	49.2	5.8	35	960.7	1.32	0
23.7	-85.3	54.8	5.5	35	949.8	1.31	0
24.4	-85.9	56.5	5.8	35	946.4	1.30	0
25.2	-86.5	57.9	6.0	35	943.5	1.29	0
26.0	-86.9	55.6	6.1	35	948.2	1.28	0
26.9	-87.1	52.5	6.1	35	954.4	1.27	0
27.8	-87.2	51.9	6.5	35	955.6	1.26	0
28.6	-87.2	52.8	6.3	35	953.8	1.25	0
29.5	-87.0	52.3	6.6	35	954.8	1.23	0
30.4	-86.8	47.6	6.8	35	963.6	1.22	1
31.3	-86.6	34.5	7.7	35	985.0	1.21	1
32.2	-86.3	23.9	12.9	35	998.6	1.20	1

4.5 Estimates of Wind Speeds and Wind Damage Losses From HAZUS HM

Hurricane wind damage results from winds circulating through the storm as it moves inland. HAZUS constructs a two-dimensional wind field associated with a hurricane based on a set of vitals. As the vitals change along the track so does the wind field. The vitals can be provided by a user (deterministic mode), or intrinsic to HAZUS based on a historical event (historical mode) or a collection of synthetic hurricane events (probabilistic mode). In each mode, HAZUS uses the set of wind fields to generate a wind swath containing the fastest winds at any location and a resulting set of damages and loss estimates.

HAZUS was developed in the early 1990s and the hurricane component was added in 1997. It was released for research purposes in 2005 (Schneider and Schauer, 2006) and it continues with periodic updates. This work uses version MR4 to generate a wind swath and loss estimates from the set of vitals (Table 4.2). The HAZUS deterministic winds generated with the set of hurricane vitals is compared to the 100-year wind gusts using the HAZUS probabilistic mode. This is also compared to a historical run of Hurricane Opal.

4.5.1 Deterministic Mode

In the deterministic mode, a single set of user-defined vitals is used to generate a wind swath across the area of interest. The HAZUS HM is described in detail in Vickery et al. (2000a,b), and in the introduction of this dissertation. All wind swaths created from a set of hurricane vitals (whether deterministic or probabilistic) are done in the same way. Wind estimates are made using two model components; the hurricane hazard model and the terrain model. The hurricane hazard model uses the hurricane vitals to create wind fields through the length of the track. The terrain model alters the wind fields based on local terrain. Greater friction associated with a rougher land surface causes a weakening of the average wind speeds. Peak wind gusts on the other hand are less affected by surface roughness (Zhu, 2008). HAZUS HM incorporates a wind speed-surface roughness relationship with the terrain information from land use land cover (LULC) maps. The set of wind fields from these models result in a wind swath of the maximum winds affecting particular geographic locations.

The wind swath for the extreme event is shown in Figure 4.7a. Values on the map are estimates of the maximum wind gusts by census track. As expected, the most intense winds are experienced at landfall and for locations east. Within the region there is a 24 m s^{-1} range in the maximum wind gusts, with a maximum gust of approximately 58 m s^{-1} .

4.5.2 Historical Scenario

The HAZUS HM contains information for all tropical storms in the Atlantic Basin that occurred between 1886 and 2001 (Vickery et al., 2006a), allowing for the simulation of historical events. In historical scenario mode, the HAZUS HM uses a past hurricane's

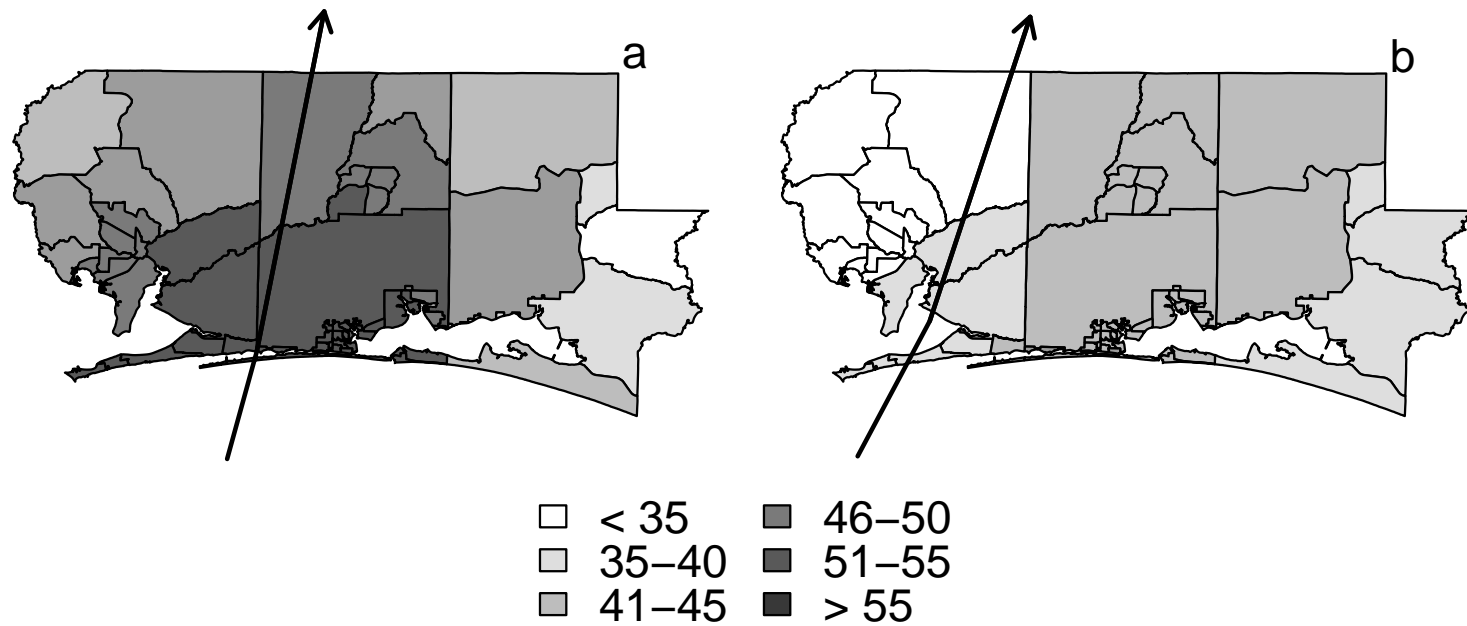


Figure 4.7: Maximum wind gusts (m s^{-1}) for a) the extreme event and b) Hurricane Opal. The respective hurricane tracks are shown as a black line. One maximum wind gust is provided for each census tract. The extreme event produces wind gusts of $34\text{--}58 \text{ m s}^{-1}$. Hurricane Opal produces wind gusts of $31\text{--}45 \text{ m s}^{-1}$.

observations to estimate the associated wind field and loss amounts. This allows us to compare the losses from the extreme event to those of Hurricane Opal.

As part of a validation procedure, Vickery et al. (2006b) compare HAZUS-modeled economic loss to actual losses for several hurricanes, including Hurricane Opal. The validation procedure shows that HAZUS loss estimates are reasonably similar to observed losses, Opal included. The largest difference between modeled and observed losses occurred at wind speeds less than 45 m s^{-1} . This was likely because at the time of the validation procedure, the HAZUS HM did not model damage from fallen trees. Fallen trees cause a large portion of damage from weaker tropical cyclones, causing them to be estimated disproportionately less than their stronger counterparts (Vickery et al., 2006b). Since then, HAZUS has been extended to include tree-fall damage, increasing the accuracy of the losses (FEMA, 2008).

HAZUS utilizes Opal's six-hourly observations to estimate wind loads and economic loss over the same region as the extreme event. THE HAZUS HM estimated wind gusts for Hurricane Opal are shown in Figure 4.7b. The strongest maximum wind gust for Opal is approximately 45 m s^{-1} , while the weakest maximum gust experienced by a census tract is approximately 31 m s^{-1} .

4.5.3 Probabilistic Mode

In the probabilistic mode, hundreds of hurricane vital sets are generated from a 10^5 -year simulation of hurricanes across the North Atlantic basin. Each vital set is used to create a wind field, and the set of winds is used to estimate return-level wind speeds for each census tract. The probabilistic results are available as a table of return levels. Here the HAZUS HM wind swath generated in deterministic mode from the 100-year wind speed along the average track is compared to the HAZUS HM 100-year wind speed generated in probabilistic mode. A comparison of maximum wind gusts is made at the census tract containing the landfall location (Figure 4.8). The probabilistic return level curve represents wind gusts of this magnitude or higher somewhere in this census tract on average once every return period. The deterministic information is gathered from the wind swath resulting from the hurricane vitals.

The deterministic wind swath shows a 100-year wind gust estimate of 58 m s^{-1} . The 90% confidence intervals ($53\text{--}63 \text{ m s}^{-1}$) on this estimate are obtained by running similar deterministic hurricanes, with intensity values of the lower and upper 90% confidence limits from Figure 4.5. This is compared to the probabilistic 100-year gust of 55 m s^{-1} , which is within the 90% confidence limits of the estimate. The probabilistic 100-year wind gust is based on a Monte Carlo simulation of 10^5 years of hurricanes across the Atlantic.

4.5.4 Economic Loss

Given the spatial variation of hurricane winds, the HAZUS HM produces wind-loss estimates at the census tract level. This integrates three model components— a wind load

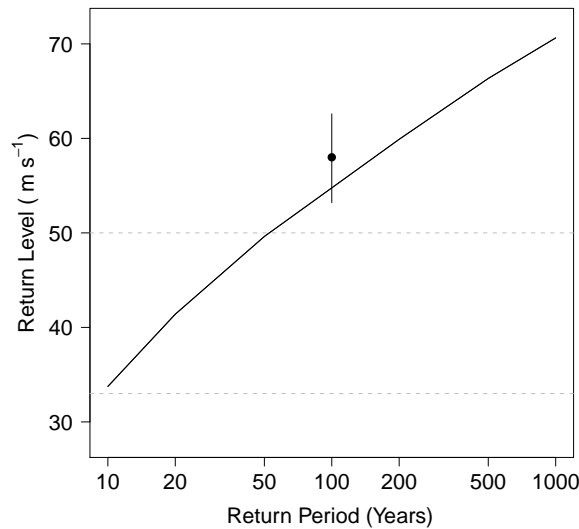


Figure 4.8: Wind speed gusts for the Santa Rosa Island census tract. The curve shows 100-year return levels of wind gusts from the HAZUS HM probabilistic output. The points and error bars are from the HAZUS HM deterministic output using extreme hurricane vitals for EAFB.

model, a physical damage model, and an economic loss model— and information on building types and materials from census data.

The wind load model includes wind pressure modeling, and windborne debris modeling. The wind pressure model uses empirical data from wind tunnel tests to estimate directionally dependent wind-induced pressures (Vickery et al., 2006a). Wind pressures are important due to their strain on buildings, resulting in building damage and causing windborne debris. Windborne debris modeling is a critical component of a physical damage model. HAZUS has two windborne debris models: one for residential debris, and another for roof gravel, which acts as a missile during high winds. The wind load model provides information to estimate wind-induced damage and loss (Vickery et al., 2006a).

Using detailed building stock information, the physical damage model estimates the damage associated with the given wind load. The physical damage model predicts the failure of building components due to progressive failures, internal pressures, duration effects, and changes in wind direction and speed. The model focuses on damage to the exterior of the buildings, including the windows, roof cover, roof deck, joint failures, and wall failures. Five damage states are used to describe the amount of damage to each of the buildings (Vickery et al., 2006b).

The economic loss model uses the information from the physical damage model to estimate hurricane wind-induced losses. The economic loss model takes into account actual building losses, loss of contents and inventory, and loss of building use (Vickery et al.,

2006b). The model does not contain data for military building stock, but provides damage estimates for residential and commercial buildings. The HAZUS HM provides a basis for assessing the military infrastructure damage, and the military building stock information may be added by the appropriate persons to estimate losses.

HAZUS estimates wind damages of \$463 million in the study region (consisting of Okaloosa, Walton and Santa Rosa counties) for the deterministic event. This is accompanied by over \$110 million in business interruption losses, including things such as income, relocation, and renting a new facility. The total building-related losses are over \$573 million. The model estimates that 461 households will be displaced due to the hurricane and require a temporary shelter. Approximately one fourth of all building types are expected to have some type of damage, providing an estimated three million tons of debris. This amount of debris would require 3359 truckloads for removal.

4.6 Summary

This chapter demonstrates a new method for estimating the risk of local extreme winds that combines historical hurricane records with a deterministic wind field model. First, a hurricane track is created for a landfall location on the island that represents a worst-case scenario. The track is based on averaging the paths of historical hurricanes in the vicinity of the landfall location. Second, an extreme-value statistical model is used estimate 100-year wind speeds at locations along the average track again based on historical hurricanes in the vicinity of the track locations. The locations are separated along the track at 100-km intervals. Third, the 100-year wind speeds together with information about hurricane size (R_{MW} , and the Holland B parameter) and forward speeds are used as input to the HAZUS HM hurricane wind field model to produce a wind swath. The R_{MW} is a constant 35 km along the track and the weakening of winds beyond the R_{MW} are characterized by the Holland B parameter.

The procedure produces a 100-year hurricane wind gust on Santa Rosa Island of $58 (\pm 5) \text{ m s}^{-1}$ (90% CI). An estimated 100-year wind gust at the same location based on a 10^5 year simulation of hurricanes is lower at 55 m s^{-1} , but within the 90% confidence limits. Based on structural damage functions and building stock data for the region contained in HAZUS, the 100-year hurricane wind swath results in \$574 million total loss to residential and commercial buildings, not including military infrastructure, with 25% of all buildings receiving at least some damage.

The 100-year wind gust estimated with the deterministic approach, while somewhat higher, has a 90% confidence interval that includes the 100-year wind gust estimated from the HAZUS HM simulation. However, the real strength of the statistical to deterministic approach is that it requires many fewer parameters than the probabilistic approach, making it useful for considering questions associated with climate variability and climate change. For instance, the extreme-value model parameters can be regressed on ocean temperature providing a way to condition the 100-year wind speed (and damage potential) on a future climate featuring warmer oceans. The methodology can be applied to other coastal regions

for local risk analysis.

CHAPTER 5

A TRACK-RELATIVE CLIMATOLOGY OF EGLIN AIR FORCE BASE HURRICANES IN A VARIABLE CLIMATE

This chapter of the dissertation is a version of a book chapter of the same title, in press with *Hurricanes and Climate Change, Volume 2*. The chapter is coauthored with Dr. James Elsner. The relevance of this work to the dissertation as a whole is that it shows the ease at which the storm statistics may be manipulated in order to analyze the affects of climate change. The work was supported with a contract from the Strategic Environmental Research and Development Program (SERDP SI-1700).

5.1 Introduction

The relationship between hurricanes and climate change has received a lot of attention. Current attempts to understand this relationship focus on the affects climate change will have on the frequency and intensity of future tropical cyclones. Some question our ability to discern changes in hurricane frequency due to climate change, as the signals may be masked by large natural variability (Trenberth, 2005). The intensity of future cyclones is also in question, but findings suggest a 30-year increase in tropical cyclone destruction potential (Emanuel, 2005), especially in the strongest hurricanes (Elsner et al., 2008b). This increase in destructiveness, coupled with an increase in coastal populations, will result in greater economic loss due to tropical cyclones (Emanuel, 2005; Hallegatte, 2007). Others suggest there is no basis for making such claims in the present state of knowledge (Pielke et al., 2005; Landsea et al., 2006), or infer that hurricane frequency variability is solely due to cyclical climate shifts (Goldenberg et al. 2001). Regardless, one can not deny the tremendous coastal devastation in the past decade due to tropical cyclone activity worldwide, and the weariness associated with a possible increase in destruction.

It is important for coastal communities to be prepared for future storms. This can be achieved through sound prediction and mitigation strategies. In this regard, it is useful to assess hurricane risk at a local, or decision-making level. This chapter serves to analyze the hurricane vulnerability of Eglin Air Force Base (EAFB), located on the Florida Pan-

handle, to help personnel understand the potential for future infrastructure damage (Figure 4.1). Utilizing a “point” analysis approach as opposed to the common method of using portions of coastline, provides a resolution suitable for understanding local-specific hurricane vulnerability (Muller and Stone, 2001) and the creation of the average track provides information additional to the standard hurricane climatology.

The method uses past hurricane events to understand the movement and characteristics of the “typical” hurricane affecting EAFB. Through creation of an average track a spatial hurricane climatology is created for the area. Additionally, we show how past tropical cyclone characteristics can be used to understand the future of EAFB hurricanes in a changing climate. In Section 5.2, I illustrate our technique for constructing a climatological hurricane track for a specific area based on the movement of past hurricanes. An average track is created to represent the typical EAFB hurricane. In Section 5.3, average hurricane characteristics (i.e. intensity and translation speed) are found along the track based on past hurricane events. Together, the track and wind characteristics serve as a track-relative climatology of EAFB hurricanes. Further, in Section 4, separate climatologies are constructed for years of warm and cool sea surface temperature (SST) anomalies. This provides a glimpse into a possible future of EAFB hurricanes associated with a change in SST. The methodology can be repeated for any location to help understand the present local-scale hurricane climate, as well as the future of these storms in a changing climate. Section 5.5 provides the summary and conclusions for the information presented in this chapter.

5.2 An Average Hurricane Track

Due to the nature of their driving forces, hurricanes move in somewhat predictable patterns (Brettschneider, 2008). Thus, hurricanes striking a particular locale are likely to follow similar pathways. It is thus possible to summarize the behavior of the typical track of hurricanes for a specific location based off of past tropical cyclone events. The goal is to provide a technique for analyzing a local-level hurricane climate, and the affect changing SST may have on the average hurricane. Thus, the first step is to create an average hurricane track for the location.

As explained in Chapter 4, the worst-case scenario track for EAFB is a hurricane making landfall on the western edge of the military base, on Santa Rosa Island, Florida. An average hurricane track is created for EAFB based on past hurricanes making landfall near the selected landfall location. The hurricane data are an hourly-interpolated version of the HURDAT data set (1851–2008). As described in Jagger and Elsner (2006), spline interpolations are used to create hourly estimations from the six-hourly HURDAT observations. Using hourly-interpolated data reduces the chance of missing a hurricane passing through a small area relative to the chance when using six-hourly data. Moreover, for an area the size of EAFB, higher temporal resolution is not needed.

Figure 5.1 shows the 26 tracks that have come within a 100-km radius of EAFB over the period 1851 through 2008. Similar to the previous chapters, the tracks have gray-scaled to reflect their closest great-circle distance to the chosen location of interest; the darker

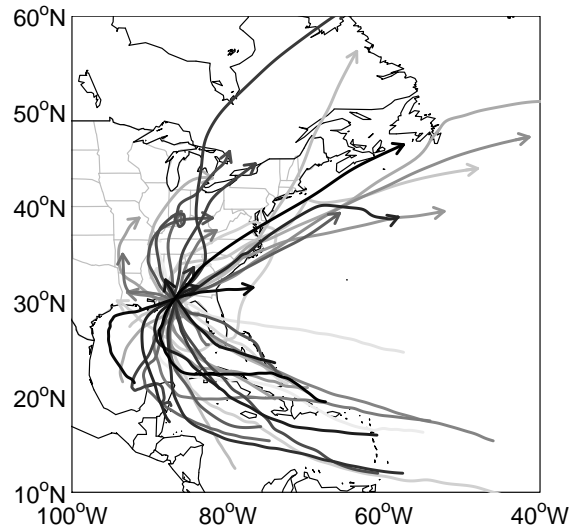


Figure 5.1: Tracks of hurricanes affecting Eglin Air Force Base (EAFB). All 26 tracks came within 100 km of Santa Rosa Island, FL (30.4°N and 86.8°W) based on data from 1851–2008. The gray shading is proportional to the distance the track came to the landfall location. Darkest tracks are those that passed nearest the island.

the track the closer it came to the location. Each of the tropical cyclones reached winds of hurricane force (33 m s^{-1}) or greater within the radius. An average of these tracks is considered to represent the typical EAFB hurricane track capable of producing catastrophic winds across the region. This is similar to Chapter 4, but inclusive of all hurricanes rather than only those Category 3 and higher. Thus, this chapter focuses on the typical EAFB hurricane (and as relative to SST) rather than the extreme EAFB hurricane.

The method used here to construct an average hurricane track uses a series of distance maps (Scheitlin et al., 2010). A distance map is created for each of the 26 hurricanes shown in Fig. 5.1. The maps are subsequently stacked and IDW averaged based on their distance from the chosen landfall point (Figure 5.2). The average track is the line down the center of the distance contours. This represents the track of a typical EAFB hurricane. Here the track is drawn within a threshold of 2.5° longitude of distance, but it can be drawn longer or shorter depending on the purpose. The next step is to gather information about the typical hurricane characteristics along this track.

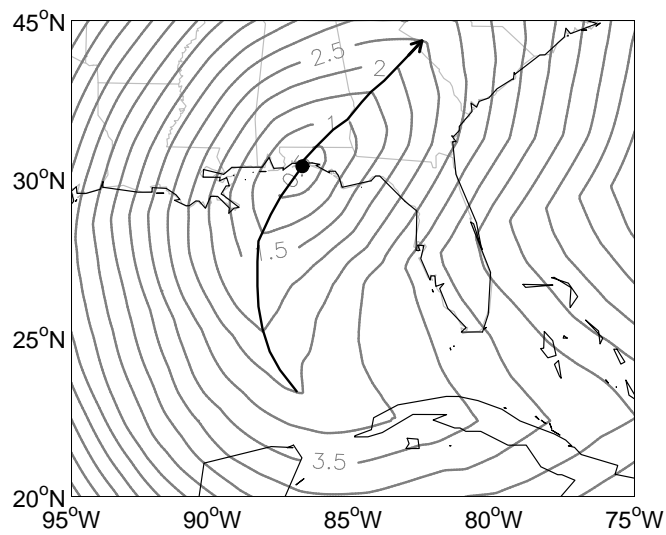


Figure 5.2: Average hurricane track for EAFB. The average track is the solid line drawn through the minimum distance contours of the average-distance map. The average-distance map is based on 26 hurricanes affecting EAFB over the period 1851–2008.

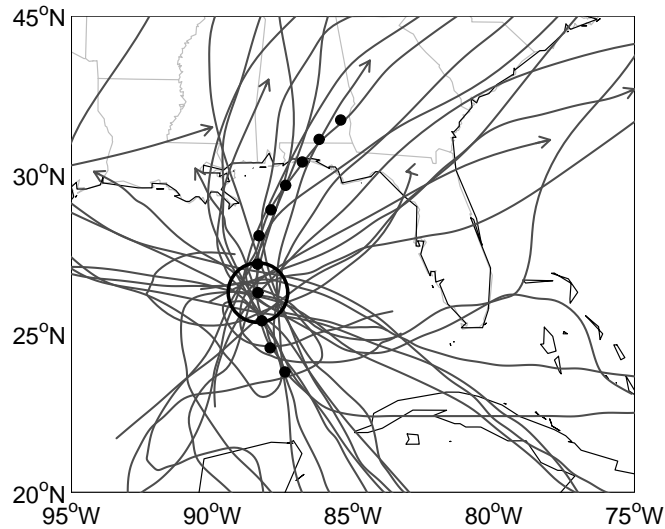


Figure 5.3: The average EAFB hurricane track depicted as a series of equal-interval points spaced 100 km apart and centered on the landfall location of EAFB. The tracks of all hurricanes passing within 100-km radius of the point 500 km from landfall are also depicted. Hurricane characteristics (intensity, forward speed, etc) are averaged based on the maximum value obtained from the hourly data as the hurricane passes through the circle. The process is repeated for each point.

5.3 Hurricane Characteristics Along the Track

An important consideration for a spatial hurricane climatology is the hurricane characteristics along the track, such as intensity and translation speed. In this section, the average track is sampled at equal-distant points, and the data used to characterize each point comes from past hurricanes that passed nearby the sampled points.

Figure 5.3 shows the average EAFB track represented by points spaced in 100-km intervals before and after landfall. Tracks of all hurricanes passing within a 100-km radius of the point 500 km from landfall are also depicted. The radius about this point contains the most hurricane tracks compared to the other track points, with 39 historical hurricanes passing within 100 km. Hurricane characteristics (intensity, forward speed, etc.) are averaged based on the maximum value obtained from the hourly data as the hurricane passes through the circle. For example, if the hurricane spends 8 hours within 100 km of the point, only the single maximum wind speed value is used in the average. The average of the maximum value of each hurricane is found.

This process is repeated along the track, selecting a set of hurricanes coming within 100 km of each of the track points. The average translation speed and intensity are calculated from the selected hurricanes, again using the maximum hourly-observation within the radii for each event. Information regarding the average decay and intensification behavior is gathered from the change of average intensity over track distance.

Figure 5.4 shows the profiles of the average hurricane characteristics along the length of the average track. The number of hurricanes used in the average is given inside the horizontal axis. As noted, the frequency peaks at locations 300 to 600 km from the landfall point. As expected there are fewer hurricanes closer to the coast and over land as the tropical cyclones weaken below hurricane intensity during their decay around landfall.

For the intensity profile, which is based on the maximum wind speed, the dashed line marks the Category 3 threshold. The hurricane stays above this major hurricane threshold for some distance prior to landfall. The hurricane reaches its maximum intensity of approximately $52 \text{ m s}^{-1} \pm 2 \text{ m s}^{-1}$ (s.e.) 400 km before reaching the coast. After that point, hurricanes approaching EAFB, on average, begin to weaken until making landfall with wind speeds of approximately 45 m s^{-1} , a Category 2 hurricane. The downward slope of the intensity profile provides information about the typical decay rate of hurricanes approaching the coast.

Although the intensity profile shown in Fig. 5.4 is based on an average, a similar intensity profile was exhibited by Hurricane Opal in 1995, which affected EAFB. While much more intense than the average EAFB hurricane, Opal experienced rapid intensification in the Gulf of Mexico and subsequent decay prior to landfall, similar to the average cyclone. Approximately 450 km prior to making landfall just west of Santa Rosa Island, Florida, a warm-core ring in the Gulf of Mexico helped Opal reach Category 4 intensity (Hong et al. 2000). The late onset of intensification surprised forecasters and an unsuspecting coastline. However, the average intensity profile shows that Opal's intensification profile is the rule rather than the exception. Although Opal is a more extreme case, the average EAFB hurricane exhibits some degree of intensification until 500–400 km from landfall before decaying during its final advancement towards the shore.

What is known about Hurricane Opal and other Gulf of Mexico hurricanes can provide insight into the average EAFB hurricane intensity profile. Similar to Opal, it is likely that the increased intensification exhibited by the average hurricane approximately 500–400 km before landfall is due to especially warm SSTs in the Gulf of Mexico. Areas of warm SST are often associated with warm-core rings that separate from the Loop Current and travel across the Gulf of Mexico (Vukovich and Crissman, 1986). The Loop Current is a stream of warm upper-ocean water in the Gulf of Mexico that flows northward between Cuba and the Yucatán peninsula into the Gulf of Mexico then exits east through the Florida Straits.

Once a tropical cyclone reaches tropical storm strength, the thermodynamic structure of the upper ocean plays an important role on storm intensity (Emanuel, 1999). For Opal and the average EAFB hurricane, the extra heat content of the warm-core ring increases the thermodynamic instability that fuels the hurricane as it travels northward toward the Gulf coast.

While the intensification of the average EAFB hurricane is easily interpreted, the decay

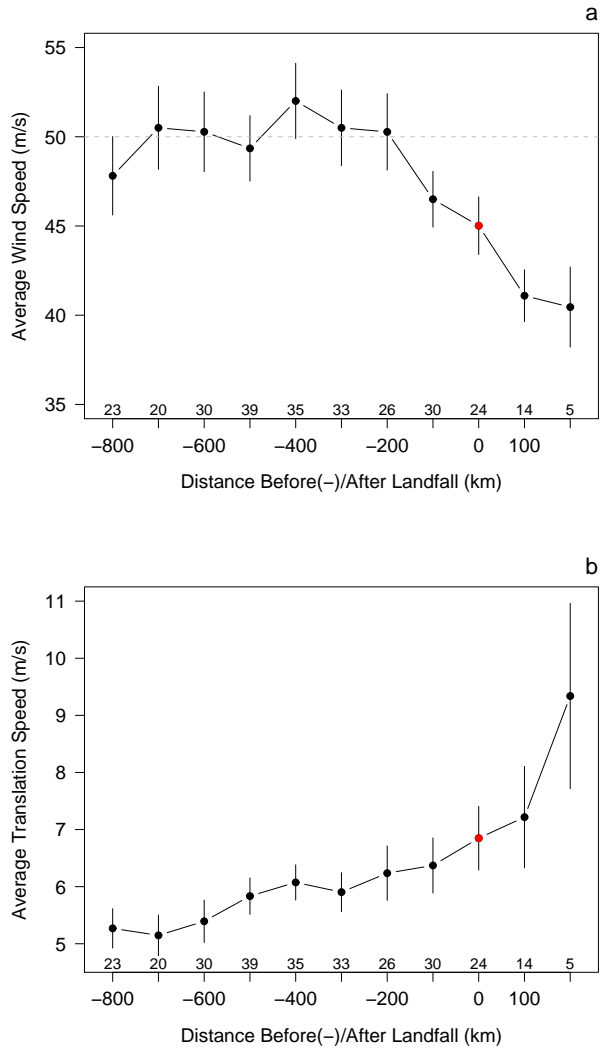


Figure 5.4: Hurricane characteristics along the average track. Average a) wind speeds and b) translation speeds at 100-km intervals along the track. Distances in kilometers before (negative) and after landfall are plotted on the horizontal axis. Standard errors (s.e.) about the mean are drawn as vertical lines and the number of hurricanes used in the averaging are shown above the horizontal axis.

of the hurricane as it approaches inland has a more complex explanation. That being said, it is no surprise that the hurricane decays in such a manner. Hurricane Opal experienced similar pre-landfall decay, and Vickery and Wadhwa (2008) note that this 12–24 hour pre-landfall decay is common in, and exclusive to, hurricanes making landfall along the Gulf Coast. Levinson et al. (2009) add that this pre-landfall weakening is more prominent in stronger Gulf of Mexico hurricanes.

There are at least three factors associated with the pre-landfall decay of the EAFB hurricane. One obvious factor is the movement of the hurricane away from the warmest waters associated with the warm-core rings of the Loop Current. Second, the entrainment of dry continental air works to “fill in” a hurricane as a portion of it begins to reach the coast (Levinson et al., 2009). This will affect larger storms first, as they will interact with the drier air earlier than smaller storms as they approach landfall. A third, lesser-known factor in the pre-landfall decay is the effect of continental aerosols near the coast. Khain et al. (2008) found that aerosols decrease the convective intensity in the center of a simulated hurricane leading to weakening. These three factors help explain the pre-landfall weakening.

In addition to intensity, the average EAFB hurricane translation speed is also gathered from the historical data set. Figure 5.4b displays the translational speed profile along the average track. On average, hurricanes are accelerating as they approach EAFB. And the acceleration rate increases, especially after landfall. For a large portion of the track, the average forward speed is in the range of 6–7 m s⁻¹. Extrapolation from a constant translation speed of 6.5 m s⁻¹ from the location of maximum intensity, the hurricane would reach EAFB in about 17 hours. This extrapolation would error on the wrong side for coastal communities and EAFB employees as the tendency is for an acceleration of the hurricane resulting in an arrival earlier than anticipated.

5.4 Warm versus Cool SST Years

A major concern about hurricane risk is the possibility that the risk will change in a warming world. Once again, it is useful to take a local-scale approach to this research in order to provide information at the decision-making level. This also allows us to account for different affects of climate change based on location, as previous studies have shown that intense hurricanes in different ocean basins are affected somewhat differently by a warming environment (Elsner et al. 2008). The next analysis is on how SST variability has affected past EAFB hurricane characteristics. This may provide information regarding the affects of future SST changes on local hurricane activity.

SST data are obtained from the Caribbean SST Index provided by NOAA Earth System Research Laboratory. The data set contains monthly SST anomalies for the Caribbean Sea from 1951–2006. For this analysis, an August-September-October anomaly average is calculated each year. The yearly averages are divided into thirds (terciles), with the top third representing warm years, and the bottom third representing cool years. The lower tercile is a -0.060°C temperature anomaly with a minimum value being a -0.374°C anomaly. The upper tercile is a 0.194°C temperature anomaly with a maximum value being a 0.472°C

anomaly. Intensity and translation speed profiles are created for cool and warm years by finding the average maximum values for each cyclone passing within 100 km of each track point during the appropriate years. The track stops 100 km inland due to decreasing sample size.

Figure 5.5 displays the EAFB intensity profile for the a) cool and b) warm years, along with the standard error of the mean. It is important to note that the time frame for these graphs is 1951–2006, differing from that of Figure 5.4, which is based on data over the period 1851–2008. The number of events used to calculate the means are given above the horizontal axis. Larger samples during the cooler years mean that since 1951, more tropical cyclones have passed nearby the average track in cooler years than warmer years. However, the warmer years exhibit greater wind speeds at each location. The highest average wind speed for warm years is 50 m s^{-1} (threshold for a Category 3 hurricane), occurring 800 km before landfall. The large standard error associated with the warm years suggests the possibility of much greater intensities. The warm years also exhibit the largest range of wind speeds along the track. During cooler years the average wind speed peaks at 42 m s^{-1} (a Category 2 hurricane), 600 km prior to landfall. On average, the hurricane makes landfall at Category 1 intensity for warm and cool years.

Figure 5.6 shows the average translation speed for the a) cool and b) warm years. There is little difference in forward speed of the average hurricane approaching EAFB between warm and cool years. The exception is near the coast. On average the warm years feature slower moving hurricanes as they approach and cross the coast. For warmer years, the slightly more intense hurricane will move more slowly over the landfall area. While it is difficult to draw conclusions from such a small sample size, these data suggest that more destruction may be expected from hurricanes occurring in warm years, or in a warming environment.

5.5 Summary

This chapter provides a methodology for developing a local-scale hurricane climatology and assessing the impact of SST on hurricane characteristics. Using Eglin Air Force Base (EAFB) as an example, an average hurricane track is created, and the average characteristics along the track are attained based off of past hurricane events. The process is repeated for warm and cool SST years. The results produce a track-relative climatology of the average EAFB hurricane, as well as the average warm- and cool-year EAFB hurricanes.

First, an average EAFB hurricane track is created based off of past hurricanes. A landfall point just west of EAFB on Santa Rosa Island, Florida is chosen because it places EAFB in the front right quadrant of the cyclone. Historical hurricanes (1851–2008) coming within 150 km of this point are selected, resulting in 26 hurricanes. A distance map is created for each hurricane, the values of which display the distance from the hurricane track to any point on the map. The distance maps are averaged using an inverse-distance weighted approach favoring the hurricanes that passed nearest the landfall point. A line down the center of the averaged distance map is the climatological EAFB hurricane track.

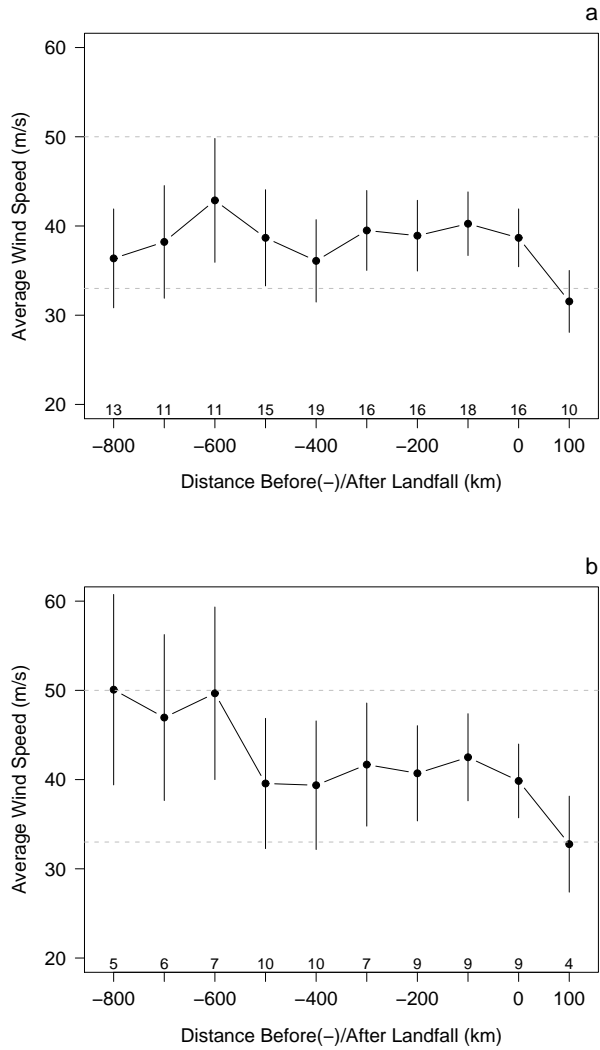


Figure 5.5: Average hurricane intensities along the average track for hurricanes during a) cool and b) warm SST years. Distances in kilometers before (negative) and after landfall are plotted on the horizontal axis. Standard errors (s.e.) about the mean intensities are drawn as vertical lines and the number of hurricanes used in the averaging are shown above the horizontal axis.

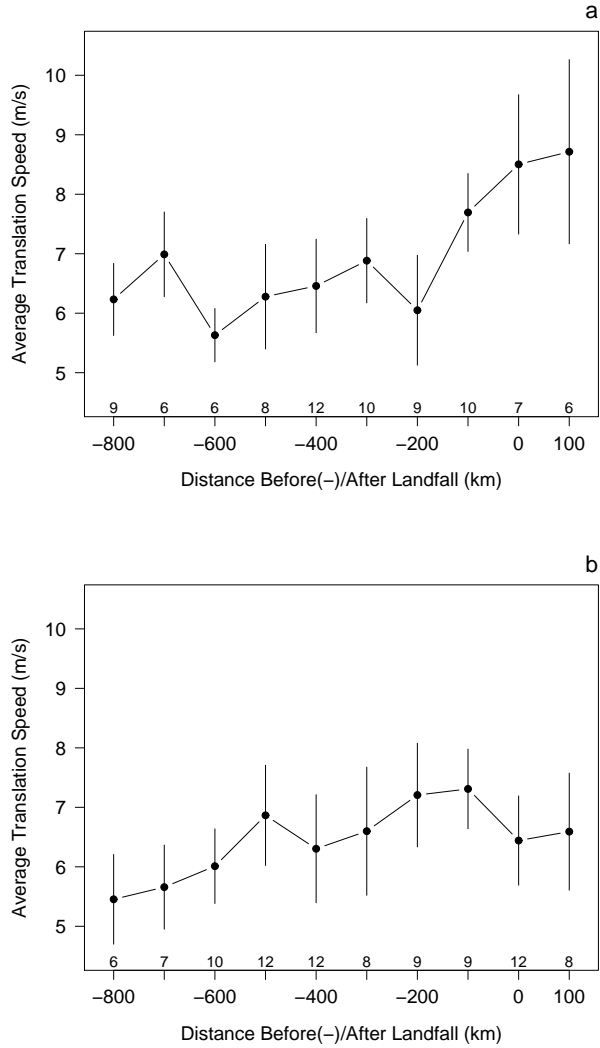


Figure 5.6: Average hurricane forward speed along the average track for hurricanes during a) cool and b) warm SST years. Distances in kilometers before (negative) and after landfall are plotted on the horizontal axis. Standard errors (s.e.) about the mean translation speed are drawn as vertical lines and the number of hurricanes used in the averaging are shown above the horizontal axis.

Next, hurricane characteristics are assigned to the average track. This is done by representing the track with a series of equal interval points, spaced in 100 km intervals before and after landfall. Past hurricanes coming within 100 km of these points are selected, and their maximum hourly-observation within the radii are averaged to represent the mean characteristics for that location. The average intensity and translation speed are shown in the form of track profiles, creating a track-relative climatology. The average EAFB hurricane reaches its maximum intensity of $52 \text{ m s}^{-1} \pm 2 \text{ m s}^{-1}$ (s.e.) 400 km prior to landfall. The cyclone continues to travel towards the coast at approximately 6.5 m s^{-1} , before making landfall with winds of 45 m s^{-1} .

The characteristics along the track are determined, this time using only those hurricanes occurring in warm or cool SST epochs. The lack of Caribbean SST data prior to 1951 makes it difficult to discern the impact of SSTs on EAFB hurricanes. However, since 1951, warm-year hurricanes have exhibited slightly higher wind speeds and moved a slower pace than their cold-year counterparts. In addition to increased wind speed, higher storm surge should also occur with warmer SSTs for two reasons. First, greater wind speeds result in a higher surge. Second, storm surge is best correlated with wind speeds farther from the coast, rather than wind speeds at landfall (Jordan and Clayson, 2008). Thus, the relatively larger difference between the pre-landfall wind speeds in warm versus cool years will likely result in large differences of surge damage. Since an increase in surge and wind speeds will cause more destruction, the economic impacts of warmer SSTs should be further analyzed.

While EAFB is likely to accrue greater hurricane damages per hurricane in a warmer climate, it may be especially worthwhile to look at strongest storms. Since the most intense hurricanes are the most destructive, and are already exhibiting strengthening in the North Atlantic (Elsner et al., 2008b), it would be useful to analyze the affect of changing SSTs on major hurricanes. This chapter provides a methodology for obtaining a local-scale hurricane climate and the basis for understanding the affects of SSTs on the hurricane characteristics. The technique can be made more useful with additional variables such as storm surge and economic loss, and by employing return levels to look at the most extreme events relative to warmer and cooler SST years.

CHAPTER 6

CONCLUSION

A hurricane spins poleward like a top, steered by high and low pressure patterns and the coriolis force. Sometimes the hurricane is pushed towards land, and suddenly nature's mechanism for distributing global heat has catastrophic effects. Understanding the tracking of hurricanes is integral for coastline preparation and mitigation. This dissertation investigates a technique for visualizing hurricane tracks that helps decipher their overall patterns. This involves constructing an average track from a selected set of hurricanes.

The technique involves using distance maps to average polylines. Presented in Chapter 2, this method provides a way to summarize large sets of spatial polyline data. Each polyline has its own distance map, which shows the distance from the polyline to any point on the map. The distance maps are subsequently stacked and the values averaged. The average distance map can be visualized as contours of average distance in units of x (longitude for most spatial data). A line digitized down the center of the contours through a chosen range of values is the average polyline. The average polyline can be thought of as the line of smallest average distance to the original polyline set. Two examples are shown where this technique may be used in hurricane research which utilize an inverse-distance weighted average that weights some of the hurricane tracks more heavily. These ideas are applied in more detail in Chapters 3–5.

In Chapter 3 the distance-map averaging technique is used to reconstruct historical hurricane tracks. Historical hurricanes are those prior to 1851 that have been uncovered through written documents, such as ship logs and newspapers. For example, Chenoweth (2006) is a comprehensive list of hurricanes from 1700–1855 that have been uncovered using historical documents. Each of the hurricanes is listed as a series of 1–4 locations of observation. These locations are largely qualitative, so the first step is digitizing the locations by approximating their latitude and longitude coordinates. Now the location data can be plotted, but there are large gaps between most hurricane observations. Since hurricanes move in predictable patterns, the average track of similar recent hurricanes provides clues about where the historical event was likely to travel. Recent hurricanes passing nearest the known historical hurricane landfall points are averaged, constructing a possible track for the series of points.

Chapter 4 is an example of using the distance map technique for a more operational problem- local hurricane risk analysis. A spatial climatology is created for Eglin Air Force

Base (EAFB), which is located on the Florida Panhandle, in order to obtain information about major hurricane tracks affecting the base. This is achieved by using distance maps of past major (Category 3 or higher) EAFB hurricanes to find an average major hurricane track. Next, characteristics (intensity, size, etc.) of a 100-year EAFB hurricane are added to the track, creating a track-relative climatology. This climatology is entered into a deterministic model to obtain wind fields and damage estimates associated with a 100-year event. The process of using local hurricane statistics in a deterministic model is a simple, dynamic way to address local hurricane risk.

Chapter 5 also looks at EAFB hurricane risk, but this time in a variable climate. A track is made for the “typical” EAFB hurricane, meaning all hurricane strengths are included in the averaging. Then, using information from past hurricanes, characteristics are applied to the track for both warm and cool SST anomaly years. Combining the methods of Chapters 4 and 5 can begin to provide information about how economic loss may change relative to climate. This is discussed in section 6.2. The remainder of this chapter summarizes the outcomes of this dissertation and additional applications of distance-map averaging in hurricane climate research.

6.1 Summary of Outcomes

The outcomes of this research include a set of tools, data, and analysis. Also, the research is clearly a basis for future spatial hurricane climatology research.

6.1.1 Tools

Three specific tools (or techniques) were created in this research. In Chapter 2 I introduce a tool for averaging polylines that may adapted for various spatial datasets. The technique was developed using R, but is described in generic terms so that any GIS software with distance map functionality may be employed. This dissertation applies the technique to hurricanes, but it is useful for any relevant spatial polyline data set. In Chapter 3 I describe a tool for constructing historical hurricane tracks. This is also done using R, and the R code for selecting modern tracks is available on the Hurricane Climate Lab’s website at myweb.fsu.edu/jelsner/Data.html. The remainder of the technique uses the methods described in Chapter 2 for averaging distance maps. Finally, in Chapter 4 I create a track-relative climatology- a tool for local-scale hurricane risk analysis. This involves creating an average track for a location using the distance map technique, and adding hurricane characteristics that enable simulation of the hurricane. The specific example is for EAFB, but may be easily adjusted to analyze any hurricane-prone area.

6.1.2 Data

In Chapter 3, the Chenoweth Archive is digitized, meaning the qualitative locations are given approximate latitude and longitude coordinates. The digitization method is based

on the type of location given. For example, for an island the central point of the island is found. The entire archive is digitized, providing approximate coordinates for all of the listed locations. These data are available online at myweb.fsu.edu/jelsner/extspace/ChenowethArchive.csv, and in the appendix (Table A.1). Also, there is the potential to provide a set of historical hurricane tracks based off of the Chenoweth Archive and the methods in this paper. Prior to creating a database of tracks the methods may be further analyzed, as discussed in Section 6.2.1.

6.1.3 Analysis

In addition to providing a tool set for spatial hurricane studies, this dissertation provides an analysis of the techniques that were created for this dissertation. Chapter 3 analyzes the abilities of using known past hurricane tracks to reconstruct historical events. The technique is tested by attempting to construct known tracks using only a few of their locations. Specifically, this is done for Hurricanes Charley and Dennis. It was shown that the methods are capable of constructing a fairly accurate track with the use of only a few locations. The technique is more reliable with a large number of locations that are more dispersed over space. Filtering the track analogs by time of year may also help the track-construction reliability.

The application of the techniques also provides an analysis of the risk of hurricane winds specific to EAFB, and how EAFB hurricanes are affected by climate variability. Chapter 4 concludes with information about hurricane wind risk to the area, and associated economic loss estimates. It was shown that EAFB can expect sustained winds of approximately 58 m s^{-1} every 100 years. A hurricane of this force will cause over \$500 million worth of wind damage alone. This information is the beginning of an assessment of EAFB hurricanes in a changing climate and assists the military in proper mitigation and preparation.

6.2 Future Research

This work describes two applications of spatial hurricane climatologies, but opens the door for additional research that may utilize the presented techniques. Here I discuss two specific continuations of this research.

6.2.1 Comparing Constructed Hurricane Tracks

In Chapter 3 I present a methodology for constructing historical hurricane tracks. The methodology is especially useful for constructing tracks when provided only a few locations, such as in Chenoweth (2006). While the archived data are useful for hurricane researchers, Michael Chenoweth, the author of the chronology, has more data (from both sources and his own intuition) in the form of hand drawn maps. These maps are not digital, therefore not available to the public, and are partly based on his best estimate of the cyclone's behavior.

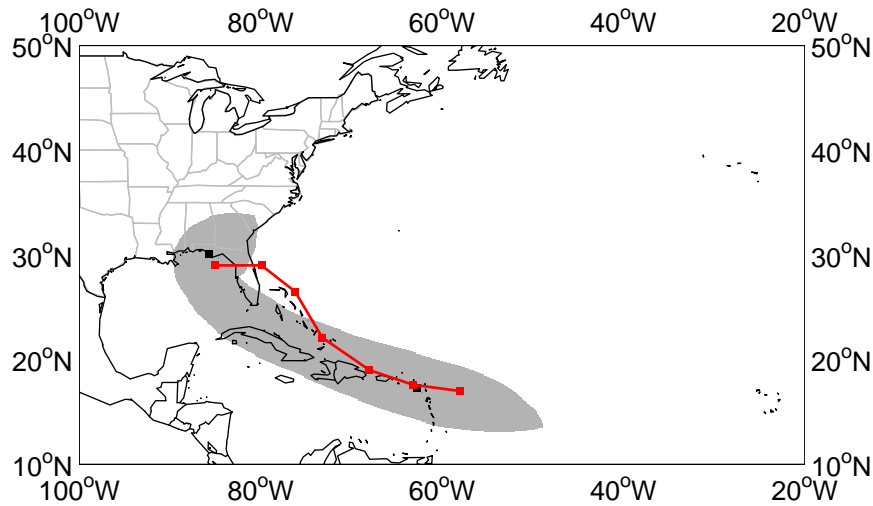


Figure 6.1: Two reconstructions of Storm No. 314. The shaded area is our climatological pathway, and the line is a digitized version of the hand-drawn track of Michael Chenoweth. Comparisons like this may help refine the technique for reconstructing historical hurricanes.

One way to testing the methodology presented in this dissertation is to compare the constructed tracks to the hand-drawn tracks of Michael Chenoweth. While we will never know the exact track of the hurricane, we will see if this methodology produces a similar track to one that is produced using all uncovered knowledge of the cyclone. This will give a general idea of the validity of the track construction methodology presented in this work.

To compare the constructed tracks to those of Michael Chenoweth, a small sample of hand-drawn tracks have been obtained from Chenoweth. Figure 6.1 depicts two renditions of Storm 314. The line shows the hurricane as constructed by Michael Chenoweth using historical information, while the gray pathway is constructed using the technique described above. The approximation of the pathway's ability to represent Chenoweth's hurricane account can be obtained from the contour values of the average distance map. If it shows that it is worthwhile to use the distance map method to construct the tracks, an entire set of historical hurricane tracks may be constructed and available for use in modern hurricane climate research.

One weakness with the methodology presented here may be the lack of modern tracks. Some hurricanes are limited to only a few realistic analogs for use in track construction.

Additionally, Chapter 3 shows that filtering the analogs by time of year may provide a more realistic track, but in most cases this is too limiting on the data set. A way to overcome this would be using synthetic tracks, such as those of Kerry Emanuel. This way, an unlimited number of track analogs can be created based on the physical possibilities, rather than only those that have occurred. This will allow for increased screening of the analogs as well-based on time of year, intensity, or other information that will help provide the most realistic hurricane analogs for the archived event. Using these hurricanes in place of the best track data provides a third comparison that will help develop the best possible technique for historical hurricane reconstruction.

6.2.2 Spatial Patterns of Major Hurricanes

Chapters 2 and 4 use the average major hurricane tracks for Galveston and the Florida Panhandle, respectively. During both of these constructions, it was noticed that the major hurricane tracks have more in common (average distances are less) than the track sets inclusive of weaker events. For example, Figure 6.2 shows the ten hurricanes (wind speeds $\geq 33 \text{ m s}^{-1}$) passing nearest Galveston, and their average distance map. Further, Figure 6.3 shows the same for the ten nearest tropical storms (wind speeds $\geq 18 \text{ m s}^{-1}$). When comparing the map of major hurricanes to one inclusive of all hurricanes and tropical storms, it is evident that the weaker storm tracks are more random, and travel an increased number of directions. This causes the contours to be more circular rather than suggestive of a reasonable track. Polyline similarity testing, as mentioned in Chapter 2, would provide more information regarding their spatial similarities.

Much of this dissertation focuses on the spatial patterns of hurricanes, and, in this section in particular, the clustering of the strongest tracks. There may also be some temporal clustering of the strongest hurricanes. For example, in the late 19th century Georgia was hit by a handful of major hurricanes. However, approximately 110 years have passed and Georgia is yet to be hit by another hurricane of such intensity. This could perhaps be related to the climate scenarios that encourage a major Georgia hurricane. This section shows that in order for a hurricane to reach major intensities it may require more specific standards-including a specific track on top of favorable climate conditions along that track. Thus, since the 19th century, the specific standards may have not been met. This is another example of how the tracking of hurricanes is seen as a return rate at the local level- not only for frequency, but also on intensity. It is also another illustration of the space-time hurricane problem.

The methods presented in this dissertation provide a way to further analyze the spatial and temporal clustering of major hurricane tracks. For example, creating average major hurricane tracks for locations relative to climate controls such as El Niño Southern Oscillation and sea surface temperatures may provide more information regarding their spatial patterns. It is shown that the spatial patterns of hurricanes is important for adequate coast-line preparation, and this dissertation provides the tools and analysis to provide a deeper understanding of these patterns.

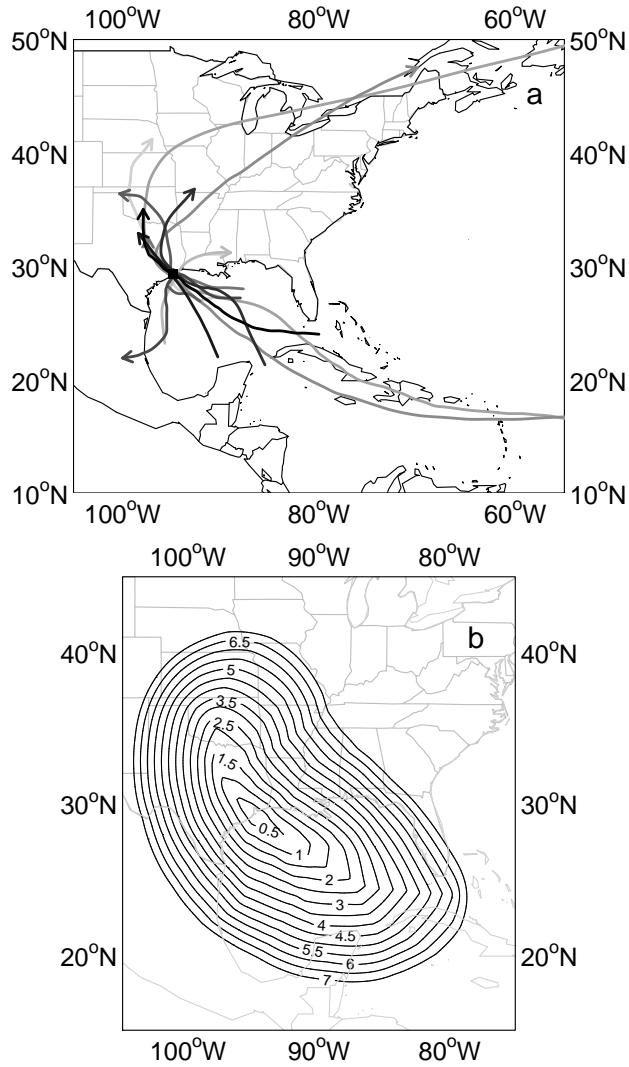


Figure 6.2: Creating an average Galveston hurricane track. a) The 10 hurricanes (wind speeds $\geq 33 \text{ m s}^{-1}$) passing nearest Galveston between 1851 and 2008. b) The average distance map of the 10 tracks. These tracks have slightly less in common than the 10 major hurricane (wind speeds $\geq 50 \text{ m s}^{-1}$) tracks used in Figure 2.2 as indicated by their average distance map in Figure 2.3.

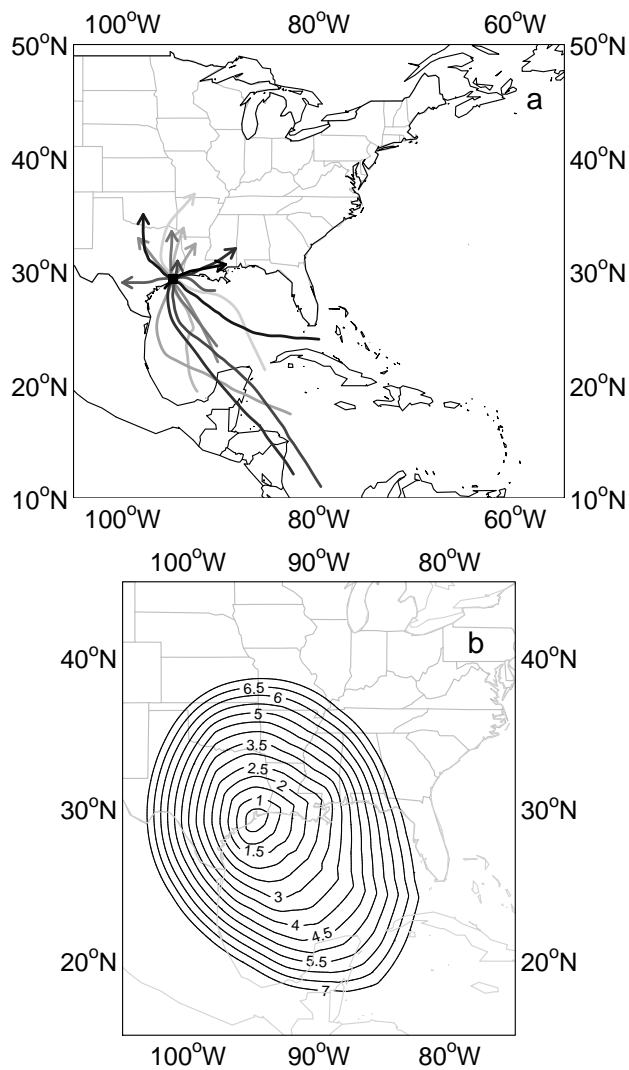


Figure 6.3: Creating an average Galveston tropical storm track. a) The 10 tropical storms and hurricanes (wind speeds $\geq 18 \text{ m s}^{-1}$) passing nearest Galveston between 1851 and 2008. b) The average distance map of the 10 tracks. These tracks have slightly less in common than the 10 hurricane tracks used in Figure 6.2 as indicated by their average distance map.

6.2.3 Return Levels of Economic Loss

In Chapter 4, economic loss is estimated for a 100-year EAFB hurricane. The losses are obtained from HAZUS, which bases the estimations on damage from hurricane winds. Repeating this process for hurricanes of various return rates (10-year, 20-year, etc) provides a set of return levels for economic loss of hurricane winds. Further, by modeling the hurricanes in a storm surge model such as SLOSH, storm surge heights and perhaps total economic loss estimates can be obtained. This information is useful for insurance companies, emergency managers, and other stakeholders, providing them with information about the return rates of hurricanes of various intensities and their likely effects based on the current climate.

That being said, the climate is changing and hurricanes are changing with it. Emanuel (2005) shows that there is an increasing trend in hurricane destruction that may be partially due to a warming climate. I have mentioned several times that the combination of methods used here- statistics to deterministic modeling- is useful because it can easily be altered to represent a changing climate, compared to the widely-used “downscaling approach” to climate research. Chapter 5 shows how a track-relative climatology may be created for warm and cool SST anomalies. In this case, a track climatology should be made that merges the methods from Chapters 4 and 5 by finding the return levels associated with the warmer and cooler years. Then, a “100-cooler-year” hurricane can be compared to its warmer year counterpart. Ultimately, this can result in economic loss information from a set of hurricanes in warmer and cooler years, which can provide a glimpse into what may happen with a change in climate. Indeed, the impacts of climate change are more far-reaching than SST variability, but this is still a valuable way to examine possible climate impacts on hurricane damage.

6.3 Concluding Remarks

Understanding the tracking of a hurricane is an important part of assessing local hurricane risk. This dissertation provides the basis for analyzing hurricane tracks and other spatial polyline data. The previous chapters display the broad utility of this technique in hurricane climate research- from constructing historical hurricane tracks to estimating economic loss from a hypothetical 100-year event.

This work challenges hurricane climatologists to take a step back and think of the hurricane as an event across space rather than a local event with point characteristics. In doing so, a spatial hurricane climatology is created. The spatial climatology is useful in local hurricane risk assessment as well as basin-wide tracking patterns. Assessing a range of scales using the same technique may provide information about the hurricane-climate relationship that is not evident with a more narrow research scope.

In addition to hurricane tracks, the distance-map averaging technique is applicable for the geovisualization and exploration of any spatial polyline data set. Perhaps, similarly to my experience with hurricane climate, upon adopting this technique researchers will find the potential for numerous applications of the methodology for investigation in their field.

It is my hopes that this work will encourage exploration of the spatial patterns of geographic phenomena, and further, more techniques for the analysis of spatial polyline data.

APPENDIX A

**DIGITIZED CHENOWETH ARCHIVE
LOCALITIES**

Table A.1: Digitized Version of the Chenoweth Archive. The year, month (M1 and M2) and days (D1 and D2) of the first and last event from the hurricane are given. The Storm Number (SN) and maximum intensity (hurricane (HU) or tropical storm (TS)) are as listed in the Chenoweth Archive. The track is the description listed in the archive. The point (Pt) refers to the event number of the given event (1–4) and the location is the description Chenoweth assigned to that point. Last are the method used to digitize the point (M), and the resulting latitude and longitude locations.

Year	M1	D1	M2	D2	SN	Int	Track	Pt	Location	M	LAT	LON
1700	9	13	9	14	1	HU	South Carolina and Virginia	1	South Carolina	3	32.87	-79.63
1700	9	13	9	14	1	HU	South Carolina and Virginia	2	Virginia	3	37.29	-75.58
1700	9	20	9	20	2	HU	Barbados	1	Barbados	4	13.18	-59.56
1702	9	24	9	26	3	HU	Barbados to 1711N 6949W	1	Barbados	4	13.18	-59.56
1702	9	24	9	26	3	HU	Barbados to 1711N 6949W	2	1711N 6949W	1	17.18	-69.82
1703	10	18	10	19	4	HU	Virginia to New England	1	Virginia	3	37.29	-75.58
1703	10	18	10	19	4	HU	Virginia to New England	2	New England	9	42.80	-70.66
1705	8	16	8	18	5	HU	Havana, southeast coast of Florida	1	Havana	2	23.13	-82.38
1705	8	16	8	18	5	HU	Havana, southeast coast of Florida	2	Southeast Coast of Florida	8	26.71	-80.06
1706	10	5	10	15	6	TS	Barbados to New England	1	Barbados	4	13.18	-59.56
1706	10	5	10	15	6	TS	Barbados to New England	2	New England	9	42.80	-70.66
1707	9	9	9	11	7	HU	Nevis, Antigua, Montserrat, St. Thomas	1	Antigua	4	17.28	-61.79
1707	9	9	9	11	7	HU	Nevis, Antigua, Montserrat, St. Thomas	2	St. Thomas	4	18.33	-64.92
1707	10	30	10	30	8	HU	St. Augustine, Florida	1	St. Augustine, FL	2	29.53	-81.19
1712	9	6	9	10	9	HU	Barbados-Jamaica-Cuba	1	Barbados	4	13.18	-59.56
1712	9	6	9	10	9	HU	Barbados-Jamaica-Cuba	2	Jamaica	4	18.15	-77.31
1712	9	6	9	10	9	HU	Barbados-Jamaica-Cuba	3	Cuba	4	21.61	-79.03
1712	9	19	9	19	10	HU	Bermuda	1	Bermuda	4	32.31	-64.75
1713	9	4	9	6	11	HU	Lesser Antilles, Puerto Rico	1	Lesser Antilles	9	13.90	-60.97
1713	9	4	9	6	11	HU	Lesser Antilles, Puerto Rico	2	Puerto Rico	4	18.23	-66.48
1713	9	10	9	17	12	HU	North of Antigua to South Carolina	1	North of Antigua	6	18.28	-61.79
1713	9	10	9	17	12	HU	North of Antigua to South Carolina	2	South Carolina	3	32.87	-79.63
1713	10	7	10	15	13	HU	Antigua to Nova Scotia	1	Antigua	4	17.28	-61.79
1713	10	7	10	15	13	HU	Antigua to Nova Scotia	2	Nova Scotia	4	44.85	-63.20
1713	10	24	10	26	14	HU	Jamaica (to Bermuda?)	1	Jamaica	4	18.15	-77.31
1713	10	24	10	26	14	HU	Jamaica (to Bermuda?)	2	Bermuda	4	32.31	-64.75
1714	8	13	8	14	15	HU	Guadeloupe	1	Guadeloupe	9	16.24	-61.53
1714	9	5	9	9	16	TS	Barbados to Jamaica	1	Barbados	4	13.18	-59.56
1714	9	5	9	9	16	TS	Barbados to Jamaica	2	Jamaica	4	18.15	-77.31
1715	7	21	7	31	17	HU	Barbados to Florida	1	Barbados	4	13.18	-59.56
1715	7	21	7	31	17	HU	Barbados to Florida	2	Florida	9	28.66	-82.50
1715	8	26	8	26	18	HU	Tampico, Mexico	1	Tampico, Mexico	2	22.23	-97.85
1715	10	14	10	20	19	HU	West of Jamaica to Mobile, Alabama	1	West of Jamaica	6	18.27	-79.37
1715	10	14	10	20	19	HU	West of Jamaica to Mobile, Alabama	2	Mobile, AL	2	30.68	-88.03
1716	8	20	8	20	20	HU	Bermuda	1	Bermuda	4	32.31	-64.75

1716	10	13	10	22	21	HU	Jamaica to Alabama to off New England	1	Jamaica	4	18.15	-77.31
1716	10	13	10	22	21	HU	Jamaica to Alabama to off New England	2	Alabama	3	30.27	-87.89
1716	10	13	10	22	21	HU	Jamaica to Alabama to off New England	3	off New England	6	41.11	-69.43
1718	9	6	9	7	22	HU	Antigua, Puerto Rico	1	Antigua	4	17.28	-61.79
1718	9	6	9	7	22	HU	Antigua, Puerto Rico	2	Puerto Rico	4	18.23	-66.48
1718	9	19	9	21	23	HU	Martinique	1	Martinique	4	14.65	-61.01
1720					24	HU	North of Puerto Rico to Florida Straits	1	North of Puerto Rico	6	19.38	-66.58
1720					24	HU	North of Puerto Rico to Florida Straits	2	Florida Straits	9	23.93	-80.93
1722	9	6	9	12	25	HU	Jamaica to Louisiana	1	Jamaica	4	18.15	-77.31
1722	9	6	9	12	25	HU	Jamaica to Louisiana	2	Louisiana	3	29.33	-91.38
1722	9	18	9	23	26	TS	Charleston, South Carolina	1	Charleston, SC	2	32.77	-79.92
1723	8	4	8	9	27	HU	North of Antigua to New York City	1	North of Antigua	6	18.28	-61.79
1723	8	4	8	9	27	HU	North of Antigua to New York City	2	New York City	2	40.70	-74.00
1724	8	22	8	30	28	HU	Lesser Antilles to South Carolina to Pennsylvania	1	Lesser Antilles	9	13.90	-60.97
1724	8	22	8	30	28	HU	Lesser Antilles to South Carolina to Pennsylvania	2	South Carolina	3	32.87	-79.63
1724	8	22	8	30	28	HU	Lesser Antilles to South Carolina to Pennsylvania	3	Pennsylvania	3	39.72	-76.38
1725	9	23	9	24	29	HU	Martinique	1	Martinique	4	14.65	-61.01
1726	9	11	9	19	30	HU	North of Antigua to Bermuda	1	North of Antigua	6	18.28	-61.79
1726	9	11	9	19	30	HU	North of Antigua to Bermuda	2	Bermuda	4	32.31	-64.75
1726					31	HU	Bermuda	1	Bermuda	4	32.31	-64.75
1726	11	1	11	2	32	HU	Jamaica	1	Jamaica	4	18.15	-77.31
1727	9	24	9	27	33	HU	3837N 6715W; Eastern New England	1	3837N 6715W	1	38.62	-67.25
1727	9	24	9	27	33	HU	3837N 6715W; Eastern New England	2	Eastern New England	9	42.80	-70.66
1728	8	13	8	14	34	HU	Charleston, South Carolina	1	Charleston, SC	2	32.77	-79.92
1728	8	28	9	2	35	HU	Antigua to St. Thomas to Hispanolia	1	Antigua	4	17.28	-61.79
1728	8	28	9	2	35	HU	Antigua to St. Thomas to Hispanolia	2	St. Thomas	4	18.33	-64.92
1728	8	28	9	2	35	HU	Antigua to St. Thomas to Hispanolia	3	Hispaniola	4	19.00	-70.67
1728	8	31	9	8	36	HU	North of Leewards to Bermuda to 42N 53W	1	North of Leewards	6	18.71	-61.85
1728	8	31	9	8	36	HU	North of Leewards to Bermuda to 42N 53W	2	Bermuda	4	32.31	-64.75
1728	8	31	9	8	36	HU	North of Leewards to Bermuda to 42N 53W	3	42N 53W	1	42.00	-53.00
1728	9	21	9	30	37	HU	Antigua to 33N 71W	1	Antigua	4	17.28	-61.79
1728	9	21	9	30	37	HU	Antigua to 33N 71W	2	33N 71W	1	33.00	-71.00
1729	8	14	8	19	38	HU	Northern Leeward Islands to South Carolina	1	Northern Leeward Islands	8	17.28	-69.79
1729	8	14	8	19	38	HU	Northern Leeward Islands to South Carolina	2	South Carolina	3	32.87	-79.63
1730	8	26	9	7	39	HU	Barbados to South Carolina	1	Barbados	4	13.18	-59.56
1730	8	26	9	7	39	HU	Barbados to South Carolina	2	South Carolina	3	32.87	-79.63
1730	10	15	10	20	40	HU	Jamaica, Cuba	1	Jamaica	4	18.15	-77.31
1730	10	15	10	20	40	HU	Jamaica, Cuba	2	Cuba	4	21.61	-79.03
1731	8	24	9	5	41	HU	Barbados to Windward Passage to off SC to 41N 51W	1	Barbados	4	13.18	-59.56
1731	8	24	9	5	41	HU	Barbados to Windward Passage to off SC to 41N 51W	2	Windward Passage	9	20.00	-75.83
1731	8	24	9	5	41	HU	Barbados to Windward Passage to off SC to 41N 51W	3	off SC	6	32.77	-78.92
1731	8	24	9	5	41	HU	Barbados to Windward Passage to off SC to 41N 51W	4	41N 51W	1	41.00	-51.00
1733	7	10	7	16	42	HU	Central Lesser Antilles to Florida Straits	1	Central Lesser Antilles	8	13.90	-60.97
1733	7	10	7	16	42	HU	Central Lesser Antilles to Florida Straits	2	Florida Straits	9	23.93	-80.93
1733	9		9		43	HU	Florida Keys to Alabama	1	Florida Keys	9	24.67	-81.54

1733	9				43	HU	Florida Keys to Alabama		2	Alabama	3	30.27	-87.89
1734	9	9	9	12	44	HU	Barbados to Jamaica		1	Barbados	4	13.18	-59.56
1734	9	9	9	12	44	HU	Barbados to Jamaica		2	Jamaica	4	18.15	-77.31
1736	9	16	9		45	HU	West of Grand Cayman to Pensacola, Florida		1	West of Grand Cayman	6	19.28	-82.37
1736	9	16	9		45	HU	West of Grand Cayman to Pensacola, Florida		2	Pensacola, FL	2	30.42	-87.22
1737	9	7	9	10	46	HU	Antigua to Hispanolia		1	Antigua	4	17.28	-61.79
1737	9	7	9	10	46	HU	Antigua to Hispanolia		2	Hispaniola	4	19.00	-70.67
1738	8	7	8	31	47	HU	Antigua to Puerto Rico		1	Antigua	4	17.28	-61.79
1738	8	7	8	31	47	HU	Antigua to Puerto Rico		2	Puerto Rico	4	18.23	-66.48
1740	9	8	9	22	48	HU	Antigua to Nassau to Dry Tortugas to Louisiana		1	Antigua	4	17.28	-61.79
1740	9	8	9	22	48	HU	Antigua to Nassau to Dry Tortugas to Louisiana		2	Nassau	2	25.08	-77.35
1740	9	8	9	22	48	HU	Antigua to Nassau to Dry Tortugas to Louisiana		3	Dry Totugas	9	24.65	-82.85
1740	9	8	9	22	48	HU	Antigua to Nassau to Dry Tortugas to Louisiana		4	Louisiana	3	29.33	-91.38
1740	9	29	9	29	49	HU	Mobile, Alabama		1	Mobile, AL	2	30.68	-88.03
1742	10	25	10	31	50	TS	Virgin Islands to Puerto Rico to Hispanolia		1	Virgin Islands	9	18.34	-64.75
1742	10	25	10	31	50	TS	Virgin Islands to Puerto Rico to Hispanolia		2	Puerto Rico	4	18.23	-66.48
1742	10	25	10	31	50	TS	Virgin Islands to Puerto Rico to Hispanolia		3	Hispaniola	4	19.00	-70.67
1743	9	10	9	10	51	HU	Jamaica Fleet and South Carolina coast		1	Jamaica Fleet	9	18.15	-77.31
1743	9	10	9	10	51	HU	Jamaica Fleet and South Carolina coast		2	South Carolina coast	7	32.87	-79.63
1743	10	28	11	4	52	TS	Jamaica to off coast of U.S.		1	Jamaica	4	18.15	-77.31
1743	10	28	11	4	52	TS	Jamaica to off coast of U.S.		2	off coast of U.S.	6	29.38	-76.45
1744	10	31	11	1	53	HU	Jamaica, Cuba		2	Cuba	4	18.15	-77.31
1744	10	31	11	1	53	HU	Jamaica, Cuba		1	Jamaica	4	21.61	-79.03
1745	10	16	10	19	54	TS	Windward Passage		1	Windward Passage	9	20.00	-75.83
1746	9	10	9	14	55	HU	Barbados to Florida Keys to central U.S. Gulf Coast		1	Barbados	4	13.18	-59.56
1746	9	10	9	14	55	HU	Barbados to Florida Keys to central U.S. Gulf Coast		2	Florida Keys	9	24.67	-81.54
1746	9	10	9	14	55	HU	Barbados to Florida Keys to central U.S. Gulf Coast		3	central U.S. Gulf Coast	8	29.79	-89.04
1747	9	26	9	27	56	HU	3847N 5423W to 4014N 5254W		1	3847N 5423W	1	38.78	-54.38
1747	9	26	9	27	56	HU	3847N 5423W to 4014N 5254W		2	4014N 5254W	1	40.23	-52.90
1747	9	29	10	6	57	HU	Lesser Antilles to 4306N 5530W		1	Lesser Antilles	9	13.90	-60.97
1747	9	29	10	6	57	HU	Lesser Antilles to 4306N 5530W		2	4306N 5530W	1	43.10	-55.50
1747	10	13	10	18	58	HU	Jamaica to Nassau to Bermuda		1	Jamaica	4	18.15	-77.31
1747	10	13	10	18	58	HU	Jamaica to Nassau to Bermuda		2	Nassau	2	25.08	-77.35
1747	10	13	10	18	58	HU	Jamaica to Nassau to Bermuda		3	Bermuda	4	32.31	-64.75
1747	11	3	11	6	59	HU	St. Kitts		1	St. Kitts	4	17.30	-62.73
1749	9	16	9	21	60	HU	Dominica to Rattan (Bay of Honduras)		1	Dominica	4	15.43	-61.36
1749	9	16	9	21	60	HU	Dominica to Rattan (Bay of Honduras)		2	Rattan	4	16.30	-86.50
1749	10	14	10	21	61	HU	Jamaica to Delaware		1	Jamaica	4	18.15	-77.31
1749	10	14	10	21	61	HU	Jamaica to Delaware		2	Delaware	3	38.70	-74.99
1750	8	29	8	30	62	HU	28-29N off Florida to Virginia Capes		1	28-29N off Florida	9	28.50	-79.53
1750	8	29	8	30	62	HU	28-29N off Florida to Virginia Capes		2	Virginia Capes	9	37.29	-75.58
1751	7	24	7	24	63	HU	Havana		1	Havana	2	23.12	-82.35
1751	9	18	9	28	64	HU	Antigua to Jamaica to Florida		1	Antigua	4	17.28	-61.79
1751	9	18	9	28	64	HU	Antigua to Jamaica to Florida		2	Jamaica	4	18.15	-77.31
1751	9	18	9	28	64	HU	Antigua to Jamaica to Florida		3	Florida	9	28.66	-82.50

1751	10	6	10	7	65	TS	Jamaica	1	Jamaica	4	18.15	-77.31
1752	9	8	9	16	66	HU	St. Kitts to South Carolina	1	St. Kitts	4	17.30	-62.73
1752	9	8	9	16	66	HU	St. Kitts to South Carolina	2	South Carolina	3	32.87	-79.63
1752	9	26	10	2	67	HU	Havana to Nova Scotia	1	Havana	2	23.12	-82.35
1752	9	26	10	2	67	HU	Havana to Nova Scotia	2	Nova Scotia	4	44.85	-63.20
1752	10	28	11	3	68	HU	Havana to Pensacola	1	Havana	2	23.12	-82.35
1752	10	28	11	3	68	HU	Havana to Pensacola	2	Pensacola, FL	2	30.42	-87.22
1753	8	24	8	25	69	TS	Cumberland Is., Georgia	1	Cumberland Is., GA	4	30.85	-81.43
1754	9	12	9	26	70	HU	Lesser Antilles to off North Carolina	1	Lesser Antilles	9	13.90	-60.97
1754	9	12	9	26	70	HU	Lesser Antilles to off North Carolina	2	off North Carolina	6	35.75	-74.55
1755	10	8	10	8	71	TS	Jamaica	1	Jamaica	4	18.15	-77.31
1756	9	12	9	17	71	HU	Leewards Islands to Jamaica	1	Leeward Islands	9	17.30	-62.73
1756	9	12	9	17	71	HU	Leewards Islands to Jamaica	2	Jamaica	4	18.15	-77.31
1756	10	1	10	3	72	HU	Cayman Islands, Cuba	1	Cayman Islands	9	19.30	-81.38
1756	10	1	10	3	72	HU	Cayman Islands, Cuba	2	Cuba	4	21.61	-79.03
1757	9	1	9	3	73	HU	Eastern New England, Nova Scotia	1	Nova Scotia	4	44.85	-63.20
1757	9	1	9	3	73	HU	Eastern New England, Nova Scotia	1	Eastern New England	9	42.80	-70.66
1758	8	22	8	24	74	HU	Lesser Antilles	1	Lesser Antilles	9	13.90	-60.97
1758	10	17	10	24	75	HU	West of Jamaica to Florida to New Jersey coast	1	West of Jamaica	6	18.27	-79.37
1758	10	17	10	24	75	HU	West of Jamaica to Florida to New Jersey coast	2	Florida	9	28.66	-82.50
1758	10	17	10	24	75	HU	West of Jamaica to Florida to New Jersey coast	3	New Jersey coast	7	39.68	-74.14
1759	9	12	9	15	76	HU	Near Jamaica to Southwest Florida	1	Near Jamaica	6	16.74	-77.27
1759	9	12	9	15	76	HU	Near Jamaica to Southwest Florida	2	Southwest, FL	8	27.74	-82.59
1760	7	6	7	6	77	TS	Charleston, South Carolina	1	Charleston, SC	2	32.77	-79.92
1760	8	12	8	12	78	HU	Pensacola, Florida	1	Pensacola, FL	2	30.42	-87.22
1760	9	7	9	8	79	HU	Vera Cruz, Mexico	1	Vera Cruz, Mexico	2	18.70	-89.07
1760	10	1	10	6	80	HU	Jamaica to South Carolina to 36N 72W	1	Jamaica	4	18.15	-77.31
1760	10	1	10	6	80	HU	Jamaica to South Carolina to 36N 72W	2	South Carolina	3	32.87	-79.63
1760	10	1	10	6	80	HU	Jamaica to South Carolina to 36N 72W	3	36N 72W	1	36.00	-72.00
1761	9	22	9	23	81	TS	West of Jamaica	1	West of Jamaica	6	18.27	-79.37
1761	10	19	10	25	82	HU	Northwest of Jamaica to Hispanolia to Quebec	1	Northwest of Jamaica	6	19.26	-79.00
1761	10	19	10	25	82	HU	Northwest of Jamaica to Hispanolia to Quebec	2	Hispaniola	4	19.00	-70.67
1761	10	19	10	25	82	HU	Northwest of Jamaica to Hispanolia to Quebec	3	Quebec	9	46.80	-71.28
1761	11	9	11	10	83	HU	Cartagena, Colombia	1	Cartagena, Colombia	2	10.38	-75.50
1762	10	4	10	5	84	TS	Southwest of Jamaica	1	Southwest of Jamaica	6	17.18	-78.31
1763	6	16	6	16	85	TS	West of Jamaica	1	West of Jamaica	6	18.27	-79.37
1763	11	5	11	6	86	TS	South of Jamaica	1	South of Jamaica	6	16.74	-77.27
1764	10	2	10	3	87	HU	Near western Jamaica	1	Near western Jamaica	6	18.27	-79.37
1764	11	16	11	20	88	HU	Apalachee Bay, Florida and western Carolinas	1	Apalachee Bay, FL	5	30.07	-84.02
1764	11	16	11	20	88	HU	Apalachee Bay, Florida and western Carolinas	2	western Carolinas	8	35.23	-80.84
1765	7	30	7	31	89	HU	Lesser Antilles	1	Lesser Antilles	9	13.90	-60.97
1765	8	7	8	16	90	HU	Lesser Antilles-Hispanolia-off New England coast	1	Lesser Antilles	9	13.90	-60.97
1765	8	7	8	16	90	HU	Lesser Antilles-Hispanolia-off New England coast	2	Hispaniola	4	19.00	-70.67
1765	8	7	8	16	90	HU	Lesser Antilles-Hispanolia-off New England coast	3	off New England coast	6	41.11	-69.43
1765	10	17	10	17	91	TS	South Carolina	1	South Carolina	3	32.87	-79.63

1765	11	13	11	14	92	TS	Caribbean to St. Domingo	1	Caribbean	5	15.16	-75.88
1765	11	13	11	14	92	TS	Caribbean to St. Domingo	2	St. Domingo	2	18.48	-69.92
1766	8	13	8	16	93	HU	Martinique to south of Jamaica	1	Martinique	4	14.65	-61.01
1766	8	13	8	16	93	HU	Martinique to south of Jamaica	2	south of Jamaica	6	16.74	-77.27
1766	9	1	9	4	94	HU	Gulf of Mexico to Texas	1	Gulf of Mexico	5	24.82	-90.14
1766	9	1	9	4	94	HU	Gulf of Mexico to Texas	2	Texas	3	28.40	-96.38
1766	9	8	9	13	95	TS	Atlantic to Off Virginia to west of New York City	1	Atlantic	9	31.36	-35.09
1766	9	8	9	13	95	TS	Atlantic to Off Virginia to west of New York City	2	Off Virginia	6	37.29	-74.58
1766	9	8	9	13	95	TS	Atlantic to Off Virginia to west of New York City	3	west of NYC	6	40.70	-75.00
1766	9	17	9	24	96	HU	Lesser Antilles to 2345N 6403W to 33N 57W to Azores	1	Lesser Antilles	9	13.90	-60.97
1766	9	17	9	24	96	HU	Lesser Antilles to 2345N 6403W to 33N 57W to Azores	2	2345N 6403W	1	23.75	-64.05
1766	9	17	9	24	96	HU	Lesser Antilles to 2345N 6403W to 33N 57W to Azores	3	33N 57W	1	33.00	-57.00
1766	9	17	9	24	96	HU	Lesser Antilles to 2345N 6403W to 33N 57W to Azores	4	Azores	9	38.65	-27.22
1766	10	5	10	13	97	HU	Lesser Antilles to Puerto Rico to off South Carolina	1	Lesser Antilles	9	13.90	-60.97
1766	10	5	10	13	97	HU	Lesser Antilles to Puerto Rico to off South Carolina	2	Puerto Rico	4	18.23	-66.48
1766	10	5	10	13	97	HU	Lesser Antilles to Puerto Rico to off South Carolina	3	off South Carolina	6	32.77	-78.92
1766	10	15	10	24	98	HU	South of Haiti and Jamaica to Pensacola, Florida	1	South of Haiti	6	16.52	-74.04
1766	10	15	10	24	98	HU	South of Haiti and Jamaica to Pensacola, Florida	2	Pensacola, FL	2	30.42	-87.22
1766	10	29	11	1	99	HU	Havana to east of Florida	1	Havana	2	23.12	-82.35
1766	10	29	11	1	99	HU	Havana to east of Florida	2	east of Florida	6	28.50	-79.53
1767	8	6	8	10	100	HU	Lesser Antilles to 3148N between SC and Bermuda	1	Lesser Antilles	9	13.90	-60.97
1767	8	6	8	10	100	HU	Lesser Antilles to 3148N between SC and Bermuda	2	3148N between SC and Bermuda	9	31.80	-72.30
1767	9	21	9	24	101	TS	Off North Carolina to southeast Massachusetts	1	Off North Carolina	6	35.75	-74.55
1767	9	21	9	24	101	TS	Off North Carolina to southeast Massachusetts	2	southeast Massachusetts	8	42.30	-71.80
1767	10	13	10	18	102	HU	Gulf of Mexico to SE US coastal waters to 35N 73W	1	Gulf of Mexico	5	24.82	-90.14
1767	10	13	10	18	102	HU	Gulf of Mexico to SE US coastal waters to 35N 73W	2	SE US coastal waters	9	29.38	-76.45
1767	10	13	10	18	102	HU	Gulf of Mexico to SE US coastal waters to 35N 73W	3	35N 73W	1	35.00	-73.00
1768	8	8	8	10	103	HU	Barbados to Grenada	1	Barbados	4	13.18	-59.56
1768	8	8	8	10	103	HU	Barbados to Grenada	2	Grenada	4	12.12	-61.68
1768	10	15	10	15	104	HU	Western Cuba	1	Western Cuba	8	22.41	-81.75
1769	8	7	8	9	105	TS	South of Jamaica	1	South of Jamaica	6	16.74	-77.27
1769	9	4	9	9	106	HU	23N 64W to New England	1	23N 64W	1	23.00	-64.00
1769	9	4	9	9	106	HU	23N 64W to New England	2	New England	9	42.80	-70.66
1769	9	28	9	29	107	TS	South Carolina	1	South Carolina	3	32.87	-79.63
1770	6	6	6	6	108	TS	Charleston, South Carolina	1	Charleston, SC	2	32.77	-79.92
1770	10	19	10	20	109	HU	3530N 7330W to New England	1	3530N 7330W	1	35.50	-73.50
1770	10	19	10	20	109	HU	3530N 7330W to New England	2	New England	9	42.80	-70.66
1771	5	23	5	24	110	TS	West of Jamaica to Cuba	1	West of Jamaica	6	18.27	-79.37
1771	5	23	5	24	110	TS	West of Jamaica to Cuba	2	Cuba	4	21.61	-79.03
1771	9	30	10	4	111	HU	Florida Keys to off South Carolina coast	1	Florida Keys	9	24.67	-81.54
1771	9	30	10	4	111	HU	Florida Keys to off South Carolina coast	2	off South Carolina coast	6	32.77	-78.92
1772	8	2	8	6	112	HU	Antigua to north of Jamaica to Bayamo, Cuba	1	Antigua	4	17.28	-61.79
1772	8	2	8	6	112	HU	Antigua to north of Jamaica to Bayamo, Cuba	2	north of Jamaica	6	19.48	-77.30
1772	8	2	8	6	112	HU	Antigua to north of Jamaica to Bayamo, Cuba	3	Bayamo, Cuba	2	20.37	-76.63
1772	8	30	9	3	113	HU	3330N 7455W to off Cape Henlopen	1	3330N 7455W	1	33.50	-74.92

1772	8	30	9	3	113	HU	3330N 7455W to off Cape Henlopen	2	Cape Henlopen	5	38.80	-74.10
1772	8	28	9	3	114	HU	Havana to Louisiana	1	Havana	2	23.12	-82.35
1772	8	28	9	3	114	HU	Havana to Louisiana	2	Louisiana	3	29.33	-91.38
1772	8	27	8	29	115	HU	North of Antigua	1	North of Antigua	6	18.28	-61.79
1772	8	29	9	5	116	HU	Antigua to western Cuba	1	Antigua	4	17.28	-61.79
1772	8	29	9	5	116	HU	Antigua to western Cuba	2	western Cuba	8	22.41	-81.75
1773	6	21	6	21	117	TS	Tobago to Grenada	1	Tobago	4	11.15	-60.67
1773	6	21	6	21	117	TS	Tobago to Grenada	2	Grenada	4	12.12	-61.68
1773	7	20	7	21	118	HU	Bahamas to Cuba	1	Bahamas	9	23.53	-75.83
1773	7	20	7	21	118	HU	Bahamas to Cuba	2	Cuba	4	21.61	-79.03
1773	8	26	8	26	119	HU	North Carolina to Virginia	1	North Carolina	3	34.69	-76.45
1773	8	26	8	26	119	HU	North Carolina to Virginia	2	Virginia	3	37.29	-75.58
1773	9	10	9	19	120	HU	Tobago to Venezuela to southwest of Western Cuba	1	Tobago	4	11.15	-60.67
1773	9	10	9	19	120	HU	Tobago to Venezuela to southwest of Western Cuba	2	Venezuela	3	10.58	-66.89
1773	9	10	9	19	120	HU	Tobago to Venezuela to southwest of Western Cuba	3	Southwest of Western Cuba	6	21.04	-85.29
1774	11	1	11	3	121	HU	Cuba to north of Bahamas to 30N 67W	1	Cuba	4	21.61	-79.03
1774	11	1	11	3	121	HU	Cuba to north of Bahamas to 30N 67W	2	north of Bahamas	6	25.98	-77.48
1774	11	1	11	3	121	HU	Cuba to north of Bahamas to 30N 67W	3	30 N 67 W	1	30.00	-67.00
1775	7	30	8	1	122	TS	Martinique to Puerto Rico	1	Martinique	4	14.65	-61.01
1775	7	30	8	1	122	TS	Martinique to Puerto Rico	2	Puerto Rico	4	18.23	-66.48
1775	8	24	9	3	123	HU	Barbados to Maryland	1	Barbados	4	13.18	-59.56
1775	8	24	9	3	123	HU	Barbados to Maryland	2	Maryland	3	38.23	-75.14
1775	9	5	9	12	124	HU	Leeward Islands to Newfoundland	1	Leeward Islands	9	17.30	-62.73
1775	9	5	9	12	124	HU	Leeward Islands to Newfoundland	2	Newfoundland	3	49.00	-56.00
1775	9	12	9	14	125	TS	Antigua to Cuba	1	Antigua	4	17.28	-61.79
1775	9	12	9	14	125	TS	Antigua to Cuba	2	Cuba	4	21.61	-79.03
1775	10	16	10	19	126	TS	North and Central Leeward Islands	1	North Leeward Islands	6	17.28	-69.79
1775	10	16	10	19	126	TS	North and Central Leeward Islands	2	Central Leeward Islands	8	17.30	-62.73
1776	9	5	9	12	127	HU	Guadeloupe to Louisiana	1	Guadeloupe	9	16.24	-61.53
1776	9	5	9	12	127	HU	Guadeloupe to Louisiana	2	Louisiana	3	29.33	-91.38
1777	10	23	10	31	128	HU	Eastern Caribbean to Cuba	1	Eastern Caribbean	5	14.54	-65.26
1777	10	23	10	31	128	HU	Eastern Caribbean to Cuba	2	Cuba	4	21.61	-79.03
1777	11	22	11	23	129	TS	Southeast of Jamaica and across western Haiti	1	Southeast of Jamaica	6	17.01	-75.98
1777	11	22	11	23	129	TS	Southeast of Jamaica and across western Haiti	2	western Haiti	8	18.38	-73.09
1778	6	5	6	5	130	TS	Jamaica	1	Jamaica	4	18.15	-77.31
1778	8	7	8	13	131	HU	Bahama Banks to New England	1	Bahama Banks	9	23.53	-75.83
1778	8	7	8	13	131	HU	Bahama Banks to New England	2	New England	9	42.80	-70.66
1778	9	16	9	17	132	HU	Jamaica	1	Jamaica	4	18.15	-77.31
1778	9	29	10	10	133	HU	Tobago to Pensacola, Florida	1	Tobago	4	11.15	-60.67
1778	9	29	10	10	133	HU	Tobago to Pensacola, Florida	2	Pensacola, FL	2	30.42	-87.22
1779	5	25	5	26	134	HU	West of Jamaica	1	West of Jamaica	6	18.27	-79.37
1779	8	18	8	18	135	HU	New Orleans	1	New Orleans	2	29.95	-90.07
1779	8	28	9	3	136	TS	Martinique to near South Carolina	1	Martinique	4	14.65	-61.01
1779	8	28	9	3	136	TS	Martinique to near South Carolina	2	near South Carolina	6	32.77	-78.92
1780	8	24	8	24	137	HU	Louisiana	1	Louisiana	3	29.33	-91.38

1780	8	25	8	26	138	TS	St. Kitts	1	St. Kitts	4	17.30	-62.73
1780	10	2	10	8	139	HU	Western Jamaica to 37N 6745W	1	Western Jamaica	8	18.15	-77.82
1780	10	2	10	8	139	HU	Western Jamaica to 37N 6745W	2	37N 6745W	1	37.00	-67.75
1780	10	10	10	20	140	HU	Barbados to Bermuda to 43N 50W	1	Barbados	4	13.18	-59.56
1780	10	10	10	20	140	HU	Barbados to Bermuda to 43N 50W	2	Bermuda	4	32.31	-64.75
1780	10	10	10	20	140	HU	Barbados to Bermuda to 43N 50W	3	43N 50W	1	43.00	-50.00
1780	10	15	10	26	141	HU	near Jamaica to Gulf of Mexico to 4450N 4228W	1	near Jamaica	6	17.18	-78.31
1780	10	15	10	26	141	HU	near Jamaica to Gulf of Mexico to 4450N 4228W	2	Gulf of Mexico	5	24.82	-90.14
1780	10	15	10	26	141	HU	near Jamaica to Gulf of Mexico to 4450N 4228W	3	4450N 4228W	1	44.83	-42.47
1781	8	1	8	2	142	HU	Jamaica	1	Jamaica	4	18.15	-77.31
1781	8	9	8	11	143	HU	South Carolina and North Carolina	1	South Carolina	3	33.87	-78.58
1781	8	16	8	23	144	HU	West of Jamaica to New Orleans	1	West of Jamaica	6	18.27	-79.37
1781	8	16	8	23	144	HU	West of Jamaica to New Orleans	2	New Orleans	2	29.95	-90.07
1781	9	3	9	7	145	TS	St. Lucia to southwest of Jamaica	1	St. Lucia	4	13.90	-60.97
1781	9	3	9	7	145	TS	St. Lucia to southwest of Jamaica	2	southwest of Jamaica	6	17.18	-78.31
1781	11	2	11	3	146	TS	West of Jamaica	1	West of Jamaica	6	18.27	-79.37
1782	5	30	5	30	147	TS	Southwest of western Jamaica	1	southwest of western Jamaica	6	17.18	-78.31
1782	8	15	8	15	148	HU	Florida Straits	1	Florida Straits	9	23.93	-80.93
1782	9	16	9	16	149	HU	North Atlantic	1	North Atlantic	9	42.91	-26.96
1783	9	15	9	20	150	HU	Off U.S. coast	1	Off U.S. coast	6	29.38	-76.45
1783	10	5	10	9	151	HU	West of Jamaica to New England	1	West of Jamaica	6	18.27	-79.37
1783	10	5	10	9	151	HU	West of Jamaica to New England	2	New England	9	42.80	-70.66
1784	7	10	7	17	152	HU	Grenada to Curacao to Honduras	1	Grenada	4	12.12	-61.68
1784	7	10	7	17	152	HU	Grenada to Curacao to Honduras	2	Curacao	4	12.18	-69.00
1784	7	10	7	17	152	HU	Grenada to Curacao to Honduras	3	Honduras	3	14.82	-86.62
1784	7	27	8	5	153	HU	Dominica to Jamaica to Pensacola, Florida	1	Dominica	4	15.43	-61.36
1784	7	27	8	5	153	HU	Dominica to Jamaica to Pensacola, Florida	2	Jamaica	4	18.15	-77.31
1784	7	27	8	5	153	HU	Dominica to Jamaica to Pensacola, Florida	3	Pensacola, FL	2	30.42	-87.22
1785	8	23	8	31	154	TS	Northern Leewards to Jamaica to Belize	1	Northern Leewards	8	17.28	-69.79
1785	8	23	8	31	154	TS	Northern Leewards to Jamaica to Belize	2	Jamaica	4	18.15	-77.31
1785	8	23	8	31	154	TS	Northern Leewards to Jamaica to Belize	3	Belize	3	17.20	-88.70
1785	9	10	9	10	155	TS	Charleston, South Carolina	1	Charleston, SC	2	32.77	-79.92
1785	9	16	9	25	156	HU	Leeward Islands to Bahamas to NC to Canada	1	Leeward Islands	9	17.30	-62.73
1785	9	16	9	25	156	HU	Leeward Islands to Bahamas to NC to Canada	2	Bahamas	9	23.53	-75.83
1785	9	16	9	25	156	HU	Leeward Islands to Bahamas to NC to Canada	3	NC	3	34.69	-76.45
1785	9	16	9	25	156	HU	Leeward Islands to Bahamas to NC to Canada	4	Canada	9	44.85	-63.20
1786	6	5	6	5	157	TS	Western Jamaica	1	Western Jamaica	8	18.15	-77.82
1786	8	29	8	29	158	HU	Off US coast	1	Off US coast	6	29.38	-76.45
1786	9	2	9	10	159	HU	Barbados to Nassau to off South Carolina	1	Barbados	4	13.18	-59.56
1786	9	2	9	10	159	HU	Barbados to Nassau to off South Carolina	2	Nassau	2	25.08	-77.35
1786	9	2	9	10	159	HU	Barbados to Nassau to off South Carolina	3	off South Carolina	6	32.77	-78.92
1786	9	28	9	28	160	TS	Charleston, South Carolina	1	Charleston, SC	2	32.77	-79.92
1786	10	19	10	23	161	HU	Jamaica to Havana to Bahamas	1	Jamaica	4	18.15	-77.31
1786	10	19	10	23	161	HU	Jamaica to Havana to Bahamas	2	Havana	2	23.12	-82.35
1786	10	19	10	23	161	HU	Jamaica to Havana to Bahamas	3	Bahamas	9	23.53	-75.83

1787	8	2	8	7	162	TS	Dominica to Grand Caicos to 40N 64W	1	Dominica	4	15.43	-61.36
1787	8	2	8	7	162	TS	Dominica to Grand Caicos to 40N 64W	2	Grand Caicos	4	21.08	-73.35
1787	8	2	8	7	162	TS	Dominica to Grand Caicos to 40N 64W	3	40 N 64 W	1	40.00	-64.00
1787	8	6	8	11	163	TS	Grenada to Jamaica to Bahamas Bank	1	Grenada	4	12.12	-61.68
1787	8	6	8	11	163	TS	Grenada to Jamaica to Bahamas Bank	2	Jamaica	4	18.15	-77.31
1787	8	6	8	11	163	TS	Grenada to Jamaica to Bahamas Bank	3	Bahamas Bank	9	23.53	-75.83
1787	8	15	8	16	164	HU	South tip of Florida	1	South tip of FL	8	25.79	-80.22
1787	8	23	8	28	165	HU	Central Leewards to Bahamas to South Carolina	1	Central Leewards	8	17.30	-62.73
1787	8	23	8	28	165	HU	Central Leewards to Bahamas to South Carolina	2	Bahamas	9	23.53	-75.83
1787	8	23	8	28	165	HU	Central Leewards to Bahamas to South Carolina	3	South Carolina	3	32.87	-79.63
1787	8	29	9	2	166	HU	Dominica to Belize	1	Dominica	4	15.43	-61.36
1787	8	29	9	2	166	HU	Dominica to Belize	2	Belize	3	17.20	-88.70
1787	9	16	9	16	167	TS	South Carolina	1	South Carolina	3	32.87	-79.63
1787	9	19	9	23	168	HU	Eastern Cuba and Jamaica to Belize	1	Eastern Cuba	8	18.15	-77.31
1787	9	19	9	23	168	HU	Eastern Cuba and Jamaica to Belize	2	Jamaica	4	21.06	-77.21
1787	9	19	9	23	168	HU	Eastern Cuba and Jamaica to Belize	3	Belize	3	17.20	-88.70
1788	6	4	6	4	169	TS	Near western Jamaica	1	Near western Jamaica	6	18.27	-79.37
1788	7	19	7	24	170	HU	Bermuda to US	1	Bermuda	4	32.31	-64.75
1788	7	19	7	24	170	HU	Bermuda to US	2	US	9	42.30	-71.80
1788	8	14	8	16	171	HU	Central Leewards to Haiti	1	Central Leewards	8	17.30	-62.73
1788	8	14	8	16	171	HU	Central Leewards to Haiti	2	Haiti	4	18.93	-72.68
1788	8	17	8	19	172	TS	SE Pennsylvania to western New England	1	SE PA	8	39.72	-76.38
1788	8	17	8	19	172	TS	SE Pennsylvania to western New England	2	western New England	8	42.96	-73.50
1788	9	8	9	9	173	TS	Jamaica	1	Jamaica	4	18.15	-77.31
1788	9	19	9	23	174	TS	US Coast to Newfoundland	1	US Coast	9	35.47	-70.48
1788	9	19	9	23	174	TS	US Coast to Newfoundland	2	Newfoundland	3	49.00	-56.00
1788	9	29	10	6	175	TS	South of Jamaica to eastern Caymans to South Carolina	1	South of Jamaica	6	16.74	-77.27
1788	9	29	10	6	175	TS	South of Jamaica to eastern Caymans to South Carolina	2	eastern Caymans	8	19.73	-79.73
1788	9	29	10	6	175	TS	South of Jamaica to eastern Caymans to South Carolina	3	South Carolina	3	32.87	-79.63
1789	8	17	8	18	176	HU	New Orleans	1	New Orleans	2	29.95	-90.07
1790	8	10	8	12	177	HU	Tobago to Curacao	1	Tobago	4	11.15	-60.67
1790	8	10	8	12	177	HU	Tobago to Curacao	2	Curacao	4	12.18	-69.00
1790	8	29	9	2	178	HU	Barbados to Jamaica	1	Barbados	4	13.18	-59.56
1790	8	29	9	2	178	HU	Barbados to Jamaica	2	Jamaica	4	18.15	-77.31
1791	6	18	6	23	179	HU	Western Cuba to Florida Panhandle	1	Western Cuba	8	22.41	-81.75
1791	6	18	6	23	179	HU	Western Cuba to Florida Panhandle	2	Florida Panhandle	9	30.05	-85.74
1791	9	27	10	4	180	HU	Jamaica to Bahamas to 37N 62W	1	Jamaica	4	18.15	-77.31
1791	9	27	10	4	180	HU	Jamaica to Bahamas to 37N 62W	2	Bahamas	9	23.53	-75.83
1791	9	27	10	4	180	HU	Jamaica to Bahamas to 37N 62W	3	37N 62W	1	37.00	-62.00
1792	7	14	7	14	181	TS	St. Eustatia, St. Kitts	1	St. Eustatia	2	17.50	-62.97
1792	7	14	7	14	181	TS	St. Eustatia, St. Kitts	2	St. Kitts	4	17.30	-62.73
1792	8	1	8	12	182	HU	Leeward Islands to near Caicos Is. to 37N 57W	1	Leeward Islands	9	17.30	-62.73
1792	8	1	8	12	182	HU	Leeward Islands to near Caicos Is. to 37N 57W	2	near Caicos Is.	6	22.34	-72.67
1792	8	1	8	12	182	HU	Leeward Islands to near Caicos Is. to 37N 57W	3	37N 57W	1	37.00	-57.00
1792	10	29	10	31	183	HU	Western Cuba to South Carolina	1	Western Cuba	8	22.41	-81.75

1792	10	29	10	31	183	HU	Western Cuba to South Carolina	2	South Carolina	3	32.87	-79.63
1793	8	12	8	18	184	HU	Northern Leewards to Bahamas to Louisiana	1	Northern Leewards	8	17.28	-69.79
1793	8	12	8	18	184	HU	Northern Leewards to Bahamas to Louisiana	2	Bahamas	9	23.53	-75.83
1793	8	12	8	18	184	HU	Northern Leewards to Bahamas to Louisiana	3	Louisiana	3	29.33	-91.38
1793	10	21	10	23	185	HU	Western Jamaica to Bermuda	1	Western Jamaica	8	18.15	-77.82
1793	10	21	10	23	185	HU	Western Jamaica to Bermuda	2	Bermuda	4	32.31	-64.75
1794	5	28	5	28	186	TS	West of Jamaica	1	West of Jamaica	6	18.27	-79.37
1794	8	10	8	11	187	HU	New Orleans	1	New Orleans	2	29.95	-90.07
1794	8	25	9	1	188	HU	Cuba to Louisiana	1	Cuba	4	21.61	-79.03
1794	8	25	9	1	188	HU	Cuba to Louisiana	2	Louisiana	3	29.33	-91.38
1795	7	20	7	20	189	HU	Near Mouth of Mississippi River	1	Near Mouth of Mississippi River	6	29.20	-89.23
1795	7	27	8	3	190	HU	Central Leewards to North Carolina	1	Central Leewards	8	17.30	-62.73
1795	7	27	8	3	190	HU	Central Leewards to North Carolina	2	North Carolina	3	34.69	-76.45
1795	8	2	8	13	191	TS	North of Puerto Rico to north of Hispanolia to Virginia	1	North of Puerto Rico	6	19.38	-66.58
1795	8	2	8	13	191	TS	North of Puerto Rico to north of Hispanolia to Virginia	2	north of Hispaniola	6	20.93	-71.33
1795	8	2	8	13	191	TS	North of Puerto Rico to north of Hispanolia to Virginia	3	Virginia	3	37.29	-75.58
1795	8	18	8	21	192	HU	Northern Leewards to Caicos Islands	1	Northern Leewards	8	17.28	-69.79
1795	8	18	8	21	192	HU	Northern Leewards to Caicos Islands	2	Caicos Islands	9	21.08	-73.35
1795	10	10	10	10	193	TS	South Carolina	1	South Carolina	3	32.87	-79.63
1796	8	25	8	27	194	HU	Florida Straits to Louisiana	1	Florida Straits	9	23.93	-80.93
1796	8	25	8	27	194	HU	Florida Straits to Louisiana	2	Louisiana	3	29.33	-91.38
1796	10	2	10	4	195	HU	Jamaica to Bahamas	1	Jamaica	4	18.15	-77.31
1796	10	2	10	4	195	HU	Jamaica to Bahamas	2	Bahamas	9	23.53	-75.83
1797	10	17	10	21	196	HU	Bahamas to South Carolina	1	Bahamas	9	23.53	-75.83
1797	10	17	10	21	196	HU	Bahamas to South Carolina	2	South Carolina	3	32.87	-79.63
1799	6	2	6	9	197	HU	Central Cuba to off U.S. Coast	1	Central Cuba	4	21.61	-79.03
1799	6	2	6	9	197	HU	Central Cuba to off U.S. Coast	2	off U.S. Coast	6	29.38	-76.45
1799	9	25	9	25	198	TS	Charleston, South Carolina	1	Charleston, SC	2	32.77	-79.92
1800	8	10	8	18	199	HU	Leeward Islands to Louisiana	1	Leeward Islands	9	17.30	-62.73
1800	8	10	8	18	199	HU	Leeward Islands to Louisiana	2	Louisiana	3	29.33	-91.38
1800	8	27	8	28	200	HU	Exuma, Grand Bahamas	1	Exuma, Grand Bahamas	4	23.53	-75.83
1800	10	2	10	5	201	HU	South Carolina	1	South Carolina	3	32.87	-79.63
1800	10	31	11	5	202	HU	Jamaica to Eastern Cuba to Crooked Island to Bermuda	1	Jamaica	4	18.15	-77.31
1800	10	31	11	5	202	HU	Jamaica to Eastern Cuba to Crooked Island to Bermuda	2	Eastern Cuba	8	21.06	-77.21
1800	10	31	11	5	202	HU	Jamaica to Eastern Cuba to Crooked Island to Bermuda	3	Crooked Island	4	22.75	-74.22
1800	10	31	11	5	202	HU	Jamaica to Eastern Cuba to Crooked Island to Bermuda	4	Bermuda	4	32.31	-64.75
1801	7	22	7	25	203	HU	Nassau to Gulf of Mexico	1	Nassau	2	25.08	-77.35
1801	7	22	7	25	203	HU	Nassau to Gulf of Mexico	2	Gulf of Mexico	5	24.82	-90.14
1801	8	15	8	16	204	HU	Mobile, Alabama	1	Mobile, AL	2	30.68	-88.03
1802	10	6	10	10	205	HU	West of Jamaica	1	West of Jamaica	6	18.27	-79.37
1803	8	31	9	1	206	HU	North Carolina	1	North Carolina	3	34.69	-76.45
1803	10	2	10	3	207	HU	Norfolk, Virginia	1	Norfolk, VA	2	36.83	-76.28
1804	8	18	8	19	208	HU	Jamaica	1	Jamaica	4	18.15	-77.31
1804	9	3	9	12	209	HU	Barbados to New England	1	Barbados	4	13.18	-59.56
1804	9	3	9	12	209	HU	Barbados to New England	2	New England	9	42.80	-70.66

1804	9	22	9	24	210	TS	Cuba to South Carolina	1	Cuba	4	21.61	-79.03
1804	9	22	9	24	210	TS	Cuba to South Carolina	2	South Carolina	3	32.87	-79.63
1804	10	4	10	10	211	HU	North of Puerto Rico to southeast New England	1	North of Puerto Rico	6	19.38	-66.58
1804	10	4	10	10	211	HU	North of Puerto Rico to southeast New England	2	southeast New England	9	41.40	-71.47
1805	7	27	8	1	212	HU	27N 58W to 36N 62W	1	27N 58W	1	27.00	-58.00
1805	7	27	8	1	212	HU	27N 58W to 36N 62W	2	36N 62W	1	36.00	-62.00
1805	9	30	10	3	213	HU	Matanzas, Cuba to Maine	1	Matanzas, Cuba	2	23.05	-81.58
1805	9	30	10	3	213	HU	Matanzas, Cuba to Maine	2	Maine	3	44.38	-68.00
1806	8	17	8	24	214	HU	17N 57W to Carolinas to 4139N 59W	1	17N 57W	1	17.00	-57.00
1806	8	17	8	24	214	HU	17N 57W to Carolinas to 4139N 59W (Cape Fear, NC)	2	Carolinas	9	33.83	-77.95
1806	8	17	8	24	214	HU	17N 57W to Carolinas to 4139N 59W	3	4139N 59W	1	41.65	-59.00
1806	8	26	9	3	215	HU	Mona Passage to 35N 72W	1	Mona Passage	5	18.06	-67.91
1806	8	26	9	3	215	HU	Mona Passage to 35N 72W	2	35N 72W	1	35.00	-72.00
1806	9	8	9	18	216	HU	Dominica to Mississippi	1	Dominica	4	15.43	-61.36
1806	9	8	9	18	216	HU	Dominica to Mississippi	2	Mississippi	3	30.37	-88.95
1806	9	27	9	29	217	HU	South Carolina, North Carolina and Virginia	1	South Carolina	3	32.87	-79.63
1806	9	27	9	29	217	HU	South Carolina, North Carolina and Virginia	2	North Carolina	3	34.69	-76.45
1806	9	27	9	29	217	HU	South Carolina, North Carolina and Virginia	3	Virginia	3	37.29	-75.58
1806	10	2	10	9	218	TS	Jamaica to South Carolina	1	Jamaica	4	18.15	-77.31
1806	10	2	10	9	218	TS	Jamaica to South Carolina	2	South Carolina	3	32.87	-79.63
1807	7	25	7	25	219	TS	Leeward Islands	1	Leeward Islands	9	17.30	-62.73
1807	9	1	9	5	220	TS	Leeward Islands to Trinidad de Cuba	1	Leeward Islands	9	17.30	-62.73
1807	9	1	9	5	220	TS	Leeward Islands to Trinidad de Cuba	2	Trinidad de Cuba	2	22.73	-82.97
1807	10	16	10	20	221	HU	Tobago-Curacao-near and west of Jamaica	1	Tobago	4	11.15	-60.67
1807	10	16	10	20	221	HU	Tobago-Curacao-near and west of Jamaica	2	Curacao	4	12.18	-69.00
1807	10	16	10	20	221	HU	Tobago-Curacao-near and west of Jamaica	3	near and west of Jamaica	6	18.27	-79.37
1809	8	1	8	3	222	TS	Dominica, Guadeloupe	1	Dominica	4	15.43	-61.36
1809	8	1	8	3	222	TS	Dominica, Guadeloupe	2	Guadeloupe	9	16.24	-61.53
1809	10	9	10	13	223	TS	Northern Leeward Islands	1	Northern Leeward Islands	8	17.28	-69.79
1810	7	30	7	31	224	TS	Jamaica	1	Jamaica	4	18.15	-77.31
1810	8	12	8	15	225	HU	Trinidad to near Jamaica	1	Trinidad	4	10.42	-61.30
1810	8	12	8	15	225	HU	Trinidad to near Jamaica	2	near Jamaica	6	18.15	-77.31
1810	9	11	9	13	226	TS	South Carolina	1	South Carolina	3	32.87	-79.63
1810	9	28	9	28	227	HU	Eastern Cuba	1	Eastern Cuba	8	21.06	-77.21
1810	10	20	10	27	228	HU	South of Cuba to Southwest Atlantic	1	South of Cuba	6	20.65	-79.93
1810	10	20	10	27	228	HU	South of Cuba to Southwest Atlantic	2	Southwest Atlantic	9	21.79	-61.05
1811	9	8	9	12	229	HU	Key Sal, Cuba to Charleston, South Carolina	1	Key Sal, Cuba	4	23.70	-80.40
1811	9	8	9	12	229	HU	Key Sal, Cuba to Charleston, South Carolina	2	Charleston, SC	2	32.77	-79.92
1811	10	11	10	11	230	HU	Pensacola to Fort Stoddart, Alabama	1	Pensacola	2	30.42	-87.22
1811	10	11	10	11	230	HU	Pensacola to Fort Stoddart, Alabama	2	Fort Stoddart, Alabama	2	33.73	-87.90
1811	10	20	10	25	231	HU	West of Jamaica to Cuba	1	West of Jamaica	6	18.27	-79.37
1811	10	20	10	25	231	HU	West of Jamaica to Cuba	2	Cuba	4	21.61	-79.03
1812	6	5	6	11	232	TS	Northwest Caribbean Sea	1	Northwest Caribbean Sea	5	19.93	-83.90
1812	8	8	8	8	233	TS	South Carolina	1	South Carolina	3	32.87	-79.63
1812	8	14	8	20	234	HU	East of Jamaica to Louisiana	1	East of Jamaica	6	17.97	-75.19

1812	8	14	8	20	234	HU	East of Jamaica to Louisiana	2	Louisiana	3	29.33	-91.38
1812	10	12	10	17	235	HU	Jamaica to 37N 51W	1	Jamaica	4	18.15	-77.31
1812	10	12	10	17	235	HU	Jamaica to 37N 51W	2	37N51W	1	37.00	-51.00
1813	7	22	7	29	236	HU	Barbados to 3830N 6500W	1	Barbados	4	13.18	-59.56
1813	7	22	7	29	236	HU	Barbados to 3830N 6500W	2	3830N 6500W	1	38.50	-62.00
1813	7	29	8	3	237	HU	Leeward Islands to Belize	1	Leeward Islands	9	17.30	-62.73
1813	7	29	8	3	237	HU	Leeward Islands to Belize	2	Belize	3	17.20	-88.70
1813	8	3	8	7	238	HU	2923N 6347W to 4127N 5619W	1	2923N 6347W	1	29.38	-63.78
1813	8	3	8	7	238	HU	2923N 6347W to 4127N 5619W	2	4127N 5619W	1	41.45	-56.32
1813	8	24	8	29	239	HU	Caicos Islands to South Carolina to Virginia & Maryland	1	Caicos Islands	9	21.08	-73.35
1813	8	24	8	29	239	HU	Caicos Islands to South Carolina to Virginia & Maryland	2	South Carolina	3	32.87	-79.63
1813	8	24	8	29	239	HU	Caicos Islands to South Carolina to Virginia & Maryland	3	VA & MD	9	37.98	-75.27
1813	8	25	8	28	240	TS	Dominica to south of Jamaica	1	Dominica	4	15.43	-61.36
1813	8	25	8	28	240	TS	Dominica to south of Jamaica	2	South of Jamaica	6	16.74	-77.27
1814	7	23	7	24	241	TS	Dominica to Puerto Rico	1	Dominica	4	15.43	-61.36
1814	7	23	7	24	241	TS	Dominica to Puerto Rico	2	Puerto Rico	4	18.23	-66.48
1815	7	27	8	10	242	HU	17N 53W to Grand Banks of Newfoundland	1	17N 53W	1	17.00	-53.00
1815	7	27	8	10	242	HU	17N 53W to Grand Banks of Newfoundland	2	Grand Banks of Newfoundland	9	46.00	-51.50
1815	8	26	9	5	243	HU	16N 51W to off the U.S. Coast	1	16N 51W	1	16.00	-51.00
1815	8	26	9	5	243	HU	16N 51W to off the U.S. Coast	2	off the U.S. Coast	6	29.38	-76.45
1815	10	16	10	23	244	HU	Martinique to New England	1	Martinique	4	14.65	-61.01
1815	10	16	10	23	244	HU	Martinique to New England	2	New England	9	42.80	-70.66
1815	10	18	10	22	245	HU	Jamaica to Caicos Islands	1	Jamaica	4	18.15	-77.31
1815	10	18	10	22	245	HU	Jamaica to Caicos Islands	2	Caicos Islands	9	21.08	-73.35
1816	6	1	6	12	246	HU	West of Jamaica to South Florida to 3128N 6823W	1	West of Jamaica	6	18.27	-79.37
1816	6	1	6	12	246	HU	West of Jamaica to South Florida to 3128N 6823W	2	South Florida	8	25.79	-80.22
1816	6	1	6	12	246	HU	West of Jamaica to South Florida to 3128N 6823W	3	3128N 6823W	1	31.47	-68.38
1816	9	3	9	11	247	HU	Martinique to eastern Cuba to South Carolina	1	Martinique	4	14.65	-61.01
1816	9	3	9	11	247	HU	Martinique to eastern Cuba to South Carolina	2	Eastern Cuba	8	21.06	-77.21
1816	9	3	9	11	247	HU	Martinique to eastern Cuba to South Carolina	3	South Carolina	3	32.87	-79.63
1816	9	15	9	25	248	HU	Dominica to 38N 70W	1	Dominica	4	15.43	-61.36
1816	9	15	9	25	248	HU	Dominica to 38N 70W	2	38N 70W	1	38.00	-70.00
1817	8	1	8	9	249	HU	Tobago to Pennsylvania	1	Tobago	4	11.15	-60.67
1817	8	1	8	9	249	HU	Tobago to Pennsylvania	2	Pennsylvania	2	39.72	-76.38
1817	10	20	10	26	250	HU	Barbados to Nicaragua	1	Barbados	4	13.18	-59.56
1817	10	20	10	26	250	HU	Barbados to Nicaragua	2	Nicaragua	3	12.85	-85.03
1818	8	26	9	5	251	HU	26N 50W to 5002N 2648W	1	26N 50W	1	26.00	-50.00
1818	8	26	9	5	251	HU	26N 50W to 5002N 2648W	2	5002N 2648W	1	50.03	-26.80
1818	9	10	9	16	252	HU	Yucatan to Texas to Mississippi	1	Yucatan	9	20.83	-89.00
1818	9	10	9	16	252	HU	Yucatan to Texas to Mississippi	2	Texas	3	28.40	-96.38
1818	9	10	9	16	252	HU	Yucatan to Texas to Mississippi	3	Mississippi	3	30.37	-88.95
1818	9	21	9	28	253	HU	Leeward Islands to North Atlantic	1	Leeward Islands	9	17.30	-62.73
1818	9	21	9	28	253	HU	Leeward Islands to North Atlantic	2	North Atlantic	9	42.91	-26.96
1818	10	12	10	14	254	HU	Northeast of Jamaica to central Bahamas	1	Northeast of Jamaica	6	19.01	-76.09
1818	10	12	10	14	254	HU	Northeast of Jamaica to central Bahamas	2	Central Bahamas	8	23.53	-75.83

1818	11	6	11	13	255	HU	Southwest Caribbean to Jamaica to Cuba	1	Southwest Caribbean	8	12.33	-82.13
1818	11	6	11	13	255	HU	Southwest Caribbean to Jamaica to Cuba	2	Jamaica	4	18.15	-77.31
1818	11	6	11	13	255	HU	Southwest Caribbean to Jamaica to Cuba	3	Cuba	4	21.61	-79.03
1819	7	24	7	30	256	HU	Bahamas to Mississippi	1	Bahamas	9	23.53	-75.83
1819	7	24	7	30	256	HU	Bahamas to Mississippi	2	Mississippi	3	30.37	-88.95
1819	9	19	9	26	257	HU	1530N 56W to 3026N 6755W	1	1530N 56W	1	15.50	-56.00
1819	9	19	9	26	257	HU	1530N 56W to 3026N 6755W	2	3026N 6755W	1	30.43	-67.92
1819	10	13	10	15	258	HU	Leeward Islands	1	Leeward Islands	9	17.30	-62.73
1819	10	27	10	28	259	TS	Cuba to Bahamas	1	Cuba	4	21.61	-79.03
1819	10	27	10	28	259	TS	Cuba to Bahamas	2	Bahamas	9	23.53	-75.83
1820	9	8	9	10	260	HU	Florida to North Carolina	1	Florida	9	28.66	-82.50
1820	9	8	9	10	260	HU	Florida to North Carolina	2	North Carolina	3	34.69	-76.45
1820	9	26	10	1	261	HU	Dominica to Haiti to South Carolina	1	Dominica	4	15.43	-61.36
1820	9	26	10	1	261	HU	Dominica to Haiti to South Carolina	2	Haiti	4	18.93	-72.68
1820	9	26	10	1	261	HU	Dominica to Haiti to South Carolina	3	South Carolina	3	32.87	-79.63
1821	9	1	9	9	262	TS	Guadeloupe to western Cuba	1	Guadeloupe	9	16.24	-61.53
1821	9	1	9	9	262	TS	Guadeloupe to western Cuba	2	Western Cuba	8	22.41	-81.75
1821	9	1	9	3	263	HU	Off US Coast to New York City	1	Off US Coast	6	29.38	-76.45
1821	9	1	9	3	263	HU	Off US Coast to New York City	2	New York City	2	40.70	-74.00
1821	9	9	9	17	264	HU	Antigua to U.S. Gulf Coast	1	Antigua	4	17.28	-61.79
1821	9	9	9	17	264	HU	Antigua to U.S. Gulf Coast	2	U.S. Gulf Coast	7	29.79	-89.04
1822	7	7	7	9	265	HU	Central U.S. Gulf Coast	1	Central U.S. Gulf Coast	8	29.79	-89.04
1822	9	25	9	28	266	HU	Bahamas to North Carolina	1	Bahamas	9	23.53	-75.83
1822	9	25	9	28	266	HU	Bahamas to North Carolina	2	North Carolina	3	34.69	-76.45
1822	12	13	12	22	267	HU	Eastern Caribbean Sea to Martinique to Venezuela	1	Eastern Caribbean Sea	5	14.54	-65.26
1822	12	13	12	22	267	HU	Eastern Caribbean Sea to Martinique to Venezuela	2	Martinique	4	14.65	-61.01
1822	12	13	12	22	267	HU	Eastern Caribbean Sea to Martinique to Venezuela	3	Venezuela	3	10.58	-66.89
1823	7	8	7	10	268	TS	Curacao to near Jamaica	1	Curacao	4	12.18	-69.00
1823	7	8	7	10	268	TS	Curacao to near Jamaica	2	Near Jamaica	6	16.74	-77.27
1823	8	2	8	3	269	TS	Seas south of Jamaica	1	Seas south of Jamaica	6	15.16	-75.88
1823	9	11	9	14	270	HU	2324N 9504W to Central U.S. Gulf Coast	1	2324N 9504W	1	23.40	-95.07
1823	9	11	9	14	270	HU	2324N 9504W to Central U.S. Gulf Coast	2	Central U.S. Gulf Coast	8	29.79	-89.04
1824	8	7	8	15	271	HU	Guadeloupe to Georgia and South Carolina	1	Guadeloupe	9	16.24	-61.53
1824	8	7	8	15	271	HU	Guadeloupe to Georgia and South Carolina	2	Georgia	3	31.39	-81.17
1824	8	7	8	15	271	HU	Guadeloupe to Georgia and South Carolina	3	South Carolina	3	32.87	-79.63
1824	8	26	8	27	272	TS	1630N south of Jamaica	1	1630N south of Jamaica	6	16.50	-76.80
1825	5	28	6	5	273	HU	Southeast of Jamaica to Florida to 37N 74W	1	Southeast of Jamaica	6	17.01	-75.98
1825	5	28	6	5	273	HU	Southeast of Jamaica to Florida to 37N 74W	2	Florida	9	28.66	-82.50
1825	5	28	6	5	273	HU	Southeast of Jamaica to Florida to 37N 74W	3	37N 74W	1	37.00	-74.00
1825	7	25	8	2	274	HU	Leeward Islands to 38N 6650W	1	Leeward Islands	9	17.30	-62.73
1825	7	25	8	2	274	HU	Leeward Islands to 38N 6650W	2	38N 6650W	1	38.00	-66.83
1825	9	28	10	3	275	HU	Haiti to northeast coast of Florida	1	Haiti	4	18.93	-72.68
1825	9	28	10	3	275	HU	Haiti to northeast coast of Florida	2	Northeast coast of Florida	8	30.32	-81.66
1826	8	31	9	10	276	TS	Dominica to near Jamaica to Grand Banks	1	Dominica	4	15.43	-61.36
1826	8	31	9	10	276	TS	Dominica to near Jamaica to Grand Banks	2	Near Jamaica	6	46.00	-51.50

1826	8	31	9	10	276	TS	Dominica to near Jamaica to Grand Banks	3	Grand Banks	9	46.00	-51.50
1827	9	17	9	23	277	HU	Antigua to Jamaica to Vera Cruz, Mexico	1	Antigua	4	17.28	-61.79
1827	9	17	9	23	277	HU	Antigua to Jamaica to Vera Cruz, Mexico	2	Jamaica	4	18.15	-77.31
1827	9	17	9	23	277	HU	Antigua to Jamaica to Vera Cruz, Mexico	3	Vera Cruz, Mexico	2	18.70	-89.07
1827	8	20	8	27	278	HU	Northern Leewards to New England	1	Northern Leewards	8	17.28	-69.79
1827	8	20	8	27	278	HU	Northern Leewards to New England	2	New England	9	42.80	-70.66
1827	8	27	9	5	279	HU	Northern Leewards to Northwest Florida	1	Northern Leewards	8	17.28	-69.79
1827	8	27	9	5	279	HU	Northern Leewards to Northwest Florida	2	Northwest Florida	8	30.05	-85.74
1827	8	29	9	8	280	TS	North of Leewards to 3650N 6650W	1	North of Leewards	6	18.71	-61.85
1827	8	29	9	8	280	TS	North of Leewards to 3650N 6650W	2	3650N 6650W	1	36.83	-66.83
1828	9	15	9	20	281	HU	18N 60W to 44N 5218W	1	18N 60W	1	18.00	-60.00
1828	9	15	9	20	281	HU	18N 60W to 44N 5218W	2	44N 5218W	1	44.00	-52.30
1829	7	9	7	13	282	TS	Gulf of Mexico	1	Gulf of Mexico	5	24.82	-90.14
1829	8	23	8	30	283	HU	South Carolina to 3830N 6609W	1	South Carolina	3	32.87	-79.63
1829	8	23	8	30	283	HU	South Carolina to 3830N 6609W	2	3830N 6609W	1	38.50	-66.15
1830	8	3	8	9	284	HU	Trinidad to western Cuba	1	Trinidad	4	10.42	-61.30
1830	8	3	8	9	284	HU	Trinidad to western Cuba	2	Western Cuba	8	22.41	-81.75
1830	8	11	8	19	285	HU	Leeward Islands to South Carolina to 43N 58W	1	Leeward Islands	9	17.30	-62.73
1830	8	11	8	19	285	HU	Leeward Islands to South Carolina to 43N 58W	2	South Carolina	3	32.87	-79.63
1830	8	11	8	19	285	HU	Leeward Islands to South Carolina to 43N 58W	3	43N 58W	1	43.00	-58.00
1830	8	19	8	26	286	HU	North of Leeward Islands to 37N 69W	1	North of Leeward Islands	6	18.71	-61.85
1830	8	19	8	26	286	HU	North of Leeward Islands to 37N 69W	2	37N 69W	1	37.00	-69.00
1830	9	29	10	1	287	HU	2246N 65W to 4025N 5824W	1	2246N 65W	1	22.77	-65.00
1830	9	29	10	1	287	HU	2246N 65W to 4025N 5824W	2	4025N 5824W	1	40.42	-58.40
1830	10	6	10	6	288	TS	South Carolina	1	South Carolina	3	32.87	-79.63
1831	6	10	6	10	289	TS	Northeast coast of Florida	1	Northeast coast of Florida	8	30.32	-81.66
1831	6	22	6	28	290	HU	South of Barbados to Yucatan	1	South of Barbados	6	12.01	-59.53
1831	6	22	6	28	290	HU	South of Barbados to Yucatan	2	Yucatan	9	20.83	-89.00
1831	8	10	8	17	291	HU	Barbados to Louisiana	1	Barbados	4	13.18	-59.56
1831	8	10	8	17	291	HU	Barbados to Louisiana	2	Louisiana	3	29.33	-91.38
1831	8	27	8	30	292	HU	Western Louisiana	1	Western Louisiana	8	29.69	-92.22
1832	6	5	6	8	293	HU	Nassau to Bermuda	1	Nassau	2	25.08	-77.35
1832	6	5	6	8	293	HU	Nassau to Bermuda	2	Bermuda	4	32.31	-64.75
1832	8	12	8	18	294	HU	Key West to NW Florida to South Carolina	1	Key West	2	24.55	-81.77
1832	8	12	8	18	294	HU	Key West to NW Florida to South Carolina	2	NW Florida	8	30.05	-85.74
1832	8	12	8	18	294	HU	Key West to NW Florida to South Carolina	3	South Carolina	3	32.87	-79.63
1832	8	21	8	21	295	TS	1251N 3926W	1	1251N 3926W	1	12.85	-39.43
1832	8	23	8	27	296	HU	Central Leeward Islands to east of Jamaica	1	Central Leeward Islands	8	17.30	-62.73
1832	8	23	8	27	296	HU	Central Leeward Islands to east of Jamaica	2	east of Jamaica	6	17.97	-75.19
1832	10	14	10	14	297	TS	South Carolina	1	South Carolina	3	32.87	-79.63
1833	8	10	8	10	298	TS	South Carolina	1	South Carolina	3	32.87	-79.63
1833	8	14	8	20	299	TS	St. Kitts to 23N 66W	1	St. Kitts	4	17.30	-62.73
1833	8	14	8	20	299	TS	St. Kitts to 23N 66W	2	23N 66W	1	23.00	-66.00
1833	9	4	9	5	300	TS	Western Louisiana	1	Western Louisiana	8	29.69	-92.22
1833	9	14	9	14	301	TS	South Carolina	1	South Carolina	3	32.87	-79.63

1833	10	16	10	19	302	TS	Cuba, Gulf of Mexico	1	Cuba	4	21.61	-79.03
1833	10	16	10	19	302	TS	Cuba, Gulf of Mexico	2	Gulf of Mexico	5	24.82	-90.14
1834	9	3	9	6	303	HU	Off Georgia coast to 39N 67W	1	Off Georgia coast	6	31.39	-80.17
1834	9	3	9	6	303	HU	Off Georgia coast to 39N 67W	2	39N 67W	1	39.00	-67.00
1834	9	5	9	7	304	TS	Gulf of Mexico to Western Louisiana	1	Gulf of Mexico	5	24.82	-90.14
1834	9	5	9	7	304	TS	Gulf of Mexico to Western Louisiana	2	Western Louisiana	8	29.69	-92.22
1834	9	20	9	30	305	HU	Central Leeward Islands to Western Louisiana	1	Central Leeward Islands	8	17.30	-62.73
1834	9	20	9	30	305	HU	Central Leeward Islands to Western Louisiana	2	Western Louisiana	8	29.69	-92.22
1835	8	12	8	18	306	HU	1655N 5345W to Rio Grande, Texas	1	1655N 5342W	1	16.92	-53.75
1835	8	12	8	18	306	HU	1655N 5345W to Rio Grande, Texas	2	Rio Grande, Texas	2	26.37	-98.82
1835	9	2	9	13	307	HU	Barbados to North Carolina	1	Barbados	4	13.18	-59.56
1835	9	2	9	13	307	HU	Barbados to North Carolina	2	North Carolina	3	34.69	-76.45
1835	9	15	9	19	308	HU	Key West to 3109N 78W to South Carolina	1	Key West	2	24.55	-81.77
1835	9	15	9	19	308	HU	Key West to 3109N 78W to South Carolina	2	3109N 78W	1	31.15	-78.00
1835	9	15	9	19	308	HU	Key West to 3109N 78W to South Carolina	3	South Carolina	3	32.87	-79.63
1835	10	22	10	29	309	HU	Turks Island to South Carolina	1	Turks Island	4	21.08	-73.55
1835	10	22	10	29	309	HU	Turks Island to South Carolina	2	South Carolina	3	32.87	-79.63
1836	9	2	9	3	310	HU	Cayman Islands	1	Cayman Islands	9	19.30	-81.38
1836	10	9	10	11	311	HU	South Carolina to North Carolina	1	South Carolina	3	32.87	-79.63
1836	10	9	10	11	311	HU	South Carolina to North Carolina	2	North Carolina	3	34.69	-76.45
1837	7	9	7	12	312	TS	Barbados to Hispanolia	1	Barbados	4	13.18	-59.56
1837	7	9	7	12	312	TS	Barbados to Hispanolia	2	Hispaniola	4	19.00	-70.67
1837	7	26	8	5	313	HU	Barbados to Georgia	1	Barbados	4	13.18	-59.56
1837	7	26	8	5	313	HU	Barbados to Georgia	2	Georgia	3	31.39	-81.17
1837	8	1	8	7	314	HU	Leeward Islands to Northwest Florida	1	Leeward Islands	9	17.30	-62.73
1837	8	1	8	7	314	HU	Leeward Islands to Northwest Florida	2	Northwest Florida	8	30.05	-85.74
1837	8	13	8	23	315	HU	18N 60W to SE U.S. coast to 39N 58W	1	18N 60W	1	18.00	-60.00
1837	8	13	8	23	315	HU	18N 60W to SE U.S. coast to 39N 58W	2	SE U.S. coast	7	32.69	-79.87
1837	8	13	8	23	315	HU	18N 60W to SE U.S. coast to 39N 58W	3	39N 58W	1	39.00	-58.00
1837	8	23	8	25	316	HU	28N 61W to 3537N 5742W	1	28N 61W	1	28.00	-61.00
1837	8	23	8	25	316	HU	28N 61W to 3537N 5742W	2	3537N 5742W	1	35.62	-57.70
1837	8	30	9	2	317	HU	Northwest Florida to North Carolina	1	Northwest Florida	8	30.05	-85.74
1837	8	30	9	2	317	HU	Northwest Florida to North Carolina	2	North Carolina	3	34.69	-76.45
1837	9	11	9	16	318	HU	Nassau to 31N 71W	1	Nassau	2	25.08	-77.35
1837	9	11	9	16	318	HU	Nassau to 31N 71W	2	31N 71W	1	31.00	-71.00
1837	9	22	10	10	319	HU	Barbados to 33N 76W	1	Barbados	4	13.18	-59.56
1837	9	22	10	10	319	HU	Barbados to 33N 76W	2	33N 76W	1	33.00	-76.00
1837	10	18	10	26	320	HU	20N 75W to Cuba	1	20N 75W	1	20.00	-75.00
1837	10	18	10	26	320	HU	20N 75W to Cuba	2	Cuba	4	21.61	-79.03
1838	5	20	5	21	321	TS	West of Jamaica	1	West of Jamaica	6	18.27	-79.37
1838	6	3	6	3	322	TS	South Carolina	1	South Carolina	3	32.87	-79.63
1838	6	15	6	21	323	HU	Florida Straits to South Carolina to 4011N 44W	1	Florida Straits	9	23.93	-80.93
1838	6	15	6	21	323	HU	Florida Straits to South Carolina to 4011N 44W	2	South Carolina	3	32.87	-79.63
1838	6	15	6	21	323	HU	Florida Straits to South Carolina to 4011N 44W	3	4011N 44W	1	40.18	-44.00
1838	7	29	8	12	324	HU	Northeast Caribbean to Texas	1	Northeast Caribbean	5	16.80	-64.13

1838	7	29	8	12	324	HU	Northeast Caribbean to Texas	2	Texas	3	28.40	-96.38
1838	9	2	9	4	325	HU	2948N 6806W to 37N 66W	1	2948N 6806W	1	29.80	-68.10
1838	9	2	9	4	325	HU	2948N 6806W to 37N 66W	2	37N 66W	1	37.00	-66.00
1838	8	30	9	13	326	HU	Barbados to off U.S. Coast	1	Barbados	4	13.18	-59.56
1838	8	30	9	13	326	HU	Barbados to off U.S. Coast	2	Barbados	4	29.38	-76.45
1838	9	28	9	30	327	TS	South Carolina to off SE U.S. Coast	1	South Carolina	3	32.87	-79.63
1838	9	28	9	30	327	TS	South Carolina to off SE U.S. Coast	2	Off SE U.S. Coast	6	32.69	-79.87
1839	8	23	9	1	328	HU	17N 62W to North Carolina to Grand Banks	1	17N 62W	1	17.00	-62.00
1839	8	23	9	1	328	HU	17N 62W to North Carolina to Grand Banks	2	North Carolina	3	34.69	-76.45
1839	8	23	9	1	328	HU	17N 62W to North Carolina to Grand Banks	3	Grand Banks	9	46.00	-51.50
1839	9	11	9	16	329	TS	24N 84W to Lake Charles, Louisiana	1	24N 84W	1	24.00	-84.00
1839	9	11	9	16	329	TS	24N 84W to Lake Charles, Louisiana	2	Lake Charles, Louisiana	2	29.33	-91.38
1839	9	7	9	14	330	HU	21N 46W to Newfoundland	1	21N 46W	1	21.00	-46.00
1839	9	7	9	14	330	HU	21N 46W to Newfoundland	2	Newfoundland	3	49.00	-56.00
1840	6	19	6	23	331	TS	Gulf of Mexico to Western Louisiana	1	Gulf of Mexico	5	24.82	-90.14
1840	6	19	6	23	331	TS	Gulf of Mexico to Western Louisiana	2	Western Louisiana	8	29.69	-92.22
1840	9	17	9	18	332	TS	Galveston, Texas	1	Galveston, Texas	2	29.30	-94.78
1841	8	23	8	24	333	TS	South U.S. Atlantic Coast	1	South U.S. Atlantic Coast	8	32.69	-79.87
1841	9	7	9	16	334	HU	Barbados to Northwest Florida to South Carolina	1	Barbados	4	13.18	-59.56
1841	9	7	9	16	334	HU	Barbados to Northwest Florida to South Carolina	2	Northwest Florida	8	30.05	-85.74
1841	9	7	9	16	334	HU	Barbados to Northwest Florida to South Carolina	3	South Carolina	3	32.87	-79.63
1841	9	25	9	27	335	HU	Off Hatteras to Nova Scotia	1	Off Hatteras	6	35.75	-74.55
1841	9	25	9	27	335	HU	Off Hatteras to Nova Scotia	2	Nova Scotia	4	44.85	-63.20
1841	9	25	10	4	336	HU	Barbados to Southeast New England	1	Barbados	4	13.18	-59.56
1841	9	25	10	4	336	HU	Barbados to Southeast New England	2	Southeast New England	9	41.40	-71.47
1841	10	18	10	21	337	HU	Cuba to Bermuda	1	Cuba	4	21.61	-79.03
1841	10	18	10	21	337	HU	Cuba to Bermuda	2	Bermuda	4	32.31	-64.75
1842	7	10	7	14	338	HU	Off North Carolina coast	1	Off North Carolina coast	6	35.75	-74.55
1842	7	31	8	2	339	TS	Cedar Keys to Jacksonville	1	Cedar Keys	9	29.13	-83.03
1842	7	31	8	2	339	TS	Cedar Keys to Jacksonville	2	Jacksonville	2	30.32	-81.65
1842	8	24	9	8	340	HU	Leeward Islands to Rio Grande, Texas	1	Leeward Islands	9	17.30	-62.73
1842	8	24	9	8	340	HU	Leeward Islands to Rio Grande, Texas	2	Rio Grande, Texas	2	26.37	-98.82
1842	9	9	9	30	341	HU	Tobago to Gulf of Mexico to Newfoundland	1	Tobago	4	11.15	-60.67
1842	9	9	9	30	341	HU	Tobago to Gulf of Mexico to Newfoundland	2	Gulf of Mexico	5	24.82	-90.14
1842	9	9	9	30	341	HU	Tobago to Gulf of Mexico to Newfoundland	3	Newfoundland	3	49.00	-56.00
1842	9	30	10	9	342	HU	St. Thomas to Louisiana to Florida to Bermuda	1	St. Thomas	4	18.33	-64.92
1842	9	30	10	9	342	HU	St. Thomas to Louisiana to Florida to Bermuda	2	Louisiana	3	29.33	-91.38
1842	9	30	10	9	342	HU	St. Thomas to Louisiana to Florida to Bermuda	3	Florida	9	28.66	-82.50
1842	9	30	10	9	342	HU	St. Thomas to Louisiana to Florida to Bermuda	4	Bermuda	4	32.31	-64.75
1842	10	24	10	27	343	HU	Southwest of Madeira to northeast of Madeira	1	Southwest of Madeira	6	32.17	-17.18
1842	10	24	10	27	343	HU	Southwest of Madeira to northeast of Madeira	2	Northeast of Madeira	6	33.19	-16.17
1842	10	24	11	1	344	TS	Off Florida to Bermuda	1	Off Florida	6	28.50	-79.53
1842	10	24	11	1	344	TS	Off Florida to Bermuda	2	Bermuda	4	32.31	-64.75
1843	7	11	7	14	345	TS	Jamaica to Florida Keys	1	Jamaica	4	18.15	-77.31
1843	7	11	7	14	345	TS	Jamaica to Florida Keys	2	Florida Keys	9	24.67	-81.54

1843	8	15	8	20	346	HU	North of Leeward Islands to Nova Scotia	2	Nova Scotia	4	44.85	-63.20
1843	9	13	9	15	347	HU	Central Florida to Maryland	1	Central Florida	8	28.66	-82.50
1843	9	13	9	15	347	HU	Central Florida to Maryland	2	Maryland	3	38.23	-75.14
1844	8	4	8	5	348	HU	Matamoros, Mexico	1	Matamoros, Mexico	2	25.87	-97.50
1844	9	8	9	16	349	HU	Central Florida to South Carolina to North Atlantic	1	Central Florida	8	28.66	-82.50
1844	9	8	9	16	349	HU	Central Florida to South Carolina to North Atlantic	2	South Carolina	3	32.87	-79.63
1844	9	8	9	16	349	HU	Central Florida to South Carolina to North Atlantic	3	North Atlantic	9	42.91	-26.96
1844	9	25	10	2	350	TS	Southern Leewards to Jamaica to Key West	1	Southern Leewards	8	15.43	-61.36
1844	9	25	10	2	350	TS	Southern Leewards to Jamaica to Key West	2	Jamaica	4	18.15	-77.31
1844	9	25	10	2	350	TS	Southern Leewards to Jamaica to Key West	3	Key West	2	24.55	-81.77
1844	9	30	10	7	351	HU	Barbados to Cuba	1	Barbados	4	13.18	-59.56
1844	9	30	10	7	351	HU	Barbados to Cuba	2	Cuba	4	21.61	-79.03
1845	10	27	10	29	352	HU	Bermuda to 37N 53W	1	Bermuda	4	32.31	-64.75
1845	10	27	10	29	352	HU	Bermuda to 37N 53W	2	37N 53W	1	37.00	-53.00
1846	9	5	9	11	353	HU	Northeast of Crooked Island to 35N 7330W	1	Northeast of Crooked Island	6	23.53	-73.45
1846	9	5	9	11	353	HU	Northeast of Crooked Island to 35N 7330W	2	35N 7330W	1	35.00	-73.50
1846	9	10	9	24	354	HU	Leeward Islands to 5130N 2730W	1	Leeward Islands	9	17.30	-62.73
1846	9	10	9	24	354	HU	Leeward Islands to 5130N 2730W	2	5130N 2730W	1	51.50	-27.50
1846	9	14	9	14	355	TS	South Carolina	1	South Carolina	3	32.87	-79.63
1846	10	5	10	13	356	HU	14N 72W to Atlantic Coast	1	14N 72W	1	14.00	-72.00
1846	10	5	10	13	356	HU	14N 72W to Atlantic Coast	2	Atlantic Coast	7	35.47	-70.48
1847	10	10	10	13	357	HU	12N 54W to Venezuela	1	12N 54W	1	12.00	-54.00
1847	10	10	10	13	357	HU	12N 54W to Venezuela	2	Venezuela	3	10.58	-66.89
1848	8	19	9	2	358	HU	East of Barbados to 42N 43W	1	East of Barbados	6	13.15	-58.41
1848	8	19	9	2	358	HU	East of Barbados to 42N 43W	2	42N 43W	1	42.00	-43.00
1848	9	23	9	28	359	HU	25N 90W to Grand Banks of Newfoundland	1	25N 90W	1	25.00	-90.00
1848	9	23	9	28	359	HU	25N 90W to Grand Banks of Newfoundland	2	Grand Banks of Newfoundland	9	46.00	-51.50
1848	9	17	9	24	360	HU	Northeast of Leeward Islands to 4824N 5001W	1	Northeast of Leeward Islands	6	18.39	-61.92
1848	9	17	9	24	360	HU	Northeast of Leeward Islands to 4824N 5001W	2	4824N 5001W	1	48.40	-50.02
1848	9	28	9	29	361	TS	West of Cape Verde	1	West of Cape Verde	6	15.05	-25.91
1848	10	5	10	15	362	HU	Cuba to near South Carolina to 3900N 4930W	1	Cuba	4	21.61	-79.03
1848	10	5	10	15	362	HU	Cuba to near South Carolina to 3900N 4930W	2	near South Carolina	6	32.77	-78.92
1848	10	5	10	15	362	HU	Cuba to near South Carolina to 3900N 4930W	3	3900N 4930W	1	39.00	-49.50
1849	9	4	9	15	363	HU	26N 60W to South Texas	1	26N 60W	1	26.00	-60.00
1849	9	4	9	15	363	HU	26N 60W to South Texas	2	South Texas	8	27.74	-97.40
1849	9	10	9	22	364	HU	26N 6620W to Nassau to North Carolina to Bermuda	1	26N 6620W	1	26.00	-66.33
1849	9	10	9	22	364	HU	26N 6620W to Nassau to North Carolina to Bermuda	2	Nassau	2	25.08	-77.35
1849	9	10	9	22	364	HU	26N 6620W to Nassau to North Carolina to Bermuda	3	North Carolina	3	34.69	-76.45
1849	9	10	9	22	364	HU	26N 6620W to Nassau to North Carolina to Bermuda	4	Bermuda	4	32.31	-64.75
1850	7	10	7	19	365	HU	Leeward Islands to New England	1	Leeward Islands	9	17.30	-62.73
1850	7	10	7	19	365	HU	Leeward Islands to New England	2	New England	9	42.80	-70.66
1850	8	16	8	25	366	HU	Barbados to 36N 75W	1	Barbados	4	13.18	-59.56
1850	8	16	8	25	366	HU	Barbados to 36N 75W	2	36N 75W	1	36.00	-75.00
1850	9	2	9	9	367	HU	Cape Verde to 42N 28W	1	Cape Verde	5	15.11	-23.62
1850	9	2	9	9	367	HU	Cape Verde to 42N 28W	2	42N 28W	1	42.00	-28.00

1850	9	4	9	10	368	HU	3158N 75W to North Atlantic	1	3158N 75W	1	31.97	-75.00
1850	9	4	9	10	368	HU	3158N 75W to North Atlantic	2	North Atlantic	9	42.91	-26.96
1850	10	14	10	18	369	HU	2459N 4710W to 2558N 4119W	1	2459N 4710W	1	24.98	-47.20
1850	10	14	10	18	369	HU	2459N 4710W to 2558N 4119W	2	2558N 4119W	1	25.97	-41.32
1851	8	16	8	28	370	HU	13.4N 48.0W to 48.5N 54.2W	1	13.4N 48.0W	1	13.40	-48.00
1851	8	16	8	28	370	HU	13.4N 48.0W to 48.5N 54.2W	2	48.5N 54.2W	1	48.50	-54.20
1851	11	7	11	8	371	HU	Western Jamaica	1	Western Jamaica	8	18.15	-77.82
1852	8	19	8	30	372	HU	20.5N 67.1W to 41.0N 68.0W	1	20.5N 67.1W	1	20.50	-67.10
1852	8	19	8	30	372	HU	20.5N 67.1W to 41.0N 68.0W	2	41.0N 68.0W	1	41.00	-68.00
1852	9	3	9	13	373	HU	Antigua to Florida Keys to Tampa to 35N 6545W	1	Antigua	4	17.28	-61.79
1852	9	3	9	13	373	HU	Antigua to Florida Keys to Tampa to 35N 6545W	2	Florida Keys	9	24.67	-81.54
1852	9	3	9	13	373	HU	Antigua to Florida Keys to Tampa to 35N 6545W	3	Tampa	2	27.93	-82.45
1852	9	3	9	13	373	HU	Antigua to Florida Keys to Tampa to 35N 6545W	4	35N 6545W	1	35.00	-65.75
1852	9	21	10	3	374	HU	16.1N 58.5W to 3650N 3230W	1	16.1N 58.5W	1	16.10	-58.50
1852	9	21	10	3	374	HU	16.1N 58.5W to 3650N 3230W	2	3650N 3230W	1	36.83	-32.50
1852	10	5	10	11	375	HU	Western Jamaica to 3923N 6840W	1	Western Jamaica	8	18.15	-77.82
1852	10	5	10	11	375	HU	Western Jamaica to 3923N 6840W	2	3921N 6840W	1	39.38	-68.67
1853	8	30	9	10	376	HU	12.1N 23.2WNA 4710N 2530W	1	12.1N 23.2W	1	12.10	-23.20
1853	8	30	9	10	376	HU	12.1N 23.2WNA 4710N 2530W	2	4710N 2530W	1	47.17	-25.50
1853	9	26	9	28	377	HU	25.8N 62.0W to 3510N 5320W	1	25.8N 62.0W	1	25.80	-62.00
1853	9	26	9	28	377	HU	25.8N 62.0W to 3510N 5320W	2	3510N 5320W	1	35.17	-53.33
1853	9	28	9	29	378	TS	15N 3710W	1	15N 3710W	1	15.00	-37.17
1853	10	19	10	25	379	HU	2730N 7830W to Nova Scotia	1	2730N 7830W	1	27.50	-78.50
1853	10	19	10	25	379	HU	2730N 7830W to Nova Scotia	2	Nova Scotia	4	44.85	-63.20
1854	9	3	9	12	380	HU	Nassau to 38N 4530W	1	Nassau	2	25.08	-77.35
1854	9	3	9	12	380	HU	Nassau to 38N 4530W	2	38N 4530W	1	38.00	-45.50
1854	9	9	9	21	381	HU	Leeward Islands to Texas	1	Leeward Islands	9	17.30	-62.73
1854	9	9	9	21	381	HU	Leeward Islands to Texas	2	Texas	3	28.40	-96.38
1854	10	18	10	22	382	HU	North of St. Thomas to northeast of Bermuda	1	North of St. Thomas	6	19.58	-64.94
1854	10	18	10	22	382	HU	North of St. Thomas to northeast of Bermuda	2	northeast of Bermuda	6	33.00	-64.05
1855	9	24	9	31	383	HU	12.0N 55.9W to Louisiana	1	12.0N 55.9W	1	12.00	-55.90
1855	9	24	9	31	383	HU	12.0N 55.9W to Louisiana	2	Louisiana	3	29.33	-91.38

BIBLIOGRAPHY

- Blaut, J. M., 1961: Space and process. *The Professional Geographer*, **13**, 1–7.
- Bove, M. C., J. B. Elsner, C. W. Landsea, X. Niu, and J. J. O'Brien, 1998: Effect of El Niño on U.S. landfalling hurricanes, revisited. *Bull. Amer. Meteor. Soc.*, **79**, 2477–2482.
- Brettschneider, B., 2008: Climatological hurricane landfall probability for the United States. *J. Appl. Meteor. and Climatol.*, **47**, 704–716.
- Brown, D. P., J. L. Franklin, and C. Landsea, 2006: A fresh look at tropical cyclone pressure-wind relationships using recent reconnaissance based 'best track' data (1998–2005). *Preprints 27th Conf. on Hurricanes and Tropical Meteorology*, Orlando, Florida, Amer. Met. Soc.
- Chen, K., R. Blonga, and C. Jacobsonb, 2006: MCE-RISK: integrating multicriteria evaluation and GIS for risk decision-making in natural hazards. *Environmental Modelling and Software*, **16**, 387–397, doi:10.1016/S1364-8152(01)00006-8.
- Chenoweth, M., 2006: A reassessment of historical Atlantic basin tropical cyclone activity, 1700–1855. *Climatic Change*, **76**, 169–240.
- Chenoweth, M., 2007: Objective classification of historical tropical cyclone intensity. *J. Geophys. Res.*, **112**, doi:10/1029/2006JD009211.
- Chenoweth, M. and D. Divine, 2008: A document-based 318-year record of tropical cyclones in the lesser antilles, 1690–2007. *Geochem. Geophys. Geosyst.*, **9**, doi: 10.1029/2008GC002066.
- Chi, M. T. H., 1997: Quantifying qualitative analyses of verbal data: A practical guide. *J. Learning Sciences*, **6**, 271–315, doi:10.1207/s15327809jls0603_1.
- Corbosiero, K. L. and J. Molinari, 2003: The relationship between storm motion, vertical wind shear, and convective asymmetries in tropical cyclones. *J. Atmos. Sci.*, **60**, 366–376.
- Danielsson, P. E., 1980: Euclidean distance mapping. *Comput. Graphics Image Processing*, **14**, 227–248.

- Demuth, J. L., M. DeMaria, and J. A. Knaff, 2006: Improvement of advanced microwave sounding unit tropical cyclone intensity and size estimation algorithms. *J. Appl. Meteor.*, **45**, 1573–1581.
- Edsall, R., 2003: The parallel coordinate plot in action: design and use for geographic visualization. *Computational Statistics and Data Analysis*, **43**, 605619.
- Elsner, J. B., 2003: Tracking hurricanes. *Bull. Amer. Meteor. Soc.*, **35**, 353–356, doi:10.1175/BAMS-84-3-353.
- Elsner, J. B. and B. H. Bossak, 2001: Bayesian analysis of U.S. hurricane climate. *J. Climate*, **14**, 4341–4350.
- Elsner, J. B. and B. H. Bossak, 2004: Hurricane landfall probability and climate. *Hurricanes and Typhoons: Past, Present, and Future*, R. Murnane and K. b. Liu, Eds., Columbia University Press.
- Elsner, J. B., B. H. Bossak, and X.-f. Niu, 2001: Secular changes to the ENSOUS hurricane relationship. *Geophys. Res. Let.*, **28**, 4123–4126.
- Elsner, J. B. and T. H. Jagger, 2004: A hierarchical Bayesian approach to seasonal hurricane modeling. *J. Climate*, **17**, 2813–2827.
- Elsner, J. B. and T. H. Jagger, 2006: Prediction models for annual U.S. hurricane counts. *J. Climate*, **19**, 2935–2952.
- Elsner, J. B. and T. H. Jagger, 2008: United states and caribbean tropical cyclone activity related to the solar cycle. *Geophys. Res. Let.*, **35**, doi:10.1029/2008GL034431.
- Elsner, J. B., T. H. Jagger, and K. Liu, 2008a: Comparison of hurricane return levels using historical and geological records. *J. Appl. Meteor. Climatol.*, **47**, 368–374.
- Elsner, J. B., T. H. Jagger, and X.-f. Niu, 2000a: Changes in the rates of North Atlantic major hurricane activity during the 20th century. *Geophys. Res. Let.*, **27**, 1743–1746.
- Elsner, J. B. and A. B. Kara, 1999: *Hurricanes of the North Atlantic: Climate and Society*. Oxford University Press, 488 pp.
- Elsner, J. B., A. B. Kara, and M. A. Owens, 1999: Fluctuations in North Atlantic hurricane frequency. *J. Climate*, **12**, 427–437.
- Elsner, J. B., J. Kossin, and T. H. Jagger, 2008b: The increasing intensity of the strongest tropical cyclones. *Nature*, **455**, 92–95.
- Elsner, J. B., K.-b. Liu, and B. Kocher, 2000b: Spatial variations in major U.S. hurricane activity: statistics and a physical mechanism. *J. Climate*, **13**, 2293–2305.

- Emanuel, K., 1986: An air-sea interaction theory for tropical cyclones. part I. *J. Atmos. Sci.*, **42**, 1062–1071.
- Emanuel, K., 1987: The dependence of hurricane intensity on climate. *Nature*, **326**, 483–485.
- Emanuel, K., 1995: The behavior of a simple hurricane model using a convective scheme based on subcloud-layer entropy equilibrium. *J. Atmos. Sci.*, **52**, 3960–3968.
- Emanuel, K., 1999: Thermodynamic control of hurricane intensity. *Nature*, **401**, 665–669.
- Emanuel, K., 2000: A statistical analysis of tropical cyclone intensity. *Mon. Wea. Rev.*, **128**, 1139–1152.
- Emanuel, K., 2004: Response of tropical cyclone activity to climate change: Theoretical basis. *Hurricanes and Typhoons: Past, Present, and Future*, R. Murnane and K. b. Liu, Eds., Columbia University Press.
- Emanuel, K., 2005: Increasing destructiveness of tropical cyclones over the past 30 years. *Nature*, **436**, 686–688.
- FEMA, 2008: HAZUS MH MR3 hurricane model technical manual. Tech. rep., Federal Emergency Management Association.
- García-Herrera, R., F. R. Durán, D. Wheeler, E. H. Martín, M. R. Prieto, and L. Gimeno, 2004: The use of Spanish and British document sources in the investigation of Atlantic hurricane incidence in historical times. *Hurricanes and Typhoons: Past, Present, and Future*, R. Murnane and K. b. Liu, Eds., Columbia University Press, 149–176.
- Gregory, I. N. and P. S. Ell, 2006: Error-sensitive historical gis: Identifying areal interpolation errors in time-series data. *Intl. J. Geog. Info Sci.*, **20**, 135–152, doi:DOI: 10.1080/13658810500399589.
- Hallegatte, S., 2007: The use of synthetic hurricane tracks in risk analysis and climate change damage assessment. *J. Appl. Meteor. Climatol.*, 1956–1966.
- Hart, R., R. Maue, and M. Watson, 2007: Estimating local memory of tropical cyclones through MPI anomaly evolution. *Mon. Wea. Rev.*, 3990–4005.
- Hirata, T., 1995: A unified linear-time algorithm for computing distance maps. *Information Processing Letters*, **58**, 129–133.
- Hoke, J. E. and R. A. Anthes, 1977: Dynamic initialization of a three-dimensional primitive-equation model of Hurricane Alma of 1962. *Mon. Wea. Rev.*, **105**, 1266–1280.
- Holland, G. J., 1980: An analytical model of the wind and pressure profiles in hurricanes. *Mon. Wea. Rev.*, **108**, 1212–1218.

- Holland, G. J., 1997: The maximum potential intensity of tropical cyclones. *J. Atmos. Sci.*, **54**, 2519–2541.
- Hong, X., S. W. Chang, S. Raman, L. K. Shay, and R. Hodur, 2000: The interaction between Hurricane Opal (1995) and a warm core ring in the Gulf of Mexico. *Mon. Wea. Rev.*, **128**, 1347–1365.
- Hsu, S. A. and Z. Yan, 1998: A note on the radius of maximum winds for hurricanes. *J. Coastal Res.*, **14**, 667–668.
- Inselberg, A. and B. Dimsdale, 1990: Parallel coordinates a tool for visualizing multi-dimensional geometry. *Proceedings of the 1990 International Conference on Information Visualization*, IEEE Computer Society, 361–378.
- Jagger, T. and J. Elsner, 2006: Climatology models for extreme hurricane winds in the United States. *J. Climate*, **19**, 3220–3236.
- Jagger, T., J. Elsner, and X. Niu, 2001: A dynamic probability model of hurricane winds in coastal counties of the United States. *J. Appl. Meteor.*, **40**, 853–863.
- Jagger, T. H., J. B. Elsner, and M. A. Saunders, 2008: Forecasting U.S. insured hurricane losses. *Climate Extremes and Society*, H. Diaz and R. Murnane, Eds., Cambridge University Press, 189–208.
- Jordan, M. and C. Clayson, 2008: A new approach to using wind speed for prediction of tropical cyclone generated storm surge. *Geophys. Res. Lett.*, **35**, doi:10.1029/2008GL033564.
- Kaplan, J. and M. DeMaria, 1995: A simple empirical model for predicting the decay of tropical cyclone winds after landfall. *J. Appl. Meteor.*, **34**, 2499–2512.
- Kaplan, J. and M. DeMaria, 2001: On the decay of tropical cyclone winds after landfall in the New England area. *J. Appl. Meteor.*, **40**, 280–286.
- Keim, B. D., R. A. Muller, and G. W. Stone, 2007: Spatiotemporal patterns and return periods of tropical storm and hurricane strikes from Texas to Maine. *J. Climate*, **20**, 3498–3509.
- Khain, A., N. Cohen, B. Lynn, and A. Pokrovsky, 2008: Possible aerosol effects on lightning activity and structure of hurricanes. *J. Atmos. Sci.*, **65**, 3652–3677.
- Kuijpers, B., B. Moelans, and N. Van de Weghe, 2006: Qualitative polyline similarity testing with applications to query-by-sketch, indexing and classification. *GIS '06: Proceedings of the 14th annual ACM international symposium on Advances in geographic information systems*, ACM, New York, NY, USA, 11–18, doi:http://doi.acm.org/10.1145/1183471.1183475.

- Landsea, C., et al., 2004: The Atlantic hurricane database reanalysis project: Documentation for the 1851–1910 alterations and additions to the HURDAT database. *Hurricanes and Typhoons: Past, Present, and Future*, R. Murnane and K. b. Liu, Eds., Columbia University Press, 177–221.
- Landsea, C. W., B. A. Harper, K. Hoarau, and J. A. Knaff, 2006: Can we detect trends in extreme tropical cyclones? *Science*, **28**, 452–454.
- Levinson, D. H., P. J. Vickery, and D. T. Resio, 2009: A climatology of landfalling hurricane central pressures along the gulf of mexico coast. *Preprints*, Halifax, Canada, 11th International Workshop on Wave Hindcasting and Forecasting and 2nd Coastal Hazard Symposium.
- Lin, N., K. A. Emanuel, J. A. Smith, and E. Vanmarcke, in press: Risk assessment of hurricane storm surge for New York City. *Bull. Amer. Meteor. Soc.*
- Liu, K.-b. and M. L. Fearn, 1993: Lake-sediment record of late holocene hurricane activities from coastal Alabama. *Geology*, **21**, 793–796.
- Liu, K.-b. and M. L. Fearn, 2000: Reconstruction of prehistoric landfall frequencies of catastrophic hurricanes in Northwestern Florida from lake sediment records. *Quaternary Research*, **54**, 238–245.
- Liu, K. S. and J. C. Chan, 1999: Size of tropical cyclones as inferred from ERS-1 and ERS-2 data. *Mon. Wea. Rev.*, **127**, 2992–3001.
- Louie, K.-s. and K.-b. Liu, 2003: Earliest historical records of typhoons in China. *J. Historical Geography*, **29**, 299–316.
- Malkus, J. S., 1958: On the structure and maintenance of the mature hurricane eye. *J. Meteor.*, **15**, 337–349.
- Malmstadt, J. C., J. B. Elsner, and T. H. Jagger, in press: Risk of strong hurricane winds to Florida cities. *J. Climate*.
- Mather, E., 1944: A linear-distance map of farm population in the United States. *A. Assoc. Am. Geog.*, **34**, 173–180.
- Mock, C. J., 2004: Tropical cyclone reconstructions from documentary records: Examples for South Carolina, United States. *Hurricanes and Typhoons: Past, Present and Future*, R. J. Murnane and K. b. Liu, Eds., Columbia University Press, 121–148.
- Muller, R. A. and G. W. Stone, 2001: A climatology of tropical storm and hurricane strikes to enhance coastal vulnerability prediction for the southeast U. S. coast. *J. Coastal Res.*, **17**, 949–956.
- Murnane, R. J. and K.-b. Liu, 2004: *Hurricanes and Typhoons: Past, Present and Future*. Columbia University Press, 462 pp.

- Oouchi, K., J. Yoshimura, H. Yoshimura, R. Mizuta, S. Kusunoki, and A. Noda, 2006: Tropical cyclone climatology in a global-warming climate as simulated in a 20 km-mesh global atmospheric model: Frequency and wind intensity analyses. *J. Meteor. Soc. Japan*, **84**, 259–276.
- O’Sullivan, D. and D. J. Unwin, 2003: *Geographic Information Analysis*. John Wiley and Sons, Inc.
- Pearson, A. D. and A. F. Sadowski, 1965: Hurricane-induced tornadoes and their distribution. *Mon. Wea. Rev.*, **93**, 461–464.
- Pielke, R., C. Landsea, M. Mayfield, J. Laver, and R. Pasch, 2005: Hurricanes and global warming. *Bull. Am. Meteor. Soc.*, **86**, 1571–1575.
- Pielke Jr., R. A., J. Gratz, C. W. Landsea, D. Collins, M. A. Saunders, and R. Musulin, 2008: Normalized hurricane damage in the United States: 1900–2005. *Nat. Haz. Rev.*, **9**, 29–42.
- Pielke Jr., R. A. and C. W. Landsea, 1999: La Niña, El Niño, and Atlantic hurricane damages in the United States. *Bull. Amer. Meteor. Soc.*, **80**, 2027–2033.
- Powell, M. D. and S. H. Houston, 1998: Surface wind fields of 1995 hurricanes Erin, Opal, Luis, Marilyn, and Roxanne at landfall. *Mon. Wea. Rev.*, **126**, 1259–1273.
- Riehl, H., 1948: A radiosonde observation in the eye of a hurricane. *Quart. J. R. Meteor. Soc.*, **74**, 194–196.
- Russ, J. H., 1989: Uses of the euclidean distance map for the measurement of features in images. *Journal of Computer-Assisted Microscopy*, **1**, 343–375.
- Scheitlin, K. N. and J. B. Elsner, 2010: A track-relative climatology of Eglin Air Force Base hurricanes in a variable climate. *Hurricanes and Climate Change, Volume 2*, J. B. Elsner, R. E. Hodges, J. C. Malmstadt, and K. N. Scheitlin, Eds., Springer, 200.
- Scheitlin, K. N., J. B. Elsner, J. C. Malmstadt, R. E. Hodges, and T. H. Jagger, 2010: Toward increased utilization of historical hurricane chronologies. *J. Geophys. Res.*, **115**, doi:10.1029/2009JD012424.
- Schneider, P. J. and B. A. Schauer, 2006: HAZUS—Its development and its future. *Nat. Haz.*, **7**, 40–44.
- Shay, L. K., G. J. Goni, and P. G. Black, 2000: Effects of a warm oceanic feature on Hurricane Opal. *Mon. Wea. Rev.*, **128**, 1366–1383.
- Siirtola, H., 2000: Direct manipulation of parallel coordinates. *Proceedings of the 2000 International Conference on Information Visualization*, IEEE Computer Society, 373–378.

- Simpson, R. H. and H. Riehl, 1981: *The Hurricane and its Impact*. Louisiana State University Press, 398 pp.
- Steed, C. A., P. J. Fitzpatrick, J. E. S. II, and T. Jankun-Kelly, 2009: Tropical cyclone trend analysis using enhanced parallel coordinates and statistical analytics. *Cartography and Geographic Information Science*, **36**, 251–265.
- Trenberth, K., 2005: Uncertainty in hurricanes and global warming. *Science*, **308**, 1753–1754.
- Vickery, P. J., J. Lin, P. F. Skerlj, L. A. Twisdale Jr., and K. Huang, 2006a: HAZUS-MH hurricane model methodology. I: Hurricane hazard, terrain, and wind load modeling. *Nat. Haz. Rev.*, **7**, 82–93.
- Vickery, P. J., P. F. Skerlj, J. Lin, L. A. Twisdale Jr., M. A. Young, and F. M. Lavelle, 2006b: HAZUS-MH hurricane model methodology. II: Damage and loss estimation. *Nat. Haz. Rev.*, **7**, 94–103.
- Vickery, P. J., P. F. Skerlj, A. C. Steckley, and L. A. Twisdale, 2000a: Hurricane wind field model for use in hurricane simulations. *J. Struct. Eng.*, **10**, 1203–1221.
- Vickery, P. J., P. F. Skerlj, and L. A. Twisdale, 2000b: Simulation of hurricane risk in the United States using empirical track model. *J. Struct. Eng.*, **10**, 1222–1237.
- Vickery, P. J. and D. Wadhera, 2008: Statistical models of holland pressure profile parameter and radius to maximum winds of hurricanes from flight-level pressure and H*Wind data. *J. Appl. Meteor. and Climatol.*, **47**, 2497–2517.
- Vukovich, F. M. and B. W. Crissman, 1986: Aspects of warm rings in the Gulf of Mexico. *J. Geophys. Res.*, **91**, 2649–2660.
- Walsh, K. J. E., K.-C. Nguyen, and J. L. McGregor, 2004: Fine-resolution climate model simulations of the impact of climate change on tropical cyclones near Australia. *Clim. Dynam.*, **22**, 47–56.
- Watson, C. C. and M. E. Johnson, 2008: Integrating hurricane loss models with climate models. *Climate extremes and society*, H. F. Diaz and R. J. Murnane, Eds., Cambridge University Press, 209–224.
- Webster, P. J., J. G. Holland, J. A. Curry, and H.-r. Chang, 2005: Changes in tropical cyclone number, duration, and intensity in a warming environment. *Science*, **309**, 1844–1846.
- Wentz, E. A., A. F. Campbell, and R. Houston, 2001: Impact of sea surface temperature anomalies on the Atlantic tropical storm activity and West African rainfall. *J. Atmos. Sci.*, **58**, 3477–3496.

- Wentz, E. A., A. F. Campbell, and R. Houston, 2003a: A comparison of two methods to create tracks of moving objects: linear weighted distance and constrained random walk. *Int. J. of Geogr. Inf. Sci.*, **17**, 623–645.
- Wentz, E. A., A. F. Campbell, and R. Houston, 2003b: Representation and spatial analysis in geographic information systems. *A. Assoc. Am. Geog.*, **93**, 574–594.
- Willoughby, H. E., 1998: Tropical cyclone eye thermodynamics. *Monthly Weather Review*, **126**, 3053–3067.
- Woodruff, J. D., J. P. Donnelly, K. Emanuel, and P. Lane, 2008: Assessing sedimentary records of paleohurricane activity using modeled hurricane climatology. *Geochem. Geophys. Geosyst.*, **9**, doi:10.1029/2008GC002043.
- Zandbergen, P. A., 2009: Exposure of US counties to Atlantic tropical storms and hurricanes, 1851–2003. *Nat. Haz.*, **48**, 83–99.
- Zhu, P., 2008: Impact of land-surface roughness on surface winds during hurricane landfall. *Quart. J. Roy. Meteor. Soc.*, **134**, 1051–1057.

BIOGRAPHICAL SKETCH

Kelsey N. Scheitlin

EDUCATION

Salisbury University, Salisbury, MD

B.S. Geography and Geosciences: Earth and Atmospheric Sciences track; May 2005

Mississippi State University, Starkville, Mississippi

M.S. Geosciences: Operational Meteorology; May 2007 Thesis: “Variations in Diurnal Temperature Range in the Southeast United States, 1995–2004

RESEARCH INTERESTS

Physical geography, applied meteorology and climatology, land-surface-atmosphere interaction, hurricane climatology, GIS, spatial analysis

PUBLICATIONS, BOOK, AND BOOK CHAPTER

2010

Scheitlin, K. N., J. B. Elsner, J. C. Malmstadt, R. E. Hodges, and T. H. Jagger, Toward increased utilization of historical hurricane chronologies, *J. Geophys. Res.*, **115**, D03108, doi:10.1029/2009JD012424.

Scheitlin, K. N. and P. G. Dixon: Variations in diurnal temperature range in the Southeast United States due to land use and air mass. *J. Applied Meteor. Climatol.*, in press.

Scheitlin, K. N. and J. B. Elsner: A track-relative climatology of Eglin Air Force Base hurricanes in a variable climate. *Hurricanes and Climate Change, 2nd Ed.*, in press.

Elsner, J. B., J. C. Malmstadt, R. E. Hodges and K. N. Scheitlin (eds): *Hurricanes and Climate Change, 2nd Ed*, in press.

Scheitlin, K. N., S. Lewers, J. B. Elsner, and T. H. Jagger: Assessing hurricane risk using a track-relative climatology of extreme events: A case study for Eglin Air Force Base. *Theoretical and Applied Climatology*, in rev.

2009

Malmstadt, J., K. Scheitlin, and J. Elsner: Florida hurricanes and damage costs. *Southeastern Geographer*, **49**, 108–131.

2008

Dixon, P. G., M. E. Brown, M. C. Carter, W. S. Gunter, J. S. Allen, A. M. Hayes, L. E. Becker, H. S. Eschete, R. P. Aylward, and K. N. Scheitlin: Predicting Atlantic hurricane paths using monthly surface pressure data. *The Geographical Bulletin*, **49**, 77–86.

2007

Dixon, P. G., A. N. McDonald, K. N. Scheitlin, J. E. Stapleton, J. S. Allen, W. M. Carter, M. R. Holley, D. D. Inman, and J. B. Roberts: Effects of temperature variation on suicide in five U.S. counties, 1991–2001. *Intl. J. Biometeorology*, **51**, 395–403.

TEACHING EXPERIENCE

Advanced Geographic Information Science, Laboratory Instructor, Florida State University. Spring 2009.

Physical Geography, Florida State University. Summer and Spring 2008.

Principles of Geographic Information Science, Laboratory Instructor, Mississippi State University. Spring 2007, Fall and Spring 2006, Fall 2005.

PRESENTATIONS

2010

Scheitlin, K. N. and J. B. Elsner: A geographic approach to hurricane climatology research. Annual Meeting, Association of American Geographers, Washington DC.

Scheitlin, K. N. and J. C. Malmstadt: Hurricanes and Pollution: Human Affecting vs. Human Affected. Environmental Action Research Symposium, Florida State University.

2009

Scheitlin, K. N., J. B. Elsner: A track-relative climatology of hurricanes affecting Eglin Air Force Base. Annual Meeting, American Geophysical Union, San Francisco, California.

Scheitlin, K. N., J. C. Malmstadt, R. Hodges, J. B. Elsner and T. H. Jagger: Toward increased utilization of historical hurricane chronologies. 2nd International Summit on Hurricanes and Climate Change, Corfu, Greece. <http://ciquestudios.com/hurricaneclimate/page/2/>

Scheitlin, K. N., J. C. Malmstadt, R. Hodges, J. B. Elsner and T. H. Jagger: Toward increased utilization of historical hurricane chronologies. 105th Annual Meeting, Association of American Geographers, Las Vegas, Nevada.

2008

Scheitlin, K. N., J. C. Malmstadt and J. B. Elsner: Increased losses from Florida hurricanes. Annual Meeting, Southeast Division of the Association of American Geographers. Greensboro, North Carolina.

2007

Scheitlin, K. N. and P. G. Dixon: Variations of Diurnal Temperature Range in the Southeast United States Due to Land Use/Land Cover Classification, 1995–2004. 103rd Annual Meeting, Association of American Geographers, San Francisco, California.

Dixon, P. G., A. N. McDonald, K. N. Scheitlin, J. E. Stapleton, J. S. Allen, W. M. Carter, M. R. Holley, D. D. Inman and J. B. Roberts: Effects of temperature variation on suicide in five U.S. counties, 1991–2001. 103rd Annual Meeting, Association of American Geographers, San Francisco, California.

2005

Scheitlin, K., S. Jacobs and B. Zaprowski: Using tombstones to calculate the rate of erosion on the eastern shore of Maryland, 1900–2005. Undergraduate Research Seminar, Salisbury, MD.

2004

Scheitlin, K. and C. Egan: Appearance-related stereotypes of the female meteorologist. Undergraduate Research Seminar, Salisbury, MD.